



Universiteit
Leiden
The Netherlands

A cluster density functional theory study of the interaction of the hydrogen storage system NaAlH₄ with transition metal catalysts
Marashdeh, A.A.

Citation

Marashdeh, A. A. (2008, March 5). *A cluster density functional theory study of the interaction of the hydrogen storage system NaAlH₄ with transition metal catalysts*. Retrieved from <https://hdl.handle.net/1887/12626>

Version: Corrected Publisher's Version

License: [Licence agreement concerning inclusion of doctoral thesis in the Institutional Repository of the University of Leiden](#)

Downloaded from: <https://hdl.handle.net/1887/12626>

Note: To cite this publication please use the final published version (if applicable).

**A cluster density functional theory study of the interaction of
the hydrogen storage system NaAlH₄ with transition metal
catalysts**

PROEFSCHRIFT

Ter verkrijging van
de graad van Doctor aan de Universiteit Leiden,
op gezag van Rector Magnificus Prof. Mr. P. F. van der Heijden,
volgens besluit van het College voor Promoties
te verdedigen op woensdag 5 maart 2008
klokke 13.45 uur

door

Ali Awad Marashdeh

geboren te Ramtha, Jordanië
in 1973

Promotiecommissie

Promotor: Prof. Dr. G. J. Kroes

Co-Promotor: Dr. R. A. Olsen

Referent: Prof. Dr. R. Broer

Overige leden: Prof. Dr. E. J. Baerends (Vrije Universiteit Amsterdam)
Prof. Dr. G. J. Kramer (Technische Universiteit Eindhoven)
Prof. Dr. J. Brouwer
Prof. Dr. M. T. H. Koper
Prof. Dr. M. C. van Hemert

The work described in this thesis was performed at the Leiden Institute of Chemistry, Leiden University (Einsteinweg 55, 2300 RA Leiden). It is part of the research program of Advanced Chemical Technologies for Sustainability (ACTS) and was made possible by their financial support. For the computer time, the National Computing Facilities Foundation (NCF) is acknowledged.

To my parents,
wife,
daughter,
brothers and sisters

Contents

1 Introduction	7
1.1 Renewable energy technology	7
1.1.1 The source of energy	7
1.1.2 Energy storage	7
1.2 Hydrogen	8
1.3 Hydrogen storage	8
1.4 NaAlH ₄	9
1.5 My research goal	12
1.6 The outline of my thesis	12
1.7 Outlook	13
1.7.1 Ti + NaAlH ₄	14
1.7.2 Ti ₂ + NaAlH ₄	14
1.7.3 TiH ₂ + NaAlH ₄	14
1.7.4 (Ti, Zr, Sc, Pd, Pt) + NaAlH ₄	15
1.7.5 The hydrogenation process and dehydrogenation of Na ₃ AlH ₆	16
1.8 References	16
2 Methods and approximations	21
2.1 The Born-Oppenheimer approximation: separating the nuclear and electronic motions	21
2.2 Solving the electronic Schrödinger equation by Density Functional Theory...	23
2.3 Finding (local) minima on the potential energy surface	25
2.4 A cluster approach to modeling NaAlH ₄	27
2.5 References	28
3 A density functional theory study of Ti-doped NaAlH₄ clusters	31
3.1 Introduction	31
3.2 Method	33
3.3 Results and Discussion	34
3.3.1 Undoped NaAlH ₄ clusters: Electronic structure and stability	34

3.3.2 Ti-doped NaAlH ₄ clusters	38
3.4 Conclusions	41
3.5 References	42
4 NaAlH₄ clusters with two titanium atoms added	45
4.1 Introduction	45
4.2 Method	48
4.3 Results and Discussion	50
4.3.1 The adsorption of two titanium atoms on the surface of the Z=23 cluster	50
4.3.2 The stability of the two titanium doped NaAlH ₄ clusters	54
4.3.2.1 Ti exchanging with Na	54
4.3.2.2 Ti exchanging with Na and Al	55
4.3.2.3 Ti exchanging with Al	55
4.3.2.4 Ti in interstitial sites	56
4.3.3 Is Ti found on the surface or inside the cluster?	56
4.3.4 Does Ti prefer to be inside the NaAlH ₄ cluster or in Ti bulk?	57
4.3.5 Density of electronic states of Ti doped clusters	58
4.3.6 A proposed model for the role of Ti	61
4.4 Conclusions	62
4.5 References	63
5 A density functional theory study of the TiH₂ interaction with a NaAlH₄ cluster	67
5.1 Introduction	67
5.2 Method	71
5.3 Results and Discussion	72
5.3.1 The adsorption of TiH ₂ on the (001) surface of the cluster	72
5.3.2 The stability of TiH ₂ inside the cluster	74
5.3.3 The interaction of H ₂ with a Ti, Na or Al atom on the surface of the cluster	75
5.3.4 The local structure around Ti	77

5.3.5 Further support of the zipper model	78
5.4 Conclusion	79
5.5 References	80
6 Why Some Transition Metals are Good Catalysts for Reversible Hydrogen Storage in Sodium Alanate, and Others are not: A Density Functional Theory Study	83
6.1 Introduction	83
6.2 Method	87
6.3 Results and Discussion	90
6.3.1 Adsorption of TM atoms on NaAlH ₄ (001)	90
6.3.2 Absorption of TM atoms in the surface of NaAlH ₄ (001)	93
6.3.3 Interpretation with a zipper model for mass transport	97
6.4 Conclusions	98
6.5 References	99
7 Zero point energy corrected dehydrogenation enthalpies of Ca(AlH₄)₂, CaAlH₅ and CaH₂+6LiBH₄	103
7.1 Introduction	103
7.2 Method	105
7.3 Results and Discussion	106
7.4 Conclusions	110
7.5 References	110
Summary	113
Samenvatting	119
Curriculum Vitae	125
Publication list	127
Acknowledgment	129

Chapter 1

Introduction

1.1 Renewable energy technology

1.1.1 The source of energy

Energy can be obtained from different sources [1] such as chemical (fossil fuels), solar (photovoltaic cell), nuclear (uranium) and thermo-mechanical (wind, water and hot water). Each kind of energy has its own problems. The use of fossil fuels leads to the production of the green house gas CO₂ that warms the earth; the use of nuclear energy leads to nuclear wastes from radioactive fission products; solar and wind energy require the use of large surface areas [1].

Currently, fossil fuel and nuclear sources are the main energy suppliers for the world [1]. The increase of the energy need with time is expected to lead to increased atmospheric concentrations of the green house gas CO₂ and to the depletion of fossil fuel supplies (especially oil) in the coming decades.

The continuous emission of CO₂ is a serious threat to the global environment. Increasing the CO₂ concentration in the atmosphere will lead to global warming [1] and as a result the climate will change. In the coming hundred years, the expected increase of the world population together with a rapid growth of the economies of e.g. China and India, will lead to a large increase in the world's use of energy [2].

In order to meet the growing global demand for energy, while producing less CO₂, the current energy sources have to be replaced by new ones. The use of fossil fuels such as oil, coal and natural gas has to be reduced. In their place we have to increase our use of renewable energy sources like solar, geothermal and wind [3].

1.1.2 Energy storage

The energy needs to be stored in a form that can be used for our purposes. In creation of the universe, (some of the) energy has been stored in the stars. Our sun is one of these

stars, and its energy is being used by humans either directly by solar cells or indirectly through fossil fuels, hydro power or wind power.

The widespread use of electricity and refined chemical fuels has made energy storage a major factor in economic development. All of the chemical energy carriers are readily converted to mechanical energy (and to electrical energy, e.g. with combustion engines that are used to power electrical generators). A great deal of the world's consumption of the liquid hydrocarbon fuel is accounted for by the transportation sector, especially automobiles.

Electric road vehicles powered by fuel cells (running on hydrogen) are a suitable alternative for vehicles running on combustion engines. Hydrogen is oxidized in the fuel cell to generate electricity (and heat) with only water as an exhaust gas [2].

1.2 Hydrogen

Hydrogen is a chemical energy carrier that is a possible alternative to hydrocarbon fuels. Hydrogen is the only carbon-free chemical energy carrier and this characteristic makes hydrogen a unique fuel. Hydrogen can be produced using different energy sources in our world and it can be stored for future use. It can be used to fuel combustion engines. Pure hydrogen can (together with oxygen) also be used to produce electricity through the proton exchange membrane (PEM) fuel cell [4].

1.3 Hydrogen storage

The energy density by weight of hydrogen is 142 MJ kg^{-1} , which is three times larger than that in other chemical fuels, such as e.g. liquid hydrocarbon (47 MJ kg^{-1}) [5].

Hydrogen is a gas at ambient temperatures, it has a critical temperature of 33 K and it has low energy density per volume. These are the main reasons why hydrogen is not the major fuel of today's energy consumption.

Automobiles run on hydrogen either by burning hydrogen with oxygen from air in an internal combustion engine [5] or by “burning” hydrogen electrochemically with oxygen from air in a fuel cell, which produces electricity that drives an electric engine [6].

To run a standard sized car for 400 km, 24 kg of petrol or 8 kg of hydrogen is needed in a combustion engine, while 4 kg of hydrogen is needed for an electric car with a fuel cell. 4 kg of hydrogen occupies a volume of 45 m³ at ambient conditions. This volume is not practical for automobiles and requires the development of an efficient system for on-board hydrogen storage [5].

The most important methods to store hydrogen are: as a pressurized gas [7], a cryogenic liquid [8], an adsorbent to carbon nanotubes [9, 10], to water in clathrate hydrates [11, 12], to metal organic frameworks (MOFs) [13, 14], and in chemical form [15-17]. So far, all of these systems have their specific problems. Pressurising or liquefying hydrogen requires a significant fraction of the energy present in H₂ [5]. The tanks holding liquid H₂ cannot be totally isolated, because hydrogen needs to be able to escape to avoid pressure build-up [18]. Hydrogen losses due to boil-off can reach about 3% per day, which makes liquid hydrogen a less attractive choice for hydrogen storage [18]. Carbon nanotubes seemed very promising at first [9], but their room temperature storage capacity would appear to be too low at about 1 wt% [10]. At (close to) ambient conditions, the storage capacity presently achieved for clathrates [12] and MOFs [13] is also too low.

So far, the system that comes closest to meeting practical requirements is the NaAlH₄ system [16], in which hydrogen is stored in chemical form.

1.4 NaAlH₄

The theoretical reversible storage capacity of NaAlH₄ is about 5.5 wt%. Hydrogen is released in two steps. According to thermodynamics, the first step, in which Na₃AlH₆, Al, and H₂ are produced, proceeds at close to ambient conditions. The second step, in which Na₃AlH₆ reacts to NaH, Al, and H₂ proceeds at close to 110 °C. A key point is that the release and re-uptake of H₂ can be made reversible by adding a catalyst like Ti, as demonstrated in 1997 by Bogdanovic and Schwickardi [15]. In much of the subsequent

work aimed at improving the kinetics of the release and re-uptake of H_2 , Ti was in the form of $TiCl_3$ [19] or of colloid nanoparticles [20, 21]. However, other transition metals have also been tried. An intriguing observation is that traditional hydrogenation catalysts like Pd and Pt are poor catalysts for hydrogen release from $NaAlH_4$ [22], while early transition metals like Ti, Zr [22, 23], and Sc, and the actinides Ce, and Pr are good catalysts (the latter three being even better than Ti [24]). Another interesting observation is that adding different transition metals together may produce synergistic effects, as has been demonstrated for, for instance, Ti/Zr [23] and Ti/Fe [19].

Although much progress has been made at improving catalysed hydrogen release from and uptake in $NaAlH_4$, the kinetics of these processes is still too slow [16]. As a result, much recent work aimed at clarifying the role of the much used Ti catalyst has focused on determining the form in which it is present. So far, Ti has been found to be present in at least three different forms. First, Ti has been observed to be present in Al as a Ti-Al alloy of varying compositions [25-31]. Second, Ti was observed to be present as TiH_2 upon doping a mixture of NaH and Al with pure Ti and ball milling [32, 33], following a conjecture that TiH_2 [34] should be the active catalyst. Finally, there are experiments that suggest Ti to be present in $NaAlH_4$ itself [31, 35, 36]. Calculations employing periodic density functional theory (DFT) suggest substitution of Ti into the bulk lattice of $NaAlH_4$ to be energetically unfavorable if standard states of $NaAlH_4$, Na, Al, and Ti are used as reference states [37] or if reactant and product states appropriate for describing doping reactions are used as reference states [38]. However, periodic DFT calculations also find substitution of Ti into the $NaAlH_4$ lattice to be stabler at the surface than in the bulk [38, 39]. Cluster DFT calculations have shown that Ti prefers to exchange with a surface Na ion (this thesis), and that the resulting situation is energetically preferred over the case of two separate bulk phases of $NaAlH_4$ and Ti (this thesis). Furthermore, periodic DFT calculations likewise suggest that the initial reaction of $TiCl_3$ with $NaAlH_4$ can result in Ti substituting a Na surface ion [40]. Recent experimental observations give further support to the idea that Ti can be present in the surface of $NaAlH_4$ after doping with Ti [31].

The exact role of the much used Ti catalyst still remains elusive [16], although several ideas have been put forward. Isotope scrambling experiments provided evidence that exchange of gaseous D_2 with $NaAlH_4$ only occurred in the presence of Ti used as dopant [41]. This effect was attributed to the presence of a Ti-Al alloy [41], with support coming from DFT calculations that show that dissociation of H_2 on a surface of Al(001) with Ti alloyed into it can occur without barriers [42, 43], whereas high barriers are encountered on low index surfaces of pure Al. However, the experimentalists pointed out that the hydrogen exchange observed to take place under steady state conditions occurs much faster than the full decomposition reaction, suggesting that the key role of Ti should be to enhance mass transfer of the solid as rate limiting step [41]. Experiments employing anelastic spectroscopy have suggested that Ti enhances bulk diffusion of H_2 through the alanate [44-46], but this point is controversial [47]. Another idea that has been suggested is that Ti enables the formation of mobile AlH_3 which would then enable the fast mass transfer required in the solid state reactions releasing hydrogen [48, 49], and volatile molecular aluminium hydride molecules have been identified during hydrogen release from Ti/Sn doped $NaAlH_4$ using inelastic neutron scattering spectroscopy [50]. Recent work has suggested that an additional role of Ti [51] or the associated anion [52, 53] used in doping may be to improve the thermodynamics of the system. Perhaps most crucially, several experiments have shown that the release and uptake of H_2 are associated with massive mass transfer over long (micrometers) distances [19, 27, 54, 55]. The idea that the crucial role of Ti is to enable mass transfer over large distances is further supported by experiments showing that partial decomposition of undoped $NaAlH_4$ particles is possible if they are very small (nano-sized), the decomposition starting at a temperature as low as 40 °C [56].

Three basic mechanisms were proposed in which Ti would affect the long range mass transport of Al or Na required for de- and re-hydrogenation [48]. In the first mechanism, long-range diffusion of metal species through the alanates to the catalyst would occur as a first step. Gross *et al.* already proposed that this could involve the AlH_3 species. In the second mechanism, the driving force would be hydrogen desorption at the catalyst site, followed by long range transport of the metal species, the catalyst acting as a hydrogen

dissociation and recombination site and possibly also as a nucleation site. In the third mechanism proposed, the catalyst itself would migrate through the bulk. In this mechanism, “the starting phase is consumed and product phases are formed at the catalyst while it ‘eats’ its way through the material” [48].

1.5 My research goal

The goal of my research has been to determine, by computation, the different aspects of the role good catalysts play in hydrogen release from and uptake in NaAlH₄. One of the main ideas underlying my work is that the explanation of the role of the catalyst should be able to account for the key experimental observation that traditional hydrogenation catalysts like Pd and Pt [22] are poor catalysts for NaAlH₄, while early transition metals like Ti, Zr [22, 23], and Sc [24] are good catalysts for NaAlH₄.

My starting point is a model in which the Ti, Sc, Zr, Pd, Pt is adsorbed on the face of NaAlH₄ which has the lowest surface energy [the (001) face], the Ti, Sc, Zr, Pd, Pt being present in monoatomically dispersed form. Such a situation can arise from ballmilling, a technique that employs mechanical energy to achieve a fine dispersion of the catalyst, which has been in use in Ti-doping of NaAlH₄ since 1999 [23], or it can arise from the initial reaction of TiCl₃ with NaAlH₄ [40].

1.6 The outline of my thesis

After the introduction in this chapter, **chapter 2** outlines the different methods and approximations used during my thesis work. Then, in **chapters 3** and **4** the focus is on the interaction of Ti with NaAlH₄. Next, **chapter 5** concerns the interaction of TiH₂ with NaAlH₄, and **chapter 6** describes how Ti, Sc, Zr, Pd and Pt interact with NaAlH₄. Finally, **chapter 7** presents zero-point energy corrected enthalpies of dehydrogenation for Ca(AlH₄)₂, CaAlH₅ and CaH₂+6LiBH₄.

In **chapter 3**, the electronic structure and stability of NaAlH₄ clusters of different size and shape were studied, and based on these results a (NaAlH₄)₂₃ cluster was chosen as a model system for a nano-sized NaAlH₄ particle. Results are also presented on the interaction of monoatomically dispersed Ti atom with the (NaAlH₄)₂₃ cluster.

In **chapter 4**, the interaction of the NaAlH_4 cluster with two Ti atoms, either as a dimer or two separated Ti atoms, and adsorbed on the (001) surface of the cluster, was studied. The calculations on surface adsorption were supplemented with a large number of calculations where one or two Ti atoms had been either inserted into interstitial sites or exchanged with a surface Na or Al atom.

In **chapter 5**, the interaction of TiH_2 with the (001) face of NaAlH_4 was studied, again using the cluster model. The adsorption of the TiH_2 molecule on the surface was investigated. Also, the TiH_2 molecule or its Ti atom was moved inside the cluster either by exchanging the whole TiH_2 molecule with Na or Al, or by exchanging only the Ti atom with Na or Al and leaving the two hydrogen atoms on the surface together with the exchanged atom.

In **chapter 6**, the role of transition metal catalysts in promoting de- or rehydrogenation was investigated coming from another angle. Rather than only addressing the popular Ti catalyst, the following question was asked: why are Sc, Ti, and Zr good catalysts for promoting hydrogen release from and uptake in NaAlH_4 , while traditional hydrogenation catalysts, like Pd and Pt, are poor for NaAlH_4 ?

In **chapter 7**, DFT calculations were performed on the dehydrogenation reactions of $\text{Ca}(\text{AlH}_4)_2$, CaAlH_5 and $\text{CaH}_2+6\text{LiBH}_4$. The DFT model used was somewhat different from that employed in the calculations on NaAlH_4 . A periodic model was used of the hydrogen storage materials, using the plane wave DFT code VASP. Harmonic phonon densities of states (DOSs) were calculated by the direct method using the PHONON code.

1.7 Outlook

As known in science, while one answers questions more interesting ideas and questions appear that make the scientific research exciting and motivating. This thesis is not an exception to that rule. This section provides an outlook summarizing some of the new questions that have arisen during my research.

1.7.1 Ti + NaAlH₄

Using mono-atomically dispersed Ti adsorbed on the surface of NaAlH₄ as a reference system to study Ti + NaAlH₄, the research done on Ti + NaAlH₄ has shown that Ti preferably exchanges with a lattice Na atom near the surface. This particular reference system may be the most relevant when studying the role of Ti in dehydrogenation/hydrogenation reactions. However, this research opens other questions: what is the barrier for the Na exchange process compared to the barrier for exchange with Al and for absorption in a surface interstitial site?

1.7.2 Ti₂ + NaAlH₄

The results of Ti₂ + NaAlH₄ research imply that Ti is more stable in the subsurface region of the cluster than on the surface, and that exchange with Na is preferred. Almost equally stable is the exchange with one Na and one Al, as long as the resulting structure contains a direct Ti-Ti bond. The calculations also show that when considering adsorption on the surface only, Ti prefers to adsorb as atomic Ti rather than as a Ti₂. In this case the Ti atoms adsorb above Na sites, with the Na atoms being displaced towards the subsurface region. An interesting question not yet addressed in this thesis is whether the dissociation of Ti₂ on the surface has a barrier associated with it, and if so, how high that barrier is?

1.7.3 TiH₂ + NaAlH₄

After studying the adsorption of the TiH₂ molecule on the (001) surface of NaAlH₄ in different sites, the TiH₂ molecule or its Ti atom was moved inside the cluster either by exchanging the whole TiH₂ molecule with Na or Al, or by exchanging only the Ti atom with Na or Al and leaving the two hydrogen atoms on the surface together with the exchanged atom. In the case that the possible outcomes were restricted to adsorption, we found that TiH₂ adsorbs on the surface above a Na atom, bonding with 4 AlH₄ units and pushing the surface Na atom into the subsurface region. However, it was energetically preferred to exchange the whole TiH₂ unit with the subsurface displaced Na atom. All other exchanges were unstable compared to the situation where TiH₂ was adsorbed on the surface.

After determining the thermodynamic fate of the TiH_2 in NaAlH_4 , it is important to study the diffusion path of the $\text{TiH}_2 + \text{NaAlH}_4$ species. This will provide information about barriers for TiH_2 diffusion and exchange with Na. A question that could be addressed is whether TiH_2 has to dissociate at some point along the reaction path to reform at a later stage.

Relevant barrier heights can be computed by taking appropriate adsorption and absorption states as reactants and products, and locating the barrier between them using a suitable transition state searcher, such as the nudged elastic band (NEB) [57] method. Such calculations should be expensive but feasible.

1.7.4 (Ti, Zr, Sc, Pd, Pt) + NaAlH_4

I have also studied the interaction of Zr, Sc, Pd, and Pt with the (001) surface of NaAlH_4 after doing research on $\text{Ti} + \text{NaAlH}_4$. The importance of this study is to understand why Ti, Zr, and Sc are good catalysts for hydrogenation and dehydrogenation of NaAlH_4 while Pd and Pt are not. The results have shown that a key difference between Ti, Zr, and Sc on the one hand, and Pd and Pt on the other hand is that exchange of the early transition metal (TM) atoms with a surface Na ion, whereby Na is pushed on to the surface, is energetically preferred over surface absorption in an interstitial site, as found for Pd and Pt. The theoretical findings are consistent with a crucial feature of the TM catalyst being that it can be transported with the reaction boundary as it moves into the bulk, enabling the starting material to react away while the catalyst eats its way into the bulk, and effecting a phase separation between a Na-rich and a Al-rich phase. However, so far I have only looked at energy minima in my studies, and I have not computed barrier heights to see if the exchanges between the TM atoms and surface Na atoms are kinetically allowed. This is clearly the next step to be taken. In addition, it should be interesting to study H_2 desorption from the $\text{TM} + \text{NaAlH}_4$ clusters, to see whether H_2 desorption might become easier (occur with a lower barrier) upon exchange of the TM atom with a surface Na atom.

Based on my results I think there is one urgent experiment that has been done using Ti [41] that should be performed: The hydrogen–deuterium exchange experiment should be

repeated with both Pd and Pt as catalysts. The question is whether exchange still will take place. If this is indeed the case one would have firmly established that the dissociation of hydrogen is not an important part of the overall process with respect to the role the TMs play in improving the kinetics.

1.7.5 The hydrogenation process and dehydrogenation of Na_3AlH_6

Starting from totally dehydrogenated material ($\text{NaH} + \text{Al}_x\text{Ti}_{1-x}$) is important to understand the H_2 interaction with an Al surface with Ti atoms in it. By comparing the dissociation of H_2 on Al surface with H_2 on an $\text{Al}_x\text{Ti}_{1-x}$ surface, as has already been done computationally for specific surface coverage of Ti in Al [42, 43], we will get a complete picture about the role of Ti in the hydrogenation process. Besides that, the dissociation of H_2 on Al(Zr, Sc, Pd, Pt) surfaces becomes an important playing ground for comparing the role of the TM catalysts in the hydrogenation process.

My study has completely focused on dehydrogenation of doped NaAlH_4 . So far, few researches have tackled the dehydrogenation of Na_3AlH_6 . It would be interesting to investigate how Ti and other good TM catalysts interact with stable Na_3AlH_6 faces, in a manner similar to that used here. Also it should be interesting to investigate the role of the TM catalyst in rehydrogenation of $\text{NaH} + \text{Al}$. Earlier studies have already established that Ti in the surface of Al may help the dissociation of H_2 into atoms [42, 43]. An interesting question is whether the same would be true for Sc and Zr, but not for Pd and Pt. Another interesting question is whether TMs might also play additional roles in rehydrogenation (like e.g. improving mass transport to the reaction center).

1.8 References

- [1] M. S. Dresselhaus and I. L. Thomas, *Nature* 414, 332 (2001).
- [2] A. B. Stambouli and E. Traversa, *Renewable and Sustainable Energy Reviews* 6, 297 (2002).
- [3] R. M. Dell and D. A. J. Rand, *J. Power Sources* 100, 2 (2001).
- [4] H. A. Gasteiger, S. S. Kocha, B. Sompalli and F. T. Wagner, *Applied Catalysis B: Environmental* 56, 9 (2005).
- [5] L. Schlapbach and A. Züttel, *Nature* 414, 353 (2001).

- [6] B. C. H. Steele and A. Heinzl, *Nature* 414, 345 (2001).
- [7] R. S. Irani, *MRS Bull.* 27, 680 (2002).
- [8] J. Wolf, *MRS Bull.* 27, 684 (2002).
- [9] A. C. Dillon, KM Jones, T. A. Bekkedahl, C. H. Kiang, D. S. Bethune and M. J. Heben, *Nature* 386, 377 (1997).
- [10] A. Züttel and S. Orimo, *MRS Bull.* 27, 705 (2002).
- [11] W. L. Mao, H-k Mao, A. F. Goncharov, V. V. Struzhin, Q. Guo, J. Hu, J. Shu, R. J. Hemley, M. Somayazulu and Y. Zhao, *Science* 297, 2247 (2002).
- [12] L. J. Florusse, C. J. Peters, J. Schoonman, K. C. Hester, C. A. Koh, S. F. Dec, K. N. Marsh and E. D. Sloan, *Science* 306, 469 (2004).
- [13] N. L. Rosi, J. Eckert, M. Eddaoudi, D. T. Vodak, J. Kim, M. O'Keeffe and O. M. Yaghi, *Science* 300, 1127 (2003).
- [14] Z. Zhao, B. Xiao, A. J. Fletcher, K. M. Thomas, D. Bradshaw and M. J. Rosseinsky, *Science* 306, 1012 (2004).
- [15] B. Bogdanovic and M. Schwickardi, *J. Alloys Comp.* 253-254, 1 (1997).
- [16] F. Schüth, B. Bogdanovic and M. Felderhoff, *Chem. Comm.* 2249 (2004).
- [17] W. Grochala and P. P. Edwards, *Chem. Rev.* 104, 1283 (2004).
- [18] M. Conte, A. Iacobazzi, M. Ronchetti and R. Vellone, *J. Power Sources* 100, 171 (2001).
- [19] B. Bogdanovic, R. A. Brand, A. Marjanovic, M. Schwickardi, and J. Tölle, *J. Alloys Comp.* 302, 36 (2000).
- [20] B. Bogdanovic, M. Felderhoff, S. Kaskel, A. Pommerin, K. Schlichte and F. Schüth, *Adv. Mater.* 15, 1012 (2003).
- [21] M. Fichtner, O. Fuhr, O. Kircher and J. Rothe, *Nanotechnology* 14, 778 (2003).
- [22] D. L. Anton, *J. Alloys Comp.* 356-357, 400 (2003).
- [23] R. A. Zidan, S. Takara, A. G. Hee and C. M. Jensen, *J. Alloys Comp.* 285, 119 (1999).
- [24] B. Bogdanovic, M. Felderhoff, A. Pommerin, F. Schüth and N. Spielkamp, *Adv. Mater.* 18, 1198 (2006).
- [25] E. H. Majzoub and K. J. Gross, *J. Alloys Comp.* 356-357, 363 (2003).

- [26] C. Weidenthaler, A. Pommerin, M. Felderhoff, B. Bogdanovic and F. Schüth, *Phys. Chem. Chem. Phys.* 5, 5149 (2003).
- [27] M. Felderhoff, K. Klementiev, W. Grunert, B. Spliethoff, B. Tesche, J. M. Bellosta von Colbe, B. Bogdanovic, M. Hartel, A. Pommerin, F. Schuth and C. Weidenthaler, *Phys. Chem. Chem. Phys.* 6, 4369 (2004).
- [28] J. Graetz, J. J. Reilly, J. Johnson, A. Yu and T. A. Tyson, *Appl. Phys. Lett.* 85, 500 (2004).
- [29] A. G. Haiduc, H. A. Stil, M. A. Schwarz, P. Paulus and J. J. C. Geerlings, *J. Alloys Comp.* 393, 252 (2005).
- [30] A. Léon, O. Kircher, M. Fichtner, J. Rothe and D. Schild, *J. Phys. Chem. B* 110, 1192 (2006).
- [31] C. P. Baldé, H. A. Stil, A. M. J. van der Eerden, K. P. de Jong and J. H. Bitter, *J. Phys. Chem. C* 111, 2797 (2007).
- [32] X. D. Kang, P. Wang and H. M. Cheng, *J. Appl. Phys.* 100, 034914 (2006).
- [33] H. W. Brinks, M. Sullic, C. M. Jensen and B. C. Hauback, *J. Phys. Chem. B* 110, 2740 (2006).
- [34] V. P. Balema and L. Balema, *Phys. Chem. Chem. Phys.* 7, 1310 (2005).
- [35] D. Sun, T. Kiyobayashi, H. T. Takeshita, N. Kuriyama and C. M. Jensen, *J. Alloys Comp.* 1310, L8 (2002).
- [36] A. Léon, O. Kircher, H. Rösner, B. Décamps, E. Leroy, M. Fichtner and A. Percheron-Guégan, *J. Alloys Compd.* 414, 190 (2006).
- [37] O. M. Løvvik and S. M. Opalka, *Phys. Rev. B* 71, 054103 (2005).
- [38] O. M. Løvvik and S. M. Opalka, *Appl. Phys. Lett.* 88, 161917 (2006).
- [39] J. Íñiguez and T. Yildirim, *Appl. Phys. Lett.* 86, 103109 (2005).
- [40] T. Vegge, *Phys. Chem. Chem. Phys.* 8, 4853 (2006).
- [41] J. M. Bellosta von Colbe, W. Schmidt, M. Felderhoff, B. Bogdanovic and F. Schüth, *Angew. Chem. Int. Ed.* 45, 3663 (2006).
- [42] S. Chaudhuri and J. T. Muckerman, *J. Phys. Chem. B* 109, 6952 (2005).
- [43] S. Chaudhuri, J. Graetz, A. Ignatov, J. J. Reilly and J. T. Muckerman, *J. Am. Chem. Soc.* 128, 11404 (2006).

- [44] O. Palumbo, R. Cantelli, A. Paolone, C. M. Jensen and S. S. Shrinivan, *J. Phys. Chem. B* 109, 1168 (2005).
- [45] O. Palumbo, A. Paolone, R. Cantelli, C. M. Jensen and S. S. Shrinivan, *J. Phys. Chem. B* 110, 9105 (2006).
- [46] O. Palumbo, A. Paolone, R. Cantelli, C. M. Jensen and R. Ayabe, *Mater. Sci. Eng. A* 442, 75 (2006).
- [47] J. Voss, Q. Shi, H. S. Jacobsen, M. Zamponi, K. Lefman and T. Vegge, *J. Phys. Chem. B* 111, 3886 (2007).
- [48] K. J. Gross, S. Guthrie, S. Takara and G. Thomas, *J. Alloys Comp.* 297, 270 (2000).
- [49] R. T. Walters and J. H. Scogin, *J. Alloys Comp.* 379, 135 (2004).
- [50] Q. J. Fu, A. J. Ramirez-Cuesta and S. C. Tsang, *J. Phys. Chem. B* 110, 711 (2006).
- [51] G. Streukens, B. Bogdanovic, M. Felderhoff and F. Schüth, *Phys. Chem. Chem. Phys.* 8, 2889 (2006).
- [52] P. Wang, X. D. Kan and H. M. Cheng, *Chem. Phys. Chem.* 6, 2488 (2005).
- [53] L. C. Yin, P. Wang, X. D. Kang, C. H. Sun and H. M. Cheng, *Phys. Chem. Chem. Phys.* 9, 1499 (2007).
- [54] B. Bogdanovic, M. Felderhoff, M. Germann, M. Härtel, A. Pommerin, F. Schüth, C. Weidenthaler and B. Zibrowius, *J. Alloys Comp.* 350, 246 (2003).
- [55] G. J. Thomas, K. J. Gross, N. Y. C. Yang and C. Jensen, *J. Alloys Comp.* 330-332, 702 (2002).
- [56] C. P. Baldé, B. P. C. Hereijgers, J. H. Bitter and K. P. de Jong, *Angew. Chem. Int. Ed.* 45, 3501 (2006).
- [57] G. Henkelman, B. P. Uberuaga and H. Jónsson, *J. Chem. Phys.* 113, 9901 (2000).

Chapter 2

Methods and approximations

This chapter focuses on the theoretical methods employed in this thesis. In Section (2.1) the Born-Oppenheimer approximation is discussed. Section (2.2) gives a brief introduction to density functional theory (DFT). Section (2.3) deals with the geometry optimization method. In Section (2.4) the choice of a cluster model over a periodic model for representing the NaAlH₄ system is discussed.

2.1 The Born-Oppenheimer approximation: separating the nuclear and electronic motions

The Hamiltonian operator that describes both the nuclear and electronic motion is given by

$$\hat{H}_{tot}(q_\alpha, q_i) = \hat{K}_n(q_\alpha) + \hat{K}_e(q_i) + \hat{V}_{ee}(q_i) + \hat{V}_{ne}(q_\alpha, q_i) + \hat{V}_{nn}(q_\alpha). \quad (2.1)$$

In Eq. (2.1) $\hat{K}_n(q_\alpha)$ and $\hat{K}_e(q_i)$ are the kinetic energy operators associated with the nuclei and electrons, respectively; $\hat{V}_{nn}(q_\alpha)$ and $\hat{V}_{ee}(q_i)$ are the potential energy operators for the repulsions between the nuclei and the repulsions between the electrons, respectively; and $\hat{V}_{ne}(q_\alpha, q_i)$ is the potential energy operator describing the attractive energy between the nuclei and the electrons. Furthermore, q_α and q_i symbolize the nuclear and electronic coordinates, respectively.

The total energy of the system can be calculated from the Schrödinger equation

$$\hat{H}_{tot} \Psi(q_\alpha, q_i) = E_{tot} \Psi(q_\alpha, q_i), \quad (2.2)$$

where Ψ is the total wave function of the system.

The solution of Eq. (2.2) can be simplified with an approximation that in many cases is highly accurate. Based on the fact that the nuclei are much heavier than the electrons, the

electrons move much faster than the nuclei and to a good approximation the nuclei can be considered as fixed in describing the motion of the electrons. Equation (2.1) can be written as

$$\hat{H}_{tot} = \hat{H}_{el} + \hat{K}_n(q_\alpha), \quad (2.3)$$

where the electronic Hamiltonian is given by

$$\hat{H}_{el}(q_\alpha, q_i) = \hat{K}_e(q_i) + \hat{V}_{ee}(q_i) + \hat{V}_{ne}(q_\alpha, q_i) + \hat{V}_{nn}(q_\alpha). \quad (2.4)$$

The Schrödinger equation for the electronic motion is then

$$\hat{H}_{el}(q_\alpha, q_i) \Psi_{el}(q_i; q_\alpha) = U(q_\alpha) \Psi_{el}(q_i; q_\alpha). \quad (2.5)$$

The energy $U(q_\alpha)$ in Eq. (2.5) is the electronic energy including internuclear repulsion, and represents the potential energy surface (PES) that determines the motion of the nuclei (see below). The electronic wave function depends parametrically on the nuclear configuration:

$$\Psi_{el} = \Psi_{el,j}(q_i; q_\alpha), \quad (2.6)$$

where j labels the electronic state of the system.

Each time the electronic Schrödinger equation (2.5) is solved for a fixed set of nuclear coordinates, a “point” on the PES $U_j(q_\alpha)$ is provided. Whether calculated on the fly or represented through some fitting or interpolation scheme, this PES then determines how the positions of the nuclear coordinates will evolve through the time-dependent nuclear Schrödinger equation

$$i \frac{\partial \Psi_{nuc}(q_\alpha, t)}{\partial t} = \left(\hat{K}_n(q_\alpha) + U(q_\alpha) \right) \Psi_{nuc}(q_\alpha, t). \quad (2.7)$$

In Eq. 2.7 and throughout this chapter, atomic units have been used. The assumption that the electronic and nuclear motion can be separated, and that the nuclear dynamics takes place on a single PES representing a single electronic state, is known as the Born-Oppenheimer approximation [1]. Often it turns out that the dynamics of the nuclei can be

treated accurately through solving the classical equations of motion instead of the quantum mechanical equation in (2.7). However, in this thesis no dynamics of the nuclei is considered, the focus is on mapping out the most important and representative local minima on the PES.

2.2 Solving the electronic Schrödinger equation by Density Functional Theory

In 1964 Pierre Hohenberg and Walter Kohn proved that for a nondegenerate ground state system of N interacting electrons in an external potential, the ground state energy of the system is uniquely determined by a functional of the ground state electron density [2]. In solving the electronic structure problem within the Born-Oppenheimer approximation [Eqs. (2.4) and (2.5)] the nuclei provide the external field $[\hat{V}_{ne}(q_\alpha, q_i)]$. By using the Hohenberg-Kohn variational principle [2], Kohn and Sham [3] found that the many-electron problem [Eq. (2.5)] can be reformulated in a set of N single electron equations:

$$\left[-\frac{1}{2}\nabla^2 + v(q) + \int \frac{\rho(q')}{|q-q'|} dq' + v_{xc}(q) \right] \phi_i(q) = \epsilon_i \phi_i(q), \quad (2.8)$$

where q and q' in Eq. (2.8) are electron positions vectors; $\rho(q')$ is the electron density at q' ; $v(q)$ is the external potential, which is related to \hat{V}_{ne} in Eq. (2.1) through $V_{ne} = \int v(q)\rho(q)dr$; and v_{xc} is the exchange-correlation potential that is found from the functional derivative of the exchange-correlation energy $E_{xc}[\rho(q)]$ with respect to the electron density:

$$v_{xc}(q) = \frac{\delta E_{xc}[\rho(q)]}{\delta \rho(q)}. \quad (2.9)$$

The electron density $\rho(q)$ is given by

$$\rho(q) = \sum_i^N |\phi_i(q)|^2, \quad (2.10)$$

where $\phi_i(q)$ is the i^{th} one-electron Kohn-Sham wave function.

Equation (2.8) could be used to obtain the exact electronic ground state energy $U_0(q_\alpha)$, if the correct expression for the exchange-correlation energy functional $E_{xc}[\rho(q)]$ were known:

$$U_0(q_\alpha) = \sum_i^N \varepsilon_i - \frac{1}{2} \int \frac{\rho(q)\rho(q')}{|q-q'|} dqdq' + E_{xc}[\rho] - \int v_{xc}(q)\rho(q) dq + V_{nn}(q_\alpha), \quad (2.11)$$

where $V_{nn}(q_\alpha)$ is the nuclear-nuclear repulsion term described in Section 2.1.

The exact exchange-correlation functional described above has not yet been found, unfortunately, and only various approximations to it exist. One of these approximations is the local density approximation (LDA). This approximation employs the uniform electron gas formula for the exchange-correlation energy:

$$E_{xc}^{LDA}[\rho(q)] = \int \rho(q) \varepsilon_{xc}(\rho(q)) dq. \quad (2.12)$$

Here, $\varepsilon_{xc}(\rho(q))$ corresponds to the exchange-correlation energy per particle of a uniform electron gas of density $\rho(q)$.

The LDA gives good results for quantities like bond lengths and vibrational frequencies of molecules, despite the rather severe approximation of treating the electron density as locally uniform. However, in determining molecular binding and adsorption energies, the LDA approximation is known to fail [4, 5, 6].

For this purpose, a more successful approximation for functionals is based on the generalized gradient approximation (GGA), where the exchange-correlation energy is written as a functional of both the electron density and its gradient:

$$E_{xc}^{GGA}[\rho(q), \nabla\rho(q)] = \int f(\rho(q), \nabla\rho(q)) dq. \quad (2.13)$$

There are a number of different GGAs that give a considerable improvement over the LDA for energetics, such as the combination of the Becke correction [7] for the exchange energy and Perdew correction [8] for the correlation energy, or the gradient-corrected functional of Perdew *et al.* (PW91) [9].

In this thesis the binding energies of all the NaAlH_4 clusters have been calculated using DFT [10, 11] as implemented in the ADF code [12]. In each case, a geometry optimization is performed (see Section 2.3), starting from a suitably chosen initial geometry based on the bulk crystal structure. The exchange-correlation energy is approximated at the GGA level using the PW91 functional [9]. The basis set used is of a triple zeta plus one polarization function (TZP) type. A frozen core of 1s on Al as well as Na was chosen, together with 1s2s2p for Ti and Sc, 1s2s2p3s3p4s3d for Zr and Pd, and 1s2s2p3s3p4s3d4p5s4d for Pt. The general accuracy parameter of ADF [12] was set to 4.0 based on a series of convergence tests. In many of the calculations a non-zero electronic temperature was applied to overcome problems with the SCF convergence. However, it was ensured that the electronic ground state was reached by gradually cooling the electrons. The standard ADF fit sets (for the TZP basis sets) used to represent the deformation density were replaced by the fit sets corresponding to the quadruple zeta plus four polarization functions type basis sets. This was necessary since the standard fit sets were found to give inaccurate results. Results from tests showed that it was important to consider both spin restricted and unrestricted calculations. All calculations in this thesis have therefore been done both at the spin restricted and unrestricted levels. The spin unrestricted calculations were performed allowing one, two, three and four electrons to be unpaired. In the modeling of heavier transition metal catalysts (Zr, Pd, and Pt), scalar relativistic corrections were incorporated using the ZORA method [13].

In this thesis some periodic bulk calculations have been performed, those presented in Chapters 3 through 6 with ADF-BAND code [14] with the same basis and fit sets as used in the cluster calculations. The calculations presented in Chapter 7 were performed with the plane wave DFT code VASP [15].

2.3 Finding (local) minima on the potential energy surface

A geometry optimization method can be used to find minima on a PES $U_0(q_\alpha)$, with these minimum energy structures representing stable (global minima) or metastable (local but not global minima) structures in which the system is most likely to be found.

The method used is based on a local second order Taylor expansion [16, 17, 18] of the PES $U_0(q_\alpha^l)$ around a given current structure q_α^l ,

$$U_0(q_\alpha^{l+1}) - U_0(q_\alpha^l) = \frac{g^t \cdot \Delta q_\alpha^l + \frac{1}{2} (\Delta q_\alpha^l)^t \cdot H \cdot \Delta q_\alpha^l}{1 + (\Delta q_\alpha^l)^t \cdot S \cdot \Delta q_\alpha^l}. \quad (2.14)$$

Here $U_0(q_\alpha^{l+1})$ is the estimated PES value at the next position q_α^{l+1} , g^t the transpose of the gradient vector at q_α^l , $\Delta q_\alpha^l = q_\alpha^{l+1} - q_\alpha^l$, H the (approximate) Hessian (the second derivative matrix) at q_α^l , and S a matrix that allows for a scaling of the Hessian eigenvalues in order to follow all Hessian eigenvectors down-hill in energy towards a local minimum. Based on this Taylor expansion the best step along each eigenvector is determined to be

$$\Delta q_{\alpha,i}^l = -\frac{g_i}{\lambda_i - \gamma_i}, \quad (2.15)$$

where g_i is the component of the gradient along Hessian eigenvector i , λ_i the corresponding Hessian eigenvalue, and γ_i is chosen to satisfy

$$\lambda_i - \gamma_i = \frac{1}{2} \left(|\lambda_i| + \sqrt{\lambda_i^2 + 4g_i^2} \right). \quad (2.16)$$

This method represents an iterative scheme in searching for a local minimum: First, an initial structure is chosen, the gradient calculated and an estimate made for the Hessian. Then the Hessian is diagonalized and a step is taken along the eigenvectors according to Eqs. (2.15) and (2.16). Next, the gradient is calculated for the new geometry. If the largest component of the gradient and the previous step vector together with the change in energy are smaller than chosen thresholds, the geometry is considered to be converged. The ADF default values have been used: 0.01 Hartree/Å for the components of the gradient, 0.01 Å for the components of the step vector, and 0.001 Hartree for the energy change from one structure to the next, respectively. If the geometry is not considered converged, the new Hessian is calculated based on the initial estimate and an added finite difference term built from the new and old gradient together with the step vector, and a step is taken along its eigenvectors. This process is repeated until convergence is reached.

2.4 A cluster approach to modeling NaAlH₄

The interaction of an adsorbate with a metal substrate can be studied by modeling the substrate by a cluster with a limited number of substrate atoms [19, 20]. However, the interaction energy converges poorly with the size and shape of the cluster [19, 20]. This poor convergence behavior is associated with the metallic nature of the system. The problem can to a large degree be solved by using embedding techniques [21]. In modeling semiconductor materials, such as NaAlH₄, the interaction energy converges much better with respect to cluster size and shape. The main reason is that the electrons are more localized.

Most of the theoretical work on modeling Ti-doped NaAlH₄ has been using periodic calculations (see Chapter 1). These periodic calculations assume the system to be infinite, but from experiments it is known that the real NaAlH₄ particles are nanometer-sized [22]. This is one of the reasons why the choice was made to work with a 23 NaAlH₄ formula units ($Z=23$) semispherical cluster as a model for a nano-sized NaAlH₄ particle (see Chapter 3). The chosen cluster is about 2 nm large, which is small compared to a real NaAlH₄ particle (typical particle sizes after ball milling are 150-200 nm [22]). Nevertheless, the model cluster is structurally, electronically (density of states and band gap), and energetically (bonding energy per formula unit) close to bulk NaAlH₄ (Chapter 3). The cluster is chosen to have a large exposed (001) surface, because this has been shown to be the most stable surface of the different crystal faces [23]. In my opinion the cluster approach offers a number of advantages above the periodic approach. It is known that during dehydrogenation and hydrogenation large structural changes take place. Modeling this properly might require very large periodic unit cells, making the calculations extremely demanding. By limiting the size of the unit cell to make the calculations feasible, one might introduce artifacts by allowing structural rearrangements to interact with their periodic images, thereby not obtaining the correct energetics. Another point is that the real materials exhibit a range of surface facets, while a slab only has one. The edges and corners inherent in a cluster approach might therefore resemble the actual situation closer than when employing slabs. And, as already mentioned, the real NaAlH₄ particles are nano-sized, as is my model cluster. It has been shown that when

the alanate particles are (significantly) smaller than 100 nm, NaAlH_4 *without* Ti releases H_2 at even lower temperatures than in Ti-catalysed NaAlH_4 [24]. All this supports the view that a cluster model is worthwhile considering. Of course, I am fully aware that a cluster approach is not unproblematic, since the calculated properties might depend to some degree on both size and shape. However, since our common goal is to understand the role transition metals play in the dehydrogenation and hydrogenation of NaAlH_4 , I feel that all reasonable approaches should be explored. The cluster approach is certainly one of them, and one that could help provide important pieces of the puzzle.

2.5 References

- [1] M. Born and R. Oppenheimer, *Annalen der Physik*, 84 457 (1927).
- [2] P. Hohenberg and W. Kohn, *Phys. Rev.* 136 B864 (1964).
- [3] W. Kohn and L. J. Sham, *Phys. Rev. A* 140 1133 (1965).
- [4] J. A. White, D. M. Bird, M. C. Payne and I. Stich, *Phys. Rev. Lett.* 73 1404 (1994).
- [5] G. Wiesenekker, G. J. Kroes, E. J. Baerends and R. C. Mowrey, *J. Chem. Phys.* 102 3873 (1995).
- [6] B. Hammer, M. Scheffler, K. W. Jacobsen and J. K. Nørskov, *Phys. Rev. Lett.* 73 1400 (1994).
- [7] A. D. Becke, *Phys. Rev. A* 38 3098 (1988).
- [8] J. P. Perdew, *Phys. Rev. B* 33 8822 (1986).
- [9] J. P. Perdew, J. A. Chevary, S. H. Vosko, K. A. Jackson, M. R. Pederson, D. J. Singh and C. Fiolhais, *Phys. Rev. B* 46, 6671 (1992).
- [10] P. Hohenberg and W. Kohn, *Phys. Rev.* 136, B864 (1964).
- [11] W. Kohn and L. Sham, *J. Phys. Rev.* 140, A1133 (1965).
- [12] G. T. Velde, F. M. Bickelhaupt, E. J. Baerends, C. Fonseca Guerra, S. J. A. van Gisbergen, J. G. Snijders and T. Ziegler, *J. Comp. Chem.* 22, 931 (2001).
- [13] E. van Lenthe, E. J. Baerends and J. G. Snijders, *J. Chem. Phys.* 101, 9783 (1994).
- [14] G. T. Velde and E. J. Baerends, *Phys. Rev. B* 44, 7888 (1991).
- [15] G. Kresse and J. Furthmüller, *Phys. Rev. B* 54, 11169 (1996).
- [16] C. J. Cerjan and W. H. Miller, *J. Chem. Phys.* 75, 2800 (1981).
- [17] A. Banerjee, N. Adams, J. Simons and R. Shepard, *J. Phys. Chem.* 89, 52 (1985).

- [18] R. A. Olsen, G. J. Kroes, G. Henkelman, A. Arnaldsson and H. Jónsson, *J. Chem. phys.* 121 9776 (2004).
- [19] M. A. Nygren and P. E. M. Siegbahn, *J. Phys. Chem.* 96, 7579 (1992).
- [20] G. te Velde and E. J. Baerends, *Chemical Physics* 177 399 (1993).
- [21] J. L. Whittam and H. Yang, *Surf. Sci. Repts.* 24, 55 (1996).
- [22] H. W. Brinks, B. C. Hauback, S. S. Srinivasan and C. M. Jensen, *J. Phys. Chem. B* 109, 15780 (2005).
- [23] T. J. Frankcombe and O. M. Løvvik, *J. Phys. Chem. B* 110, 622 (2006).
- [24] C. P. Baldé, B. P. C. Hereijgers, J. H. Bitter and K. P. de Jong, *Angew. Chem. Int. Ed.* 45, 3501 (2006).

Chapter 3

A density functional theory study of Ti-doped NaAlH₄ clusters

This chapter is based on:

Marashdeh, A.; Olsen, R. A.; Løvvik, O. M.; Kroes, G.J.

Chem. Phys. Lett. 426, 180 (2006)

Density functional theory calculations have been performed on Ti-doped NaAlH₄ clusters. First the electronic structure and stability of undoped clusters of different size and shape were studied, and then one of these clusters was chosen as a model system for a nano-sized NaAlH₄ particle. A Ti atom added to the surface of this model preferably substituted a lattice Na near the surface, when using the NaAlH₄ cluster with Ti adsorbed as the reference system and keeping the substituted atoms within the model. This may be a first step towards a model explaining the role of Ti during dehydrogenation and hydrogenation.

3.1 Introduction

Non-catalyzed release of hydrogen from NaAlH₄ only occurs at high temperatures with slow kinetics [1], and the reverse reaction starting from the decomposed material hardly takes place at all [2]. However, in 1997 Bogdanovic and Schwickardi showed that the reaction can be made reversible at relatively low temperatures and pressures, and with greatly improved kinetics, by adding Ti to NaAlH₄ [3]. As a result, sodium alanate has become a possible candidate for a low cost and high density hydrogen storage material.

Among the large number of additives employed in improving the performance of the NaAlH₄ hydrogen storage system, Ti is currently believed to be one of the best catalysts for enhancing the reaction kinetics [4]. However, in spite of the intense research efforts to determine the location of Ti in the sodium alanate and the role it plays in improving the kinetics (see e.g. Refs. [5-17]), our understanding of the system is still rudimentary. From experimental studies we know that the final oxidation state of (most of) the titanium is zero [10, 12-13], independent of the initial oxidation state and of how Ti is added to the alanate. It is also known that a large part of the Ti is forming an intermetallic phase with Al. This is either identified as a

crystalline Al_3Ti alloy in the surface region [7, 8, 17] or as an amorphous Ti-Al phase of the form $\text{Al}_{1-y}\text{Ti}_y$, with y between 0.1 and 0.18 [11, 13, 14, 17]. The temperature during cycling determines which of these phases is obtained [8, 17]. The remaining Ti has been suggested to occupy bulk Na sites [5, 6, 9], or to be present as a TiH_x species [15, 16].

Several theoretical studies have sought to determine the location of Ti in the sodium alanate. Løvvik and Opalka studied Ti-doped NaAlH_4 using as reference bulk systems NaAlH_4 , Ti, Na, Al and gaseous H_2 , finding that Ti is unstable on the surface or when substituted into the lattice, with substitution of Al by Ti being the least unfavorable [18]. Íñiguez *et al.* found that Ti preferably substitutes lattice Na in the first layer [9, 19], and that such substitution is stable when using gas phase atomic elements as reference. Also in the study of Araújo *et al.* it was found that titanium prefers to occupy a Na site when using the gas phase atomic elements as reference [20]. However, when they used the cohesive energies of Al, Na, and Ti as the reference, their results were in agreement with those of Løvvik and Opalka. Løvvik and Opalka recently repeated their study using comparisons of the product side of various reaction equations involving all known and a number of hypothetical phases in the doped system [21]. This eliminated the necessity of an external reference system for studying the thermodynamic equilibrium of the system, and gave conclusions similar to their previous study.

The questions we seek to answer in this theoretical study are related to the ones addressed by many other studies: Where can Ti be located in NaAlH_4 ? Does it always stay on the surface or may it move subsurface or into the bulk? Would it occupy an interstitial position, or rather exchange positions with a Na or Al atom? However, our approach to the issue is different than that employed by others. We take as starting point a Ti atom absorbed on the surface of NaAlH_4 , define this as our reference system, and subsequently move the Ti atom to different places or exchange it with Na or Al atoms, asking the question whether any of the resulting structures are more stable than our starting structure. Although our starting point can easily be justified, using this as a reference system is not unproblematic. We will address this in detail and discuss the relevance of our chosen reference system with respect to those employed in other studies.

In this study we have chosen to model the sodium alanate using clusters, in contrast to most other studies where periodically repeated supercells are employed. The main advantage of the cluster approach is that we will (in future studies) be able to describe the dehydrogenation/hydrogenation cycling, including phase separation, without being hindered by the periodic boundary conditions. We also think that it will be fruitful to approach the NaAlH_4 hydrogen storage system from the nano-sized particle perspective, since it will provide us with a different (or complementary) view to the one offered from an infinite bulk/surface approach—after all, the real Ti-doped NaAlH_4 storage system consists of nano-sized particles [14]. Also, this gives us the possibility to keep the number of atoms constant during substitution, making it possible to directly compare total energies of various models. To the best of our knowledge, only one previous study has been based on a cluster approach, and there it was used to assist in the interpretation and assignment of the characteristic Raman bands of NaAlH_4 [22].

This Chapter is organized as follows. In Section 3.2 the computational method is described. This is followed by a presentation of our results and a discussion of them in Section 3.3, with the undoped clusters being addressed in Section 3.3.1, and the Ti-doped cluster in Section 3.3.2. Our conclusions are given in Section 3.4.

3.2 Method

Our ultimate goal is to describe the full dehydrogenation/hydrogenation cycling of NaAlH_4 , and in particular to determine the role of the Ti catalyst in improving the kinetics. This can best be accomplished through a cluster approach. Our calculations have been performed within a density functional theory (DFT) [23, 24] framework at the PW91 [25] generalized gradient approximation level, as implemented in the ADF code [26]. We have employed a triple zeta plus one polarization function (TZP) type basis set. A frozen core of 1s on Al as well as Na was chosen, together with 1s2s2p for Ti. A large set of tests was performed to ensure that the chosen basis set and frozen core approximation give results reasonably close to the basis set limit and all electron calculations. The general accuracy parameter of ADF [26] was set to 4.0 based on a series of convergence tests. In many of the calculations we applied a non-zero electronic temperature to avoid problems with the SCF convergence. However, we ensured that we eventually ended up in the electronic ground state by gradually

cooling the electrons. The standard ADF fit sets (for the TZP basis sets) used to represent the deformation density were replaced by the fit sets corresponding to the quadruple zeta plus four polarization functions type basis sets. This was necessary since the standard fit sets were found to give inaccurate results. Periodic bulk and slab reference calculations were performed using ADF-BAND [27] with the same basis and fit sets as used in the cluster calculations.

The clusters were built with large exposed (001) surfaces, because the (001) surface has been shown to be the most stable of the different crystal faces [28]. Next, the electronic structure and stability was examined both for bulk-terminated structures and after full geometric relaxations (Section 3.3.1). Based on these results we could choose an appropriate model cluster for studying Ti-doped NaAlH₄. Subsequently, the preferred adsorption/absorption site of Ti in the cluster was determined, after allowing for full structural relaxations, and using mono-atomically dispersed Ti adsorbed on the surface of NaAlH₄ as a reference (Section 3.3.2). In all geometry optimizations of both the bare clusters and the Ti-doped clusters, I use the standard ADF convergence criteria concerning the force, step length and the energy to locate the minimum.

3.3 Results and Discussion

3.3.1 Undoped NaAlH₄ clusters: Electronic structure and stability

A number of differently sized and shaped clusters were selected based on suitably chosen cuts from the bulk crystal. They are divided in two classes: (i) Tetragonal clusters with $Z = 1, 2, 4, 8, 12, 16, 20,$ and $42,$ respectively (Z denotes the number of NaAlH₄ formula units), and (ii) semispherical clusters with $Z = 23$ and $45,$ respectively. Some structurally optimized clusters are shown in Fig. 3.1, the starting bulk-cut structures can be inferred from them.

As already indicated in Section 3.2, we encountered difficulties with converging the single point calculations to the electronic ground state for clusters with bulk geometries. This problem was overcome by first applying a non-zero electronic

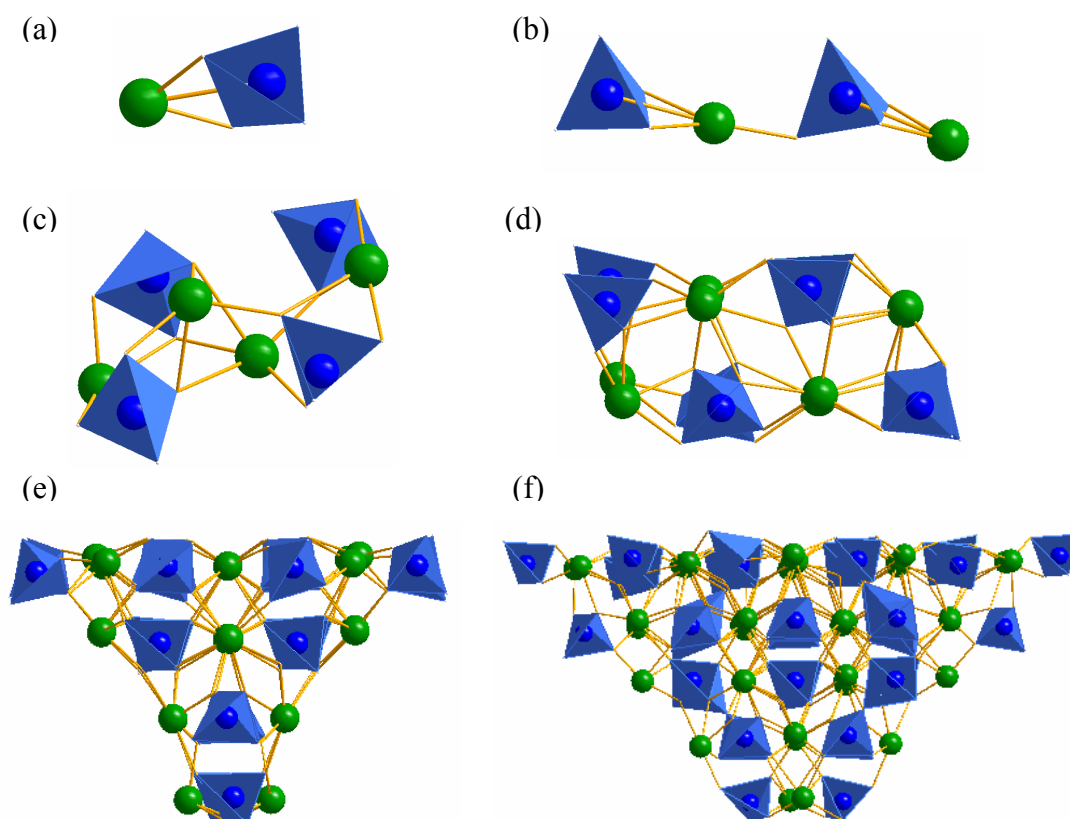


Fig. 3.1: Optimized NaAlH_4 clusters of different shape and size. Tetragonal clusters with $Z = 1$ (a), 2 (b), 4 (c), and 8 (d), respectively, and semispherical clusters with $Z = 23$ (e) and 45 (f), respectively, are displayed. Z denotes the number of NaAlH_4 formula units. Al atoms are represented by blue spheres, Na atoms by green spheres. Hydrogen atoms are located at the corners of the blue tetrahedra.

temperature, followed by subsequent cooling until the electronic ground state configuration was reached. The densities of states (DOSs) of two of the clusters are displayed in Figs. 3.2(a) and 3.2(b), and we see that there is no gap between the valence and conduction bands, i.e., the bulk-cut clusters are metallic. However, after allowing for full structural relaxation, a band gap [i.e., a HOMO-LUMO (highest occupied molecular orbital - lowest unoccupied molecular orbital) gap] opens up and we find quite good agreement between the electronic structure of the geometry optimized cluster and that from periodic surface and bulk calculations [Figs. 3.2(c) through 3.2(f)], although the band gaps are somewhat smaller for the clusters. A more detailed look at the electronic structure of the geometry optimized large clusters and that of the periodic surface and bulk NaAlH_4 reveals equally strong similarities between the partial densities of states associated with Na, Al, and H (results not shown). They all show mainly H 1s and Al 3s3p contributions to the valence band and

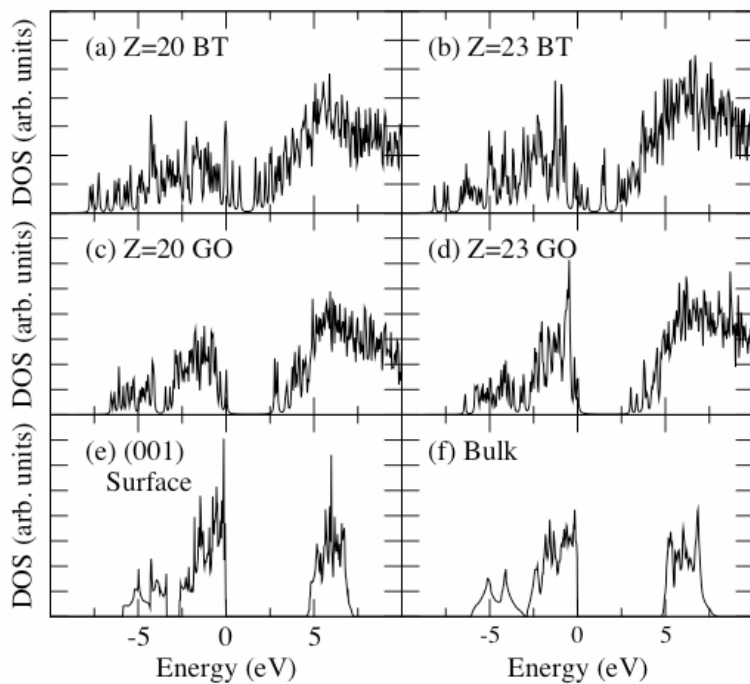


Fig. 3.2: The density of states (DOS) for bulk terminated (BT) (a, b) and geometry optimized (GO) (c, d) $Z = 20$ and 23 clusters, respectively, compared to that of the periodic (001) surface (e) and bulk (f) NaAlH_4 .

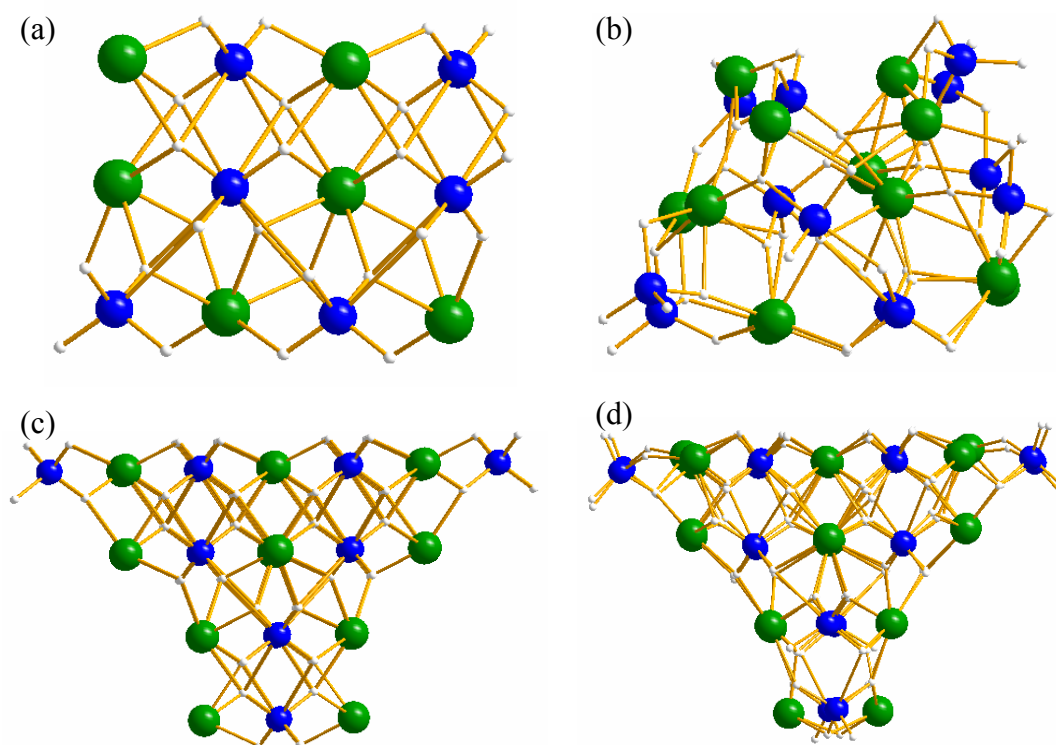


Fig. 3.3: Comparison of $Z = 12$ and 23 cluster structure before (a, c) and after geometry optimization (b, d), respectively. Al atoms are represented by blue spheres, Na atoms by green spheres, and H atoms by small white spheres.

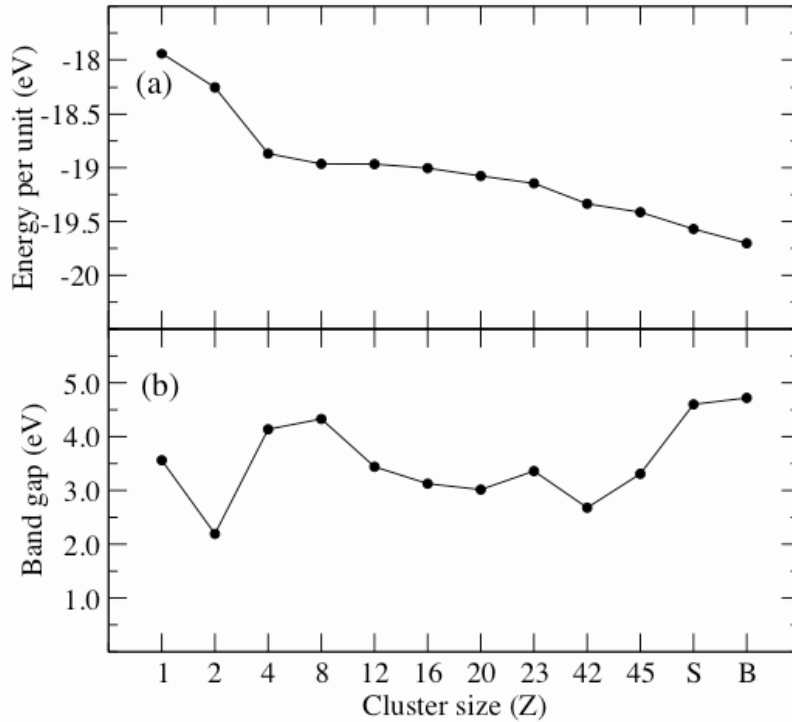


Fig. 3.4: The binding energy per formula unit (a) and band gap (b) of geometry optimized clusters is shown as a function of cluster size, also comparing to results for a slab of NaAlH_4 with exposed (001) surfaces (S) and for bulk NaAlH_4 (B).

mainly Na 3s3p and Al 3p character of the conduction band.

The structures of small clusters change considerably upon geometry optimization [Figs. 3.3(a) and 3.3(b)], while the structures of large clusters remain similar to that of the bulk cuts [Figs. 3.3(c) and (d)].

We have also considered how the binding energy per formula unit changes as a function of the cluster size. As Fig. 3.4(a) shows, with increasing size of the cluster there is a smooth convergence of binding energy per formula unit towards the slab and bulk values. While the band gap [Fig. 3.4(b)] shows some oscillatory behavior as a function of Z for low Z , its dependence on Z becomes smoother at large Z . That the values do not converge to the (001) surface slab and bulk band gap is to be expected since the clusters also have other exposed surfaces than the (001) surface (Figs. 3.1 and 3.3). The smaller values [compared to that of the (001) surface and bulk] found for the large clusters are consistent with the lower band gap found for slabs with exposed surfaces other than the (001) surface [28].

	Ti @ top	Ti @ Na	Ti @ Al	Ti @ inter12	Ti @ inter2
E_B (SR)	-446.03	-447.03	-445.92	-446.38	-446.50
E_{Rel} (SR)	0.00	-1.00	0.11	-0.35	-0.48
E_B (SU)	-446.07	-447.18	-445.92	-446.75	-446.86
E_{Rel} (SU)	0.00	-1.11	0.15	-0.68	-0.79

Table 3.1: The binding energy (E_B) and the energetic stability of the clusters relative to Ti @ top (E_{Rel}) are given both for spin restricted (SR) and spin unrestricted (SU) calculations. The labels used to refer to a given structure are defined in Fig. 3.5. All the energies are given in eV, and all results have been obtained from fully relaxed geometries.

In choosing an appropriate cluster model for a small NaAlH₄ particle, we are forced to make certain compromises. It is known from experiments that the typical particle size is 150-200 nm after ball milling [14]. A cluster of this size is out of reach for current Kohn-Sham DFT based codes, and unfortunately orbital-free DFT, which can be computationally much more efficient, so far fails to describe NaAlH₄ even qualitatively [29]. Furthermore, extensive geometry optimizations have to be performed in order to address the question of where the Ti resides in the sodium alanate during dehydrogenation/hydrogenation cycling. Thus a smaller cluster must be chosen. However, the chosen cluster should of course resemble the real particles both electronically and structurally. Based on these considerations and the results discussed above, we believe that the $Z = 23$ semispherical cluster represents an appropriate model system for a small NaAlH₄ particle, for modeling processes on the (001) face of the cluster.

3.3.2 Ti-doped NaAlH₄ clusters

We started with adsorbing a Ti atom on the surface on the C_2 symmetry axis of the $Z = 23$ cluster chosen in the previous section by allowing the structure to relax completely [Fig. 3.5(b)]. Next, different other positions on the surfaces of and inside the cluster were chosen together with a number of adsorption/absorption sites reached by permutation of the Ti atom and a lattice Na or Al. In all cases full structural relaxation was performed. Some of the most stable structures are shown in Fig. 3.5.

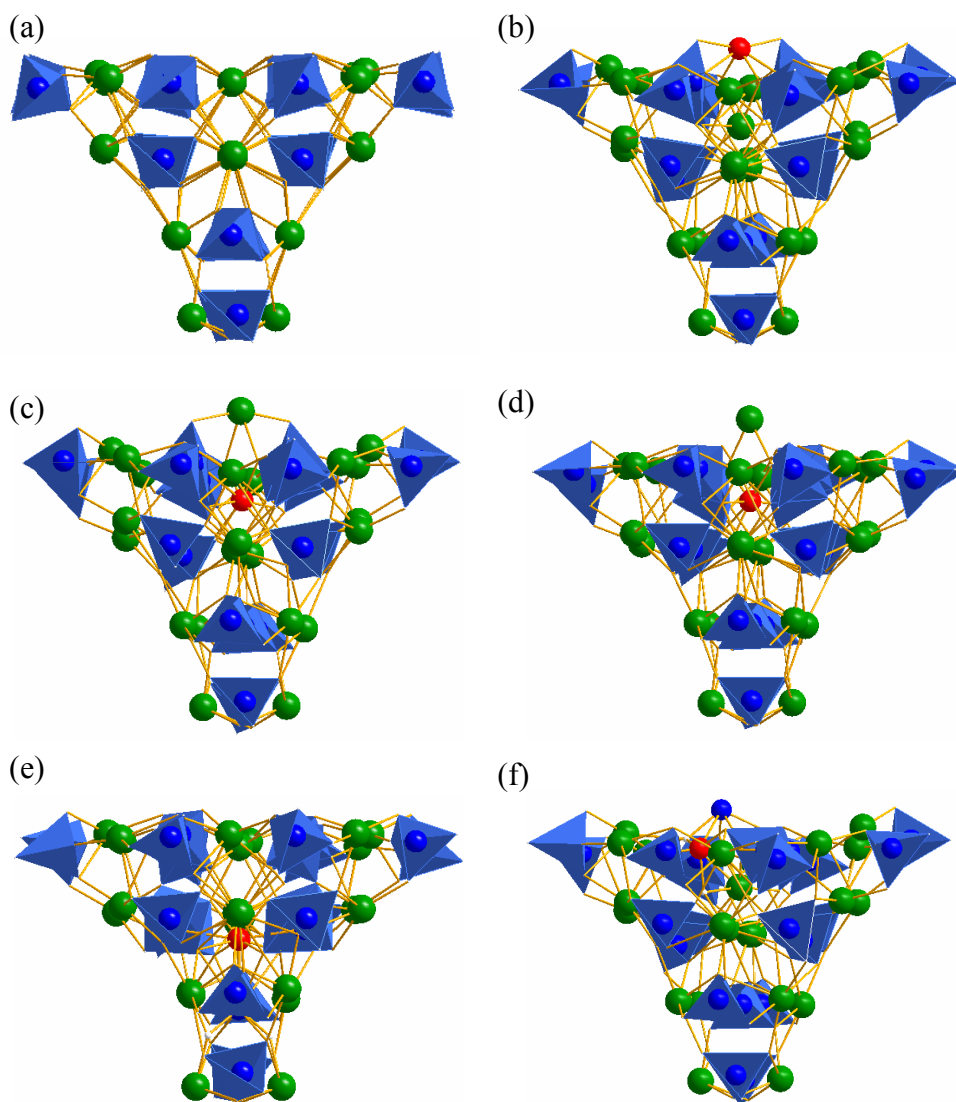


Fig. 3.5: The figure shows some of the $Z = 23$ model systems used to determine the relative stability of Ti-doped NaAlH_4 . (a) The undoped cluster, (b) Ti on the surface on the C_2 symmetry axis [Ti @ top], (c) Ti replaces a Na atom on the C_2 axis with Na in the original position of Ti [Ti @ Na], (d) Ti in interstitial site between first and second layer on the C_2 axis [Ti @ inter12], (e) Ti in interstitial site in second layer on the C_2 axis [Ti @ inter2], (f) Ti replaces an Al atom away from the C_2 axis with Al in the original position of Ti [Ti @ Al]. In all cases full structure relaxations have been performed. The labels in the brackets are used in Table 3.1 and in the text to refer to a specific structure. The Ti atom is represented as a red ball, while the other atoms are represented as in Fig. 3.1.

The binding energy of these clusters and their stability relative to our chosen reference are given in Table 3.1, both for spin restricted and unrestricted calculations. (In the spin restricted calculations the α - and β -spin orbitals are assumed to be

degenerate with equal occupations, whereas spin polarization can take place in the spin unrestricted calculations by allowing α - and β -spin orbitals and occupations to be different.)

The results in Table 3.1 clearly show the importance of doing the calculations spin unrestricted. By comparing the results for spin restricted and unrestricted calculations we see that the relative stability of the different configurations change by more than 0.3 eV. Similar effects are present in periodic surface and bulk calculations [21], and should be taken into account in future studies. In the following we will focus on the results obtained from spin unrestricted calculations.

According to the results in Table 3.1 Ti prefers to substitute a Na atom close to the surface [Fig. 3.5(c)]. It is less favorable to place Ti in an interstitial position in the second layer [Fig. 3.5(e)] or between the first and second layer [Fig. 3.5(d)]. Substitution of Al [Fig. 3.5(f)] is not stable compared to leaving the Ti on the surface [Fig. 3.5(b)]. This would probably be somewhat stabilized if substitution could take place subsurface [18], but such a site is unfortunately not available in this cluster. On the one hand, these results are in agreement with what was found in Refs. [9, 19, 20] when gas phase atomic elements were used as reference. Conversely, our conclusions disagree with those obtained when using bulk systems as reference, where Ti substitution of Al is favored above Na substitution [18, 20, 21] (this is mainly due to the about 2 eV larger cohesive energy of Al compared to Na). This, of course, immediately raises the question of which reference system is the most appropriate. In the following we will offer our view on this issue, but we would like to stress that there is still a lot of work to be done before it can be properly settled.

As mentioned above, experimental studies have shown that most of the Ti has a final oxidation state of zero [10, 12-13] and may be alloyed with Al [7, 8, 11, 13, 14, 17]. However, it is not yet known whether this constitutes the active phase of the catalyst. It is possible that a minor part of Ti is the active form of the catalyst, and that it might be present as mono-atomically dispersed Ti. If this is the case, the present reference system is indeed an appropriate starting point, and we can quite safely conclude that the catalytically active Ti prefers to go into the lattice rather than staying at the surface. However, the validity of our conclusions regarding the substitution with Al or

Na, or near-surface interstitial sites, must be treated with more care. As seen from Figs. 3.5(c), 3.5(d) and 3.5(f) the resulting structures leave rather exposed Na or Al atoms on the surface. These structures might represent possible physical transients during the hydrogenation/dehydrogenation cycling, and therefore will be relevant for understanding the role Ti plays as a catalyst in this system. But we are also aware that we are only modeling a small part of the total system and that the presence of other particles close to the exposed atoms might alter the conclusions reached here. To address this properly, one most likely will have to resort to multi-scale modeling.

The use of bulk systems as reference is appropriate when developing notions about the main thermodynamic driving forces in the Ti-doped sodium alanate. As noted, using this reference leads to different conclusions about the most preferred position of Ti than when using mono-atomically dispersed Ti on the surface of NaAlH_4 as reference. However, we think it is conceivable that both references should be considered together in order to develop a full understanding of the catalytic activity of Ti; bulk systems when long-term thermodynamic stability is in focus, and doped clusters when studying the dehydrogenation/hydrogenation kinetics. Much depends on whether Ti is present in mono-atomically dispersed form, and on the local availability of phases stabilizing one or the other adsorbed metal species.

We find it more difficult to provide support for using gas phase atomic elements as reference, since we have not been able to come up with physical scenarios with a large presence of gas phase atoms of Al, Na, H and Ti.

Finally, we note that in Chapter 6 a large set of initial geometries has been considered for Ti in the surface of NaAlH_4 . In this Chapter, an even more stable geometry was found for exchange of Ti with Na, but the study presented there leaves the main conclusion of this Chapter, that surface adsorbed Ti atoms prefer to exchange with surface Na ions, unchanged.

3.4 Conclusions

In order to determine the preferred position of Ti in NaAlH_4 we have performed density functional theory calculations at the generalized gradient approximation level on Ti-doped NaAlH_4 clusters. For this, we have first determined what constitutes a

good model cluster. We have found that large geometry optimized clusters (tetragonal cluster of 20 and 42 NaAlH₄ formula units, and semispherical clusters of 23 and 45 NaAlH₄ formula units) are energetically, electronically and structurally close to surface and bulk NaAlH₄, and therefore form good model systems for nano-sized NaAlH₄ particles. Choosing the semispherical cluster of 23 NaAlH₄ formula units as an appropriate model system, we then doped it with a Ti atom. Using this monoatomically dispersed Ti adsorbed on the surface of NaAlH₄ as a reference system, we found that Ti preferably substitutes a lattice Na near the surface. This particular reference system may be the most relevant when studying the role of Ti in dehydrogenation/hydrogenation reactions. However, there is clearly more effort needed to resolve open questions related to both this and approaches using other reference systems, which may ultimately require multi-scale modeling. Finally, we have found that it is important to perform the calculations spin unrestricted, and that this is something that needs to be checked carefully for periodic calculations as well.

3.5 References

- [1] T. N. Dymova, Y. M. Dergachev, V. A. Sokolov, N. A. Grechanaya, Dokl. Akad. Nauk SSSR 224, 591 (1975).
- [2] T. N. Dymova, N. G. Eliseeva, S. I. Bakum, Y. M. Dergachev, Dokl. Akad. Nauk SSSR 215, 1369 (1974).
- [3] B. Bogdanovic and M. Schwickardi, J. Alloys Compd. 253, 1 (1997).
- [4] D. L. Anton, J. Alloys Compd. 356–357, 400 (2003).
- [5] C. M. Jensen, R. Zidan, N. Mariels, A. Hee and C. Hagen, Int. J. Hydrogen Energy 24, 461 (1999).
- [6] D. Sun, T. Kiyobayashi, H. T. Takeshita, N. Kuriyama and C. M. Jensen, J. Alloys Compd. 337, L8 (2002).
- [7] E. H. Majzoub and K. J. Gross, J. Alloys Comp. 356-357, 363 (2003).
- [8] C. Weidenthaler, A. Pommerin, M. Felderhoff, B. Bogdanovic and F. Schüth, Phys. Chem. Chem. Phys. 5, 5149 (2003).
- [9] J. Íñiguez, T. Yildirim, T. J. Udovic, M. Sulic and C. M. Jensen, Phys. Rev. B 70, 060101(R) (2004).
- [10] J. Graetz, J. J. Reilly, J. Johnson, A. Y. Ignatov and T. A. Tyson, Appl. Phys. Lett. 85, 500 (2004).

- [11] H. W. Brinks, C. M. Jensen, S. S. Srinivasan, B. C. Hauback, D. Blanchard and K. Murphy, *J. Alloys Compd.* 376, 215 (2004).
- [12] A. Léon, O. Kircher, J. Rothe and M. Fichtner, *J. Phys. Chem. B* 108, 16372 (2004).
- [13] M. Felderhoff, K. Klementiev, W. Grünert, B. Spliethoff, B. Tesche, J. M. Bellosta von Colbe, B. Bogdanovic, M. Härtel, A. Pommerin, F. Schüth and C. Weidenthaler, *Phys. Chem. Chem. Phys.* 6, 4369 (2004).
- [14] H. W. Brinks, B. C. Hauback, S. S. Srinivasan and C. M. Jensen *J. Phys. Chem. B* 109, 15780 (2005).
- [15] V. P. Balema and L. Balema, *Phys. Chem. Chem. Phys.* 7, 1310 (2005).
- [16] P. Wang, X. D. Kang and H. M. Cheng, *J. Phys. Chem. B* 109, 20131 (2005).
- [17] A. G. Haiduc, H. A. Stil, M. A. Schwarz, P. Paulus and J. J. C. Geerlings, *J. Alloys Compd.* 393, 252 (2005).
- [18] O. M. Løvvik and S. M. Opalka, *Phys. Rev. B* 71, 054103 (2005).
- [19] J. Íñiguez and T. Yildirim, *Appl. Phys. Lett.* 86, 103109 (2005).
- [20] C. Moysés Araújo, R. Ahuja, J. M. Osorio Guillén and P. Jena, *Appl. Phys. Lett.* 86, 251913 (2005).
- [21] O. M. Løvvik and S. M. Opalka, *Appl. Phys. Lett.* 88, 161917 (2006).
- [22] D. J. Ross, M. D. Halls, A. G. Nazri and R. F. Aroca, *Chem. Phys. Lett.* 388, 430 (2004).
- [23] P. Hohenberg and W. Kohn, *Phys. Rev.* 136, B864 (1964).
- [24] W. Kohn and L. J. Sham, *Phys. Rev.* 140, A1133 (1965).
- [25] J. P. Perdew, J. A. Chevary, S. H. Vosko, K. A. Jackson, M. R. Pederson, D. J. Singh and C. Fiolhais, *Phys. Rev. B* 46, 6671 (1992).
- [26] G. te Velde, F. M. Bickelhaupt, E. J. Baerends, C. Fonseca Guerra, S. J. A. van Gisbergen, J. G. Snijders and T. Ziegler, *J. Comp. Chem.* 22, 931 (2001).
- [27] G. te Velde and E. J. Baerends, *Phys. Rev. B* 44, 7888 (1991).
- [28] T. J. Frankcombe and O. M. Løvvik, *J. Phys. Chem. B* 110, 622 (2006).
- [29] T. J. Frankcombe, G. J. Kroes, N. I. Choly and E. Kaxiras, *J. Phys. Chem. B* 109, 16554 (2005).

Chapter 4

NaAlH₄ clusters with two titanium atoms added

This chapter is based on:

Marashdeh, A.; Olsen, R. A.; Løvvik, O. M.; Kroes, G.J.

J. Phys. Chem. C, *111*, 8206 (2007)

We present density functional theory calculations on a NaAlH₄ cluster with two titanium atoms added. The two titanium atoms were adsorbed on the (001) surface of NaAlH₄ as a Ti dimer or as two separate atoms. Various absorption sites inside the cluster were investigated, either by placing the Ti atoms in interstitial sites or exchanging them with Na and Al atoms. The results imply that Ti is more stable in the subsurface region of the cluster than on the surface, and that exchange with Na is preferred. Almost equally stable is the exchange with one Na and one Al, as long as the resulting structure contains a direct Ti-Ti bond. The calculations also show that when considering adsorption on the surface only, Ti prefers to adsorb as atomic Ti rather than as a Ti₂. In this case the Ti atoms adsorb above Na sites, with the Na atoms being displaced towards the subsurface region. A zipper model is proposed for explaining the enhanced kinetics due to Ti.

4.1 Introduction

After the finding of Bogdanovic and Schwickardi that hydrogenation and dehydrogenation kinetics of NaAlH₄ are improved by adding small amounts of Ti, NaAlH₄ has become a promising candidate for a reversible hydrogen storage material [1]. Different transition metals have been added to compare their effect on the hydrogenation kinetics, and Ti was found to be one of the best [2]. After this finding, much effort has been directed at understanding the role of Ti in improving the reaction kinetics, mainly focusing on understanding the structure of Ti in NaAlH₄. Some studies have shown that Ti is present in a dispersed amorphous phase with metallic aluminum in the form of Al₃Ti [3-6]. Brinks *et al.* showed that an amorphous phase is formed after ball milling, while a solid solution (Al_{1-x}Ti_x) is formed after cycling [7, 8]. Haiduc *et al.* found that the form of the TiAl compound depends on the cycling temperature. Below 175°C an amorphous

phase is produced. This phase was correlated with the best kinetics, while slightly poorer kinetics was observed for an ordered intermetallic $\text{Al}_{1-x}\text{Ti}_x$ phase, which is formed above 200°C [9]. Baldé *et al.* suggested that about 70% of the Ti occupied interstitial spaces in the NaAlH_4 lattice after ball milling with TiCl_3 , with the remaining Ti present on the surface of Al. After desorption at different temperatures they found results very similar to those of Haiduc *et al.* [10]. Léon *et al.* showed after ball milling and during cycling that Ti is present primarily in the zero oxidation state [11]. Streukens *et al.* suggested that due to the generation of Al in the dehydrogenation process, the Ti state changes from a Ti-rich TiAl_3 state to a Ti-poor $\text{Al}_{1-x}\text{Ti}_x$ solid solution [12]. Ti hydride (TiH_2) has also been observed during NaAlH_4 reversible hydrogenation and shown to be catalytically active [3, 13, 14].

Palumbo *et al.* have found evidence from inelastic spectroscopy that Ti increases the mobility of hydrogen vacancies, but it is not clear from this study where the active form of Ti is located [15]. A computational study by Li *et al.* concluded that hydrogen vacancies may be promoted by Ti substituted in the lattice of NaAlH_4 [16]. Inelastic neutron scattering experiments have demonstrated the existence of volatile molecular aluminum hydrides, which are proposed to be shuttles of hydrogen during (re-)hydrogenation [17]. A recent combined DFT modeling and EXAFS study concluded that the role of Ti could be explained by the catalytic effect of Ti in solid solution $\text{Al}_{1-x}\text{Ti}_x$ on the dissociation of H_2 [18]. From hydrogen isotope scrambling experiments, it was suggested that part of the role of Ti is to catalyze the dissociation of hydrogen at the surface of the material *and* to facilitate the diffusion of hydrogen into the bulk of the material [19]. However, it was also suggested that the rate-limiting step in the (de-)hydrogenation process seemed to be mass transfer of the solid [19], which emphasizes the need to understand the role Ti plays in this process.

Since three different majority phases (TiAl_3 , $\text{Al}_{1-x}\text{Ti}_x$ solid solution and TiH_2) have been observed and the kinetics is comparable when either of these phases is present, it is reasonable to believe that a minority phase may be responsible for the kinetics enhancement. Some studies have suggested that a fractional amount of the Ti diffuses and

substitutes into the alanate lattice [14, 20] where it occupies bulk Na sites [21]. Theoretical studies of Ti-doped NaAlH₄ using a standard state reference system [22-24], or the product side of the reaction equations as the reference state [25], show that, in these conceptual frameworks, Ti on the surface or substituted into the lattice is unstable compared to Ti in Ti bulk, with substitution of Al by Ti being the least unfavorable. On the other hand substitution of lattice Na by Ti is found to be stable if gas phase atoms are used as the reference state [26-28]. In summary, Na-substitution is favored if the substituted metal is not allowed to aggregate, while Al-substitution is favored if the substituted metal is allowed to aggregate, due to the larger cohesive energy of Al and AlTi compounds.

Most of the theoretical work on modeling Ti-doped NaAlH₄ has been using periodic density functional theory (DFT) calculations. These periodic calculations assume the system to be infinite, but from experiments it is known that the real NaAlH₄ particles are nanometer-sized [8]. This was one of the reasons why we recently chose to work with a 23 NaAlH₄ formula units (Z=23) semispherically shaped cluster as a model for a nano-sized NaAlH₄ particle [29]. The chosen cluster is about 2 nm large, which is small compared to a real NaAlH₄ particle (typical particle sizes after ball milling are 150-200 nm [8]). Nevertheless, our model cluster was structurally, electronically (density of states and band gap), and energetically (bonding energy per formula unit) close to bulk NaAlH₄ [29]. The cluster was chosen to have a large exposed (001) surface, because this has been shown to be the most stable surface of the different crystal faces [24, 30]. We introduced a new reference system: a Ti atom adsorbed on the surface of the cluster, assuming that some of the Ti can be present in monoatomically dispersed form, and that this could constitute the active catalyst. Subsequently, the Ti atom was exchanged with Na or Al atoms or absorbed in interstitial sites, measuring the stability relative to the newly chosen reference system. We found that the Ti atom preferably exchanges with a subsurface Na atom, while the occupation of an interstitial site was also found to be favorable [29]. Note that in these calculations the Na or Al atom being exchanged was adsorbed on the surface, and not moved into the gas phase or the bulk.

The cluster approach offers a number of advantages above the periodic approach. It is known that during dehydrogenation and hydrogenation large structural changes take place. Modeling this properly might require very large periodic unit cells, making the calculations extremely demanding. By limiting the size of the unit cells to make the calculations feasible, one might introduce artifacts by allowing structural rearrangements to interact with their periodic images, thereby not obtaining the correct energetics. Another point is that the real materials exhibit a range of surface facets, while a slab only has one. The edges and corners inherent in a cluster approach might therefore resemble the actual situation more closely than when employing slabs. An argument already stated is that the real NaAlH₄ particles are nano-sized, as is our model cluster. It has recently been shown that when the alanate particles are (significantly) smaller than 100 nm, NaAlH₄ *without* Ti can release some of the incorporated H₂ at even lower temperatures than in Ti-catalysed NaAlH₄ [31]. All this supports the view that a cluster model can provide very useful information. Of course, the cluster approach is not unproblematic, since the calculated properties might depend on both size and shape. Also, model clusters are surrounded by vacuum, while other particles surround the large majority of real-world particles. Our view is that cluster and periodic calculations are complementary with strong points contained in both of them.

In the present work, we extend our previous study by adding to our $Z=23$ model cluster two titanium atoms. This has given us access to a large range of relevant Ti adsorption and absorption geometries that have not yet been studied theoretically, and has allowed us to look for cooperative effects of the Ti added. This may be regarded as the first step towards experimental conditions in which nanosized Ti clusters are present. We have determined the most stable adsorption and absorption geometries, focusing on the overall energetics, but also looking into the local structure and bonding around the Ti.

4.2 Method

The binding energy of all the clusters has been calculated using density functional theory (DFT) [32, 33] as implemented in the ADF code [34]. In each case, a geometry optimization is performed, starting from a suitably chosen initial geometry based on the

bulk crystal structure. The exchange-correlation energy is approximated at the generalized gradient approximation (GGA) level using the functional of Perdew *et al.* (PW91) [35]. The basis set used is of a triple zeta plus one polarization function (TZP) type. A frozen core of 1s on Al as well as Na was chosen, together with 1s2s2p for Ti. The general accuracy parameter of ADF [34] was set to 4.0 based on a series of convergence tests. In many of the calculations we applied a non-zero electronic temperature to overcome problems with the SCF convergence. However, we ensured that we eventually ended up in the electronic ground state by gradually cooling the electrons. The standard ADF fit sets (for the TZP basis sets) used to represent the deformation density were replaced by the fit sets corresponding to the quadruple zeta plus four polarization functions type basis sets. This was necessary since the standard fit sets were found to give inaccurate results. In our previous study we found that it was important to consider both spin restricted and unrestricted calculations [29]. All calculations in the present study have been done both at the spin restricted and unrestricted levels, and they confirm this conclusion. The spin unrestricted calculations were performed allowing one, two, three and four electrons to be unpaired. However, note that only the value for the energetically most stable state is reported in the tables (together with the corresponding number of unpaired electrons). Other computational details can be found in Ref. [29].

The ADF code calculates the total binding energy relative to spin restricted spherically symmetric atoms. The only purpose of this reference state, is to provide a reference energy common to all calculated energies. However, since we have some freedom in how to define our energy reference, we have chosen additional reference systems that have a physical meaning and allow for a straightforward comparison of the two Ti and one Ti systems. When considering two Ti atoms adsorbed/absorbed on/in the $Z=23$ model cluster our zero of energy has been set to that of the fully optimized bare $Z=23$ cluster plus two Ti atoms in Ti bulk. When considering one Ti atom adsorbed/absorbed on/in the $Z=23$ model cluster our zero of energy has been set to that of the fully optimized bare

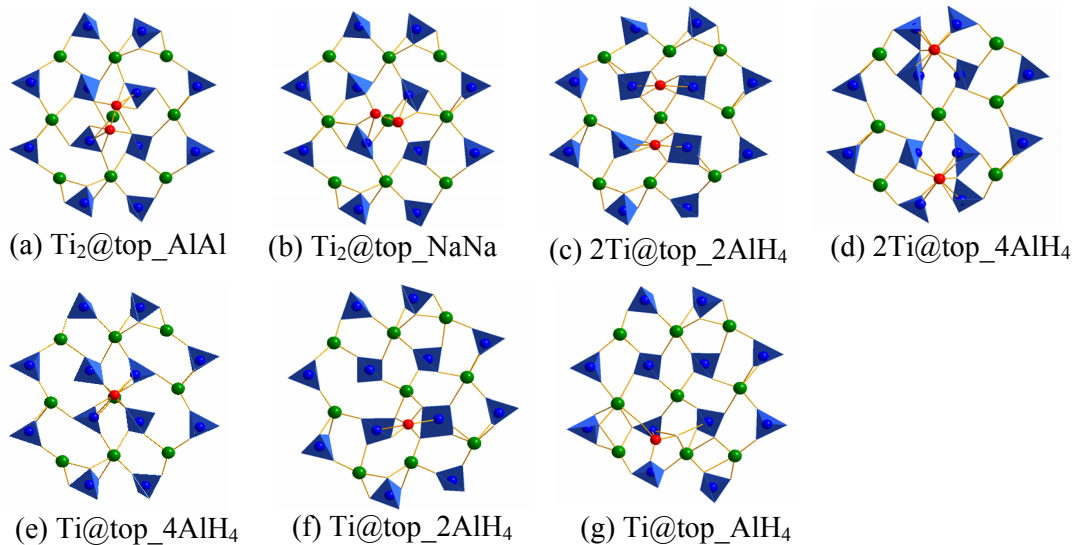


Fig. 4.1: (Results of geometry optimization.) The figure shows one and two titanium atoms adsorbed in different positions on the (001) surface of the $Z=23$ model cluster viewed from above. (a) A Ti dimer above (first layer) Na along the Al-Al direction [$\text{Ti}_2@top_AlAl$]. (b) A Ti dimer above (first layer) Na along the Na-Na direction [$\text{Ti}_2@top_NaNa$]. (c) Two Ti atoms separated, adsorbed between two AlH_4 units [$2\text{Ti}@top_2AlH_4$]. (d) Two Ti atoms separated, adsorbed above sodium atoms between four AlH_4 units [$2\text{Ti}@top_4AlH_4$]. (e) A single Ti atom adsorbed above (first layer) Na between four AlH_4 units [$\text{Ti}@top_4AlH_4$]. (f) A single Ti atom adsorbed between two AlH_4 units [$\text{Ti}@top_2AlH_4$]. (g) A single Ti atom adsorbed above an AlH_4 unit [$\text{Ti}@top_AlH_4$].

$Z=23$ cluster plus one Ti atom in Ti bulk. In this way the energies reported for the two and one Ti systems can be directly compared and represent the energy gained by taking one (two) Ti atom(s) out of Ti bulk and putting it (them) on/in the $Z=23$ cluster. Note that we have defined the adsorption/absorption energies in such a way that a negative number means that it is stable with respect to Ti in Ti bulk. Our periodic bulk Ti calculations have been performed using ADF-BAND [36] with the same basis and fit sets as used in the cluster calculations.

4.3 Results and Discussion

4.3.1 The adsorption of two titanium atoms on the surface of the $Z=23$ cluster

Two titanium atoms were adsorbed on the (001) surface of the $Z=23$ formula units NaAlH_4 cluster in different positions and orientations relative to each other. The

	2Ti@top_4AlH ₄	2Ti@top_2AlH ₄	Ti ₂ @top_AlAl	Ti ₂ @top_NaNa
E _{ads}	0.70	3.38	3.88	2.55
d _{Ti-Ti}	10.16	5.11	2.20	1.91
n	4	3	0	2

Table 4.1: The adsorption energies (E_{ads}) for the two titanium atoms adsorbed on the (001) surface of the $Z=23$ cluster are given. The energy reference used is discussed in Section 4.2. The notations used to refer to a given structure are defined in Fig. 4.1. All the energies are given in eV and all results have been obtained from fully relaxed geometries. The distance between the two Ti atoms is denoted $d_{\text{Ti-Ti}}$ and is given in Å. The number of unpaired electrons giving the lowest energy is denoted n .

adsorption energies of Ti on the relaxed clusters are listed in Table 4.1 and the surface geometries are displayed in Fig. 4.1. As a first step, a Ti dimer was adsorbed above a Na atom in the Al-Al direction [Ti₂@top_AlAl] and in the Na-Na direction [Ti₂@top_NaNa] as shown in Figs. 4.1a and 4.1b, respectively. Ti₂@top_NaNa has a shorter Ti₂ bond length (1.91 Å) than Ti₂@top_AlAl (2.20 Å) and is more stable by 1.33 eV.

The stability exhibited by the Ti₂@top_NaNa cluster might be partly attributed to its shorter Ti₂ bond length which is close to the Ti dimer bond length in the gas phase (1.93 Å). As a comparison, the energy penalty for stretching the Ti dimer bond from 1.93 Å to 2.20 Å in the gas phase is 0.45 eV. In the next step, the Ti dimer bond was broken and each Ti atom adsorbed separately between two AlH₄ units [2Ti@top_2AlH₄] or above sodium atoms between four AlH₄ units [2Ti@top_4AlH₄], as shown in Figs. 4.1c and 4.1d, respectively. As seen from the adsorption energies in Table 4.1, the 2Ti@top_2AlH₄ cluster is less stable than the Ti₂@top_NaNa cluster. This can be attributed to the loss of the Ti₂ bond: apparently, the separated titanium atoms do not compensate for this through their bonding to two AlH₄ units each. In the case of the 2Ti@top_4AlH₄ cluster, the Ti atoms have the chance to bond with four AlH₄ units each by pushing the Na atoms into the subsurface region, and thereby forming the most stable cluster (Fig. 4.1d).

The above results are in accordance with those obtained for a single Ti atom adsorbed on the surface of the $Z=23$ cluster, as can be seen from the following results (see also Ref.

	Ti@top_4AlH ₄	Ti@top_2AlH ₄	Ti@top_AlH ₄
E _{ads}	0.61	1.02	1.11
n	2	2	2

Table 4.2: The adsorption energies (E_{ads}) for one titanium atom adsorbed on the (001) surface of the $Z=23$ cluster are given. The energy reference used is discussed in Section 4.2. The notations used to refer to a given structure are defined in Fig. 4.1. All the energies are given in eV and all results have obtained from fully relaxed geometries. The number of unpaired electrons giving the lowest energy is denoted n.

[29] and Chapter 3). One Ti atom was adsorbed on the surface of the cluster above a Na atom between four AlH₄ units [Ti@top_4AlH₄], between two AlH₄ units [Ti@top_2AlH₄], and above one AlH₄ unit [Ti@top_AlH₄] as shown in Figs. 4.1e, 4.1f and 4.1g, respectively. The adsorption energies of Ti in the relaxed geometries are given in Table 4.2 indicating that Ti@top_4AlH₄ is the most stable one. In Ti@top_4AlH₄, the Ti atom pushes a Na atom into the subsurface region, thereby forming high coordination bonding with the AlH₄ units. All these results point to the same tendency: the surface Na atoms are displaced into the subsurface region, facilitating Ti adsorption above a Na surface atom.

Before continuing, we need to address the issue of possible cluster-edge effects for the two Ti systems, especially for 2Ti@top_4AlH₄. As can be seen in Fig. 4.1d the two Ti atoms are rather close to the cluster-edge as compared to the case where only one Ti atom is adsorbed on the middle of the (001) face of the cluster (Fig. 4.1e). One should note that atoms and complexes at the edge are missing some Na-H bonds, and may thus interact differently with Ti near the edge. From Table 4.2 we can calculate twice the adsorption energy of one Ti atom [Ti@top_4AlH₄] ($2 \times 0.61 \text{ eV} = 1.22 \text{ eV}$) and the adsorption energy of two Ti atoms [2Ti@top_4AlH₄] (0.70 eV) can be taken from Table 4.1. The energy difference between them is 0.52 eV, which can be mainly attributed to an edge effect. However, the edge effect is significantly smaller than the energy difference between the dissociated Ti dimer [2Ti@top_4AlH₄] and the intact Ti dimer [Ti₂@top_NaNa], which is 1.85 eV (Table 4.1). Thus, we can safely conclude that it is

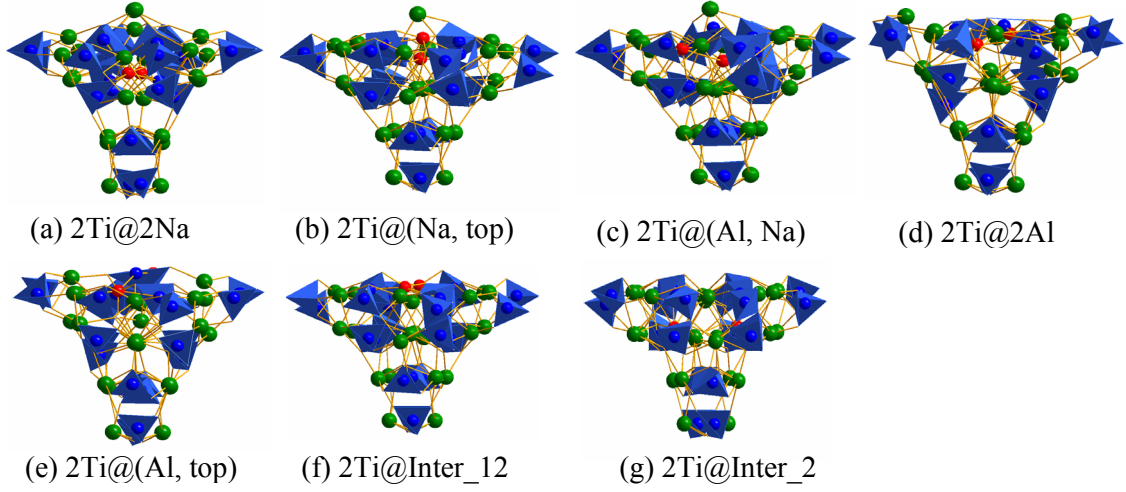


Fig. 4.2: (Results of geometry optimization.) Two titanium atoms adsorbed in different positions on or in the Z=23 cluster. (a) Two Ti atoms exchange with two Na atoms [2Ti@2Na]. (b) The first Ti atom exchanges with a Na atom and the second remains on the surface [2Ti@(Na, top)]. (c) The first Ti atom exchanges with a Na atom and the second exchanges with an Al atom [2Ti@(Al, Na)]. (d) Two Ti atoms exchanges with two Al atoms [2Ti@2Al]. (e) The first Ti atom exchanges with an Al atom and the second remains on the surface [2Ti@(Al, top)]. (f) Two Ti atoms absorb in interstitial sites between the first and the second layer [2Ti@Inter_12]. (g) Two titanium atoms are placed in interstitial sites in the second layer [2Ti@Inter_2].

	E_{abs}	CN	$d_{\text{Ti-Ti}}$	n
2Ti@2Na	-0.71	22	4.47	2
2Ti@(Na, top)	0.35	15	2.46	2
2Ti@(Al, Na)	-0.52	21	2.81	2
2Ti@2Al	0.21	16	4.90	4
2Ti@(Al, top)	2.50	14	4.89	2
2Ti@Inter_2	1.72	22	7.38	2
2Ti@Inter_12	4.10	14	5.77	2

Table 4.3: The absorption energies (E_{abs}) are given for the two Ti system. The energy reference used is discussed in Section 2. The notations used to refer to a given structure are defined in Fig. 4.2. All the energies are given in eV, and all results have been obtained from fully relaxed geometries. The number of atoms within the distance of 3 Å for the Ti atoms is denoted CN. The distance between the two Ti atoms is denoted $d_{\text{Ti-Ti}}$ and is given in Å. The number of unpaired electrons giving the lowest energy is denoted n.

energetically preferred for the Ti dimer to dissociate on the surface of NaAlH₄. Note, however, that this conclusion relates to the overall thermodynamics and not to the kinetics. It might be that there is a kinetic barrier for dissociation of Ti₂ on the surface of NaAlH₄, but we have not yet investigated this.

4.3.2 The stability of the two titanium doped NaAlH₄ clusters

The 2Ti@top_2AlH₄ cluster (Fig. 4.1c) described in the previous section was used as a starting point for putting the Ti atoms into interstitial sites, and for exchanging one or two Ti atoms with one or two Na, or Al, or with one Na and one Al. Full structural relaxation was performed for all clusters and the most stable structures are displayed in Fig. 4.2. We also investigated whether the absorption energy computed for the exchange of Ti with Na and Al could be further decreased by displacing the adsorbed atom (Na, Al) along the surface. The most favourable absorption energies are given in Table 4.3.

4.3.2.1 Ti exchanging with Na

According to the results in Table 4.3, the two Ti atoms prefer to exchange with the two Na atoms that have been displaced into the subsurface region, 2Ti@2Na (Fig. 4.2a). The number of Na, Al and H atoms within the range of 3 Å around the Ti atoms is 22, as indicated in Table 4.3 as the coordination number (CN). The local structure around the Ti atoms can be described as that of a Ti₂Al₆H₁₂ complex, possibly indicating the very first step in the formation of a (TiAl₃)₂ alloy. We also see that this structure is considerably more stable than 2Ti@(Na, top), which is formed by replacing one Ti atom with a subsurface displaced Na atom while the second Ti atom remains on the surface of the cluster (Fig. 4.2b).

An important question is whether the contribution of the second Ti atom to the stability of the cluster is the same as the first one. This can be answered by comparing the absorption energy of one and two Ti atoms in the cluster relative to bulk, as done in Table 4. It is seen that the absorption energy of one Ti atom exchanging with a Na atom [Ti@Na] is -0.50 eV, and the absorption energy of two Ti atoms exchanging with two Na atoms [2Ti@2Na] is -0.71 eV. The energy difference between them (-0.21 eV) is the second Ti atom's contribution to the stability of the cluster, which is considerably less

than that of the first Ti atom (-0.50 eV). If we assume the subsurface Ti to be the active catalyst, this might explain why the effect of adding Ti is limited to a certain concentration range with respect to its catalytic activity: As the concentration of Ti increases, the stability of NaAlH₄ containing subsurface Ti decreases, until it reaches a point where the Ti does not mix well with sodium alanate, and the subsequently added Ti goes to another (majority) phase, which does not lead to additional speed-up of the kinetics [37, 38].

4.3.2.2 Ti exchanging with Na and Al

By exchanging two Ti atoms with a subsurface displaced Na and a surface Al atom (Fig. 4.2c) a cluster [2Ti@(Al, Na)] is formed which is similar in its stability to the most stable 2Ti@2Na cluster. The energy difference is small (0.2 eV). As shown in Table 4.3, this exchange results in the two Ti atoms being in their closest position inside the cluster, forming a 2.81 Å bond. The coordination number is 21 and a Ti₂Al₅H₁₀ complex is formed which is similar to the one formed in the 2Ti@2Na cluster. This explains the similar stability of these two clusters.

4.3.2.3 Ti exchanging with Al

Exchange of the two Ti atoms with two surface Al atoms [2Ti@2Al] (Fig. 4.2d) is more stable than the exchange of one Al atom and leaving the second Ti atom on the surface [2Ti@(Al, top)] (Fig. 4.2e) or leaving the two Ti atoms on the surface [2Ti@top_4AlH₄] (Fig. 4.1d). But still these exchanges are less favourable than the exchanges of two subsurface displaced Na atoms or the exchanges with a subsurface displaced Na and a surface Al. A single Ti atom adsorbed on the surface of the cluster was found to be more stable than the Ti@Al exchanged cluster by about 0.1 eV [29]. A similar finding does not apply to the 2Ti@2Al system. From Tables 4.1 and 4.3 we see that the 2Ti@2Al system is about 0.5 eV more stable than leaving the two Ti atoms on the surface. The reason is that the two Al atoms stabilize each other on the surface by forming a 2.88 Å long bond and clustering with the exchanged Ti atoms.

4.3.2.4 Ti in interstitial sites

The two Ti atoms are placed in interstitial positions between the first and the second layer [2Ti@Inter_12] (Fig. 4.2f) and in the second layer [2Ti@Inter_2] (Fig. 4.2g), respectively. From Table 4.3 we see that the structure with two Ti atoms in the second layer is more stable than when they are inserted between the first and second layer. Actually, when the Ti atoms are placed between the first and the second layer the Ti atoms move to a final position in the surface of the cluster (Fig. 4.2f). This position is less stable than that of 2Ti@top_2AlH₄ (Fig. 4.1c) by 0.7 eV (see Tables 4.1 and 4.3). And even if the second interstitial structure [2Ti@Inter_2] is considerably more stable than the first [2Ti@Inter_12], it is still less stable than the most stable structure with both Ti atoms on the surface [2Ti@top_4AlH₄]. The latter is favored by about 1 eV if the numbers are compared directly, but also when the estimated edge-effect of 0.5 eV is subtracted there is a clear preference for leaving the Ti atoms on the surface. This is in contrast to the case where one single Ti atom was placed in an interstitial position and found to be comparable in stability to the Ti@Na exchange [29]. Having Ti atoms close together in interstitial positions is clearly unfavorable, even if the distance between them is in the range 5.8 - 7.4 Å.

4.3.3 Is Ti found on the surface or inside the cluster?

Combining the results described in Sections 4.3.1 and 4.3.2 we can address the question whether Ti prefers to stay on the surface of the cluster or prefers to move inside. This important question can be answered by comparing the most stable cluster for Ti adsorption on the surface of the cluster, 2Ti@top_4AlH₄, with the most stable clusters where Ti can be found inside the cluster, 2Ti@2Na and 2Ti@(Al, Na). From Tables 4.1 and 4.3 we see that Ti is more stable inside the cluster by 1.41 and 1.22 eV, respectively. Thus, our cluster model clearly indicates that Ti prefers to move into the subsurface region of NaAlH₄. Similar conclusions are reached when performing periodic calculations for the *exchange* reactions, supporting the results from our cluster model [39]. Note that in these calculations the Na or Al atom being exchanged is adsorbed on the surface, and not moved into the gas phase or the bulk [see also comments below].

	Ti@Na	2Ti@2Na
E_{abs}	-0.50	-0.71
n	2	2

Table 4.4: The absorption energy (E_{abs}) is given for one and two titanium atoms exchanging one and two Na atoms, Ti@Na and 2Ti@2Na, respectively. The energy reference used is discussed in Section 2. All the energies are given in eV, and all results have been obtained from fully relaxed geometries. The number of unpaired electrons giving the lowest energy is denoted n.

Note that there is no evidence from our results that Ti would move further into the lattice, and that periodic calculations imply that bulk substitution is substantially less stable than surface or subsurface substitution [22, 25]. We thus expect that the subsurface site is the most stable option for Ti in the NaAlH₄ lattice.

4.3.4 Does Ti prefer to be inside the NaAlH₄ cluster or in Ti bulk?

The preference for Ti to be in the subsurface region of the cluster or in Ti bulk can be determined for systems with one and two Ti atoms added from Tables 4.3 and 4.4.

One Ti atom is more stable inside the cluster than in Ti bulk by 0.5 eV, two Ti atoms are more stable in the cluster than two Ti atoms in bulk by 0.71 eV. Thus, when present in the form of two atoms, Ti clearly prefers to be inside the cluster than to be in Ti bulk. This is in strong contrast to the results of periodic supercell calculations where a clear preference for Ti bulk has been found [22-25]. The reason is quite obvious: The slab calculations removed the *substituted* atoms and put them in their corresponding bulk state when Ti was added, so that the cohesive energies of bulk Na, Al, etc. entered the stability calculations [22, 24, 25, 28]. Al has a higher cohesive energy than Na, and this will therefore tend to favor Al substitution. In our case the *exchanged* atom(s) is(are) placed on the surface of the cluster and the difference in cohesive energies do not play a role in the relative stabilities. Which answer is correct depends on e.g. whether Al-bulk particles are present in the vicinity of the exchanged Al atom.

The only energy being comparable to published slab studies is that of Ti being placed interstitially, since then the composition of the cluster and slab is similar. Interstitially

absorbed Ti in the second layer was found to be unstable by 2.07 eV relative to Ti bulk for the slab model [22], while for the cluster model it is stable by 0.18 eV. However, the slab model contains $Z=16$ formula units, and the cluster model $Z=23$ formula units, which means that the numbers still are not directly comparable. Perhaps most importantly, when using periodic supercell calculations the possibilities for structural rearrangements to accommodate the extra atom are much more limited than when using a cluster model. Due to the limited size of the supercells, self-interaction between the periodic images of the Ti-containing complexes may also be expected in that case. At the moment it is hard to say which approach, periodic or cluster, is better. It is known from experiments that the typical particle size is 150-200 nm after ball milling [8], although experiments have also been done on particles smaller than 100 nm [31]. On the one hand, our $Z=23$ cluster model is considerably smaller, but on the other hand, the periodic calculations assume infinite particle size and impose geometric constraints on NaAlH_4 by modeling this material as a slab. Also, the slabs only exhibit one surface termination, while clusters may have several different terminations simultaneously, in addition to edges and corners.

4.3.5 Density of electronic states of Ti doped clusters

The density of electronic states have been calculated and they are displayed for the $2\text{Ti}@2\text{Na}$ system in Fig. 4.3a, for the $\text{Ti}@\text{Na}$ system in Fig. 4.3b, and for the bare $Z=23$ cluster in Fig. 4.3c.

The bare cluster has a band gap [i.e., a HOMO-LUMO (highest occupied molecular orbital-lowest unoccupied molecular orbital) gap] of 3.0 eV, as seen from the total density of state (TDOS) plot in Fig. 4.3c. Figure 4.3c also shows the partial densities of states (PDOS) associated with Al, Na and H of the bare cluster. They show mainly H $1s$ and Al $3s3p$ contributions to the valence band and mainly Na $3s3p$ and Al $3p$ character of the conduction band. Figures 4.3a and 4.3b show the TDOS, and the PDOS associated with Ti, Al, Na and H, of doubly Ti doped [$2\text{Ti}@2\text{Na}$] and singly Ti doped [$\text{Ti}@\text{Na}$] clusters, respectively. By comparing the TDOS and the PDOS of the bare cluster with the doped clusters, we see that Ti introduces states in the band gap, forming a metallic-

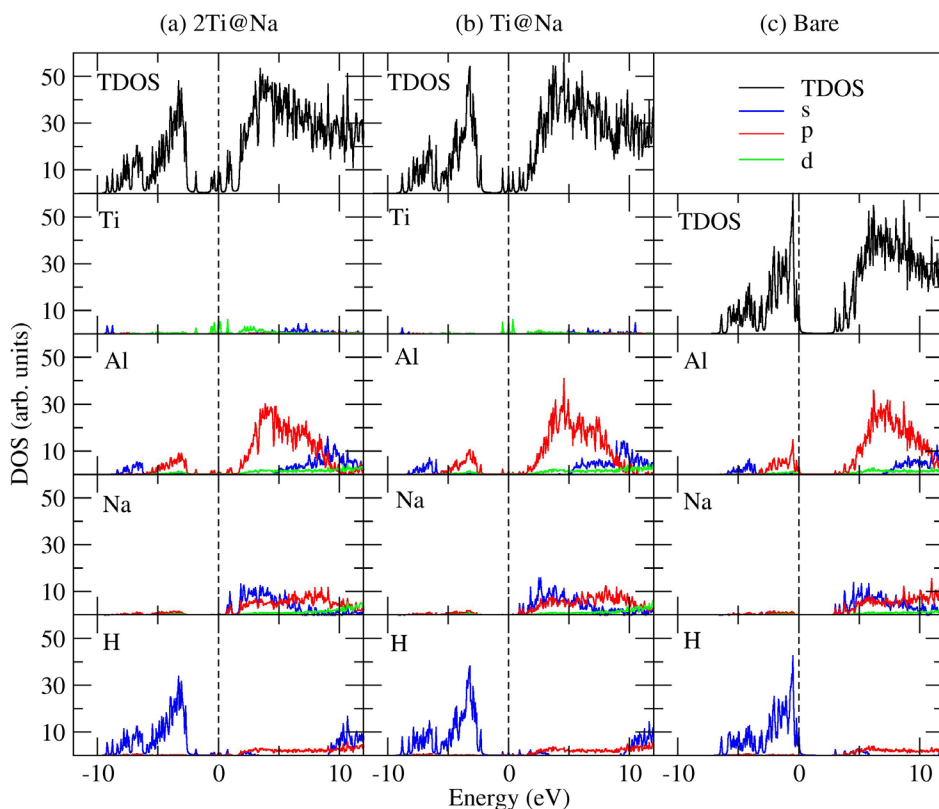


Fig. 4.3: The total density of states (TDOS) and partial densities of states associated with Ti, Na, Al, and H of the (a) $2\text{Ti}@2\text{Na}$, (b) $\text{Ti}@2\text{Na}$ and (c) bare clusters, respectively. The partial and total densities of states have been shifted so that the HOMO is at the zero of the energy scale (indicated with a dashed line).

like cluster. The difference between the singly Ti and the doubly Ti doped clusters is that in the doubly Ti doped system there are more states introduced in the band gap. One should note that the Ti $3d$ orbitals does not only introduce new states in the band gap, but it also mixes into both valence and conduction bands, as can be seen from the PDOS plots of Ti in Figs. 4.3a and 4.3b.

To unravel some more detail in the bonding of Ti to NaAlH_4 , we have plotted the overlap population density of states (OPDOS) in Figs. 4.4 and 4.5, for most of the clusters depicted in Figs. 4.1 and 4.2. Figure 4.4 shows the OPDOS between all Ti orbitals and all Na orbitals, and Fig. 4.5 shows the OPDOS between all Ti orbitals and all Al and H orbitals. From Fig. 4.4 it is clear that there is very little direct interaction between Ti and

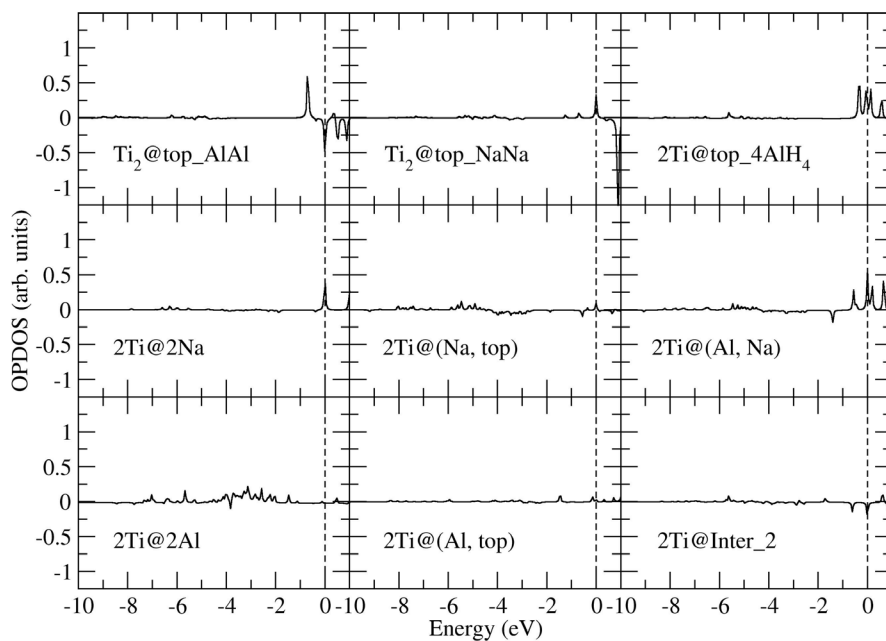


Fig. 4.4: The overlap partial densities of states (OPDOS) of the Ti with the Na. The notations used to label the different panels are defined in Figs. 4.1 and 4.2. The OPDOSs have been shifted so that the HOMO is at the zero of the energy scale (indicated with a dashed line).

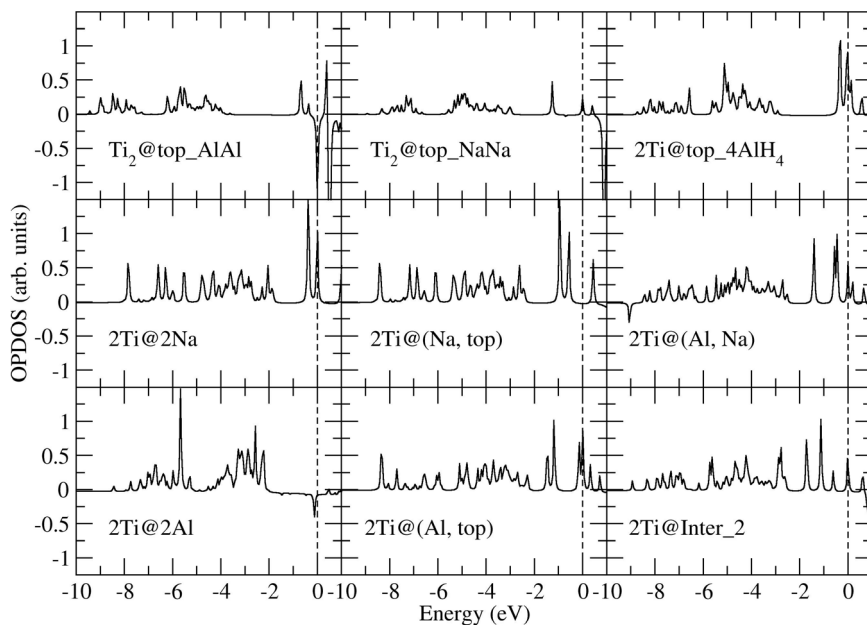


Fig. 4.5: The overlap partial densities of states (OPDOS) of the Ti with the AlH₄. The notations used to label the different panels are defined in Figs. 4.1 and 4.2. The OPDOSs have been shifted so that the HOMO is at the zero of the energy scale (indicated with a dashed line).

Na, and then only in the HOMO region. From Fig. 4.5 we see that the Ti orbitals have a positive overlap with the Al and H orbitals throughout the valence band, and that the Al and H orbitals also mix favorably into the Ti band gap states. Thus, the Ti interaction with Al and H is bonding at and below the HOMO.

4.3.6 A proposed model for the role of Ti

It is clear from the discussion above that exchange of Ti with subsurface Na atoms is preferred, or with a combination of Na and Al atoms when a direct bond between the Ti atoms can be established. These exchanged structures exhibit surfaces which most likely are very reactive (see also below). It is conceivable that the reactive species (Na, Al, H) left behind will be removed due to interactions with other subspecies, eventually leading to the removal of the whole top layer. The result of such a reaction could be that Ti again resides on the surface of the nanoparticle, and will then try to move into the subsurface of the nanoparticle once more.

This constitutes what we introduce as the zipper-model. In this model, Ti works as a novel kind of catalyst in NaAlH_4 by acting as a slider, eating itself into the nano-particle as it reacts away – effectively unzipping the structure. In this way, the fully hydrogenated alanate would be decomposed, and at the same time fresh surfaces would be exposed along the path of the zipper. Note that the most reactive of all structures is the one with Ti on the surface. The first reaction according to our zipper model is that Ti moves into the subsurface region of the structure replacing Na. In our model we assume that the Na left on the surface can easily react with other species present. The reason for claiming this is that they are exposed under-coordinated atoms.

Is this model consistent with previous studies on the Ti-enhanced sodium alanate? It is easy to envision that Ti could both work as the zipper slide and at the same time also as a traditional (de-)hydrogenation catalyst. This could explain why catalysts that usually are better hydrogenation catalysts than Ti (like Pd) do not work very well in NaAlH_4 [2]: they may be able to split hydrogen molecules, but they lack the mobility and tendency of Ti to move into the alanate lattice (see also Chapter 6). The zipper model could also be consistent with the studies observing defects in Ti-enhanced sodium alanate [15, 16] –

since defects have been shown to promote Ti substitution in the alanate lattice by several modeling studies [16, 24, 28, 40], defects could further facilitate the primary steps of the zipper model. Also, it is easy to imagine that formation of alanes could result from a zipper mechanism – this could happen in parallel to reaction of the adsorbed Na atoms on the surface.

There is one possible problem with the zipper model: the hypothesized monodispersed Ti has so far not been observed by any experimental study. The majority of Ti that has been observed seems to be in a zero-valent state, surrounded primarily by Al [41]. This could be explained by the experimental techniques not being sufficiently sensitive to find the minority phase proposed in this study. It could also be that these minority phases, being metastable of nature, only exist off equilibrium, that is during the hydrogenation and dehydrogenation process. Even so, it should be checked if subsurface exchange of Ti still is feasible when it is present together with Al. Work on this question is in progress. All in all, it seems that the zipper model may be a crucial part of the complicated role of Ti in the sodium alanate system. To the best of our knowledge we are the first to propose such a model.

4.4 Conclusions

We have performed density functional theory calculations at the generalized gradient approximation level for a NaAlH₄ cluster with two Ti atoms, either as a dimer or two separated Ti atoms, adsorbed on the (001) surface of the cluster. These calculations have been followed by a large number of calculations where one or two Ti atoms have been inserted into interstitial sites or exchanged with Na or Al. The results support the following conclusions: (i) Starting from the case that a Ti dimer is adsorbed on the surface, it is energetically preferred for the Ti dimer to dissociate on the surface of the cluster. The most stable adsorption position for the resulting atomic Ti is above first layer Na surface atoms. The surface Na atoms are found to be displaced into the subsurface region of the cluster upon Ti adsorption, allowing the Ti to interact with 4 AlH₄ units. (Note that we have not yet investigated whether there is a barrier to dissociation of the Ti dimer; so far we have only considered the initial and final stable geometries). (ii) After

dissociation the two Ti atoms prefer to move inside the cluster to the subsurface region. When the two Ti atoms move inside the cluster, exchange with two subsurface displaced Na atoms is preferred, and overall this represents the energetically most favorable case. Almost equally stable is the exchange with one subsurface displaced Na and one surface Al, provided the two Ti atoms end up close enough to each other to form a direct bond. In both cases small local TiAl clusters are formed. Absorbing two Ti atoms in interstitial sites close to each other (5.8 – 7.4 Å) is clearly unfavorable. The thermodynamically most stable situation is for Ti atoms to move into Na positions far away from each other. A zipper model is proposed, in which the mechanism by which the added Ti promotes H₂ release is explained by the Ti atom working itself down into the alanate particle, effectively unzipping the structure.

4.5 References

- [1] B. Bogdanovic, M. Schwickardi, *J. Alloys Compd.* 253, 1 (1997).
- [2] Anton, D. L. *J. Alloys Compd.* 356–357, 400 (2003).
- [3] V. P. Balema, L. Balema, *Phys. Chem. Chem. Phys.* 7, 1310 (2005).
- [4] J. Graetz, J. J. Reilly, J. Johnson, A. Y. Ignatov, T. A. Tyson, *Appl. Phys. Lett.* 85, 500 (2004).
- [5] C. Weidenthaler, A. Pommerin, M. Felderhoff, B. Bogdanovic, F. Schüth, *Phys. Chem. Chem. Phys.* 5, 5149 (2003).
- [6] E. H. Majzoub, K. J. Gross, *J. Alloys Compd.* 356–357, 363 (2003).
- [7] H. W. Brinks, C. M. Jensen, S. S. Srinivasan, B. C. Hauback, D. Blanchard, K. Murphy, *J. Alloys Compd.* 376, 215 (2004).
- [8] H. W. Brinks, B. C. Hauback, S. S. Srinivasan, C. M. Jensen, *J. Phys. Chem. B* 109, 15780 (2005).
- [9] A. G. Haiduc, H. A. Stil, M. A. Schwarz, P. Paulus, J. J. C. Geerlings, *J. Alloys Compd.* 393, 252 (2005).
- [10] C. P. Baldé, H. A. Stil, A. M. J. van der Eerden, K. P. de Jong, J. H. Bitter, *J. Phys. Chem. C* 111, 2797 (2007).
- [11] A. Léon, O. Kircher, J. Rothe, M. Fichtner, *J. Phys. Chem. B* 108, 16372 (2004).

- [12] G. Streukens, B. Bogdanovic, M. Felderhoff, F. Schüth, *Phys. Chem. Chem. Phys.* 8, 2889 (2006).
- [13] P. Wang, X. D. Kang, H. M. Cheng, *J. Phys. Chem. B* 109, 20131 (2005).
- [14] K. J. Gross, E. H. Majzoub, S. W. Spangler, *J. Alloys Compd.* 356–357, 423 (2003).
- [15] O. Palumbo, A. Paolone, R. Cantelli, C. M. Jensen, M. Sulic, *J. Phys. Chem. B* 110, 9105 (2006).
- [16] S. Li, P. Jena, *Phys. Rev. B* 73, 214107 (2006).
- [17] Q. J. Fu, A. J. Ramirez-Cuesta, S. C. Tsang, *J. Phys. Chem. B* 110, 711 (2006).
- [18] C. Santanu, G. Jason, I. Alex, J. R. James, T. M. James, *JACS* 128, 11404 (2006).
- [19] J. M. Bellosta von Colbe, W. Schmidt, M. Felderhoff, B. Bogdanovic, F. Schüth, *Angew. Chem. Int. Ed.* 45, 3663 (2006).
- [20] C. M. Jensen, R. Zidan, N. Mariels, A. Hee, C. Hagen, *Int. J. Hydrogen Energy* 24, 461 (1999).
- [21] D. Sun, T. Kiyobayashi, H. T. Takeshita, N. Kuriyama, C. M. Jensen, *J. Alloys Compd.* 337, L8 (2002).
- [22] O. M. Løvvik, S. M. Opalka, *Phys. Rev. B* 71, 054103 (2005).
- [23] E.-K. Lee, Y. W. Cho, J. K. Yoon, *J. Alloys Compd.* 416, 245 (2006).
- [24] T. Vegge, *Phys. Chem. Chem. Phys.* 8, 4853 (2006).
- [25] O. M. Løvvik, S. M. Opalka, *Appl. Phys. Lett.* 88, 161917 (2006).
- [26] J. Íñiguez, T. Yildirim, T. J. Udovic, M. Sulic, C. M. Jensen, *Phys. Rev. B* 70, 060101(R) (2004).
- [27] J. Íñiguez, T. Yildirim, *Appl. Phys. Lett.* 86, 103109 (2005).
- [28] C. M. Araújo, R. Ahuja, J. M. O. Guillén, P. Jena, *Appl. Phys. Lett.* 86, 251913 (2005).
- [29] A. Marashdeh, R. A. Olsen, O. M. Løvvik, G. J. Kroes, *Chem. Phys. Lett.* 426, 180 (2006).
- [30] T. J. Frankcombe, O. M. Løvvik, *J. Phys. Chem. B* 110, 622 (2006).
- [31] C. P. Baldé, B. P. C. Hereijgers, J. H. Bitter, K. P. de Jong, *Angew. Chem. Int. Ed.* 45, 3501 (2006).
- [32] P. Hohenberg, W. Kohn, *Phys. Rev.* 136, B864 (1964).
- [33] W. Kohn, L. J. Sham, *Phys. Rev.* 140, A1133 (1965).

- [34] G. T. Velde, F. M. Bickelhaupt, E. J. Baerends, C. Fonseca Guerra, S. J. A. van Gisbergen, J. G. Snijders, T. Ziegler, *J. Comp. Chem.* **22**, 931 (2001).
- [35] J. P. Perdew, J. A. Chevary, S. H. Vosko, K. A. Jackson, M. R. Pederson, D. J. Singh, C. Fiolhais, *Phys. Rev. B* **46**, 6671 (1992).
- [36] G. T. Velde, E. J. Baerends, *Phys. Rev. B* **44**, 7888 (1991).
- [37] B. Bogdanovic, G. Sandrock, *MRS Bull.* **27**, 712 (2002).
- [38] F. Schüth, B. Bogdanovic, M. Felderhoff, *Chem. Commun.* 2249 (2004).
- [39] A. Marashdeh, R. A. Olsen, O. M. Løvvik, G. J. Kroes, in preparation.
- [40] O. M. Løvvik, *J. Alloys Compd.* **373**, 28 (2004).
- [41] A. Léon, O. Kircher, M. Fichtner, J. Rothe, D. Schild, *J. Phys. Chem. B* **110**, 1192 (2006).

Chapter 5

A density functional theory study of the TiH_2 interaction with a NaAlH_4 cluster

To understand the role of titanium in catalyzing the de/rehydrogenation reactions in NaAlH_4 , it is necessary to determine the composition and structure of the catalytically active species that is (are) formed during ball milling and de/rehydrogenation reactions. One of the species that is thought to be catalytic active is TiH_2 . We have performed a density functional theory study of TiH_2 interacting with a NaAlH_4 cluster. First, a TiH_2 molecule was adsorbed on the (001) surface of NaAlH_4 in different sites. Next, the TiH_2 molecule or its Ti atom was moved inside the cluster either by exchanging the whole TiH_2 molecule with Na or Al, or by exchanging only the Ti atom with Na or Al and leaving the two hydrogen atoms on the surface together with the exchanged atom. Our calculations suggest that, when restricting the possible outcomes to adsorption, TiH_2 adsorbs on the surface above a Na site, pushing the Na atom subsurface. However, exchanging the whole TiH_2 unit with the subsurface displaced Na atom is favorable compared to leaving the TiH_2 on the surface. All other investigated exchanges were found to be less stable than TiH_2 adsorbed on the surface. The results are consistent with a zipper model that we recently proposed.

5.1 Introduction

“Vehicles can be run either by connecting them to a continuous supply of energy or by storing energy on board. Hydrogen would be ideal as a synthetic fuel because it is lightweight, highly abundant and its oxidation product (water) is environmentally benign, but storage remains a problem” [1]. This direct quote from a 2001 review paper unfortunately still holds true, while a safe and economic high-performance hydrogen storage system is a requirement for providing an onboard hydrogen source for fuel cells in mobile applications [1]. A considerable amount of research has been done on conventional hydrogen storage systems (high pressure or low temperature), but so far they do not meet the requirements for the mobile fuel cell applications. For a long time there seemed to be no alternative. This situation changed in 1997 when Bogdanovic and Schwickardi found that by adding small amounts of Ti to NaAlH_4 ,

the hydrogenation and dehydrogenations kinetics is greatly improved, which promoted NaAlH₄ to a promising reversible hydrogen storage candidate that is close to meeting the mobile fuel cell requirements [2].

The finding that hydrogen storage in complex metal hydrides can be made reversible with its kinetics improved by adding a catalyst (or dopant) sparked many studies on the light complex metal hydrides, in particular on NaAlH₄ with the goal of understanding the role of the Ti catalyst. Many efforts have been aimed at understanding the composition and structure of the catalytic species. There are suggestions that a fractional amount of the added Ti diffuses and substitutes into the NaAlH₄ lattice [3, 4]. Some studies have found formation of TiAl compounds with different Ti:Al compositions, depending on the ball milling and reaction conditions used [5-13].

Of special interest to this Chapter is the suggestion of Balema *et al.* [5] that the Al₃Ti alloy produced from Ti-enhanced NaAlH₄ reactions contains a catalytic titanium hydride phase. This catalytic phase may have been hard to detect and analyze in several previous experiments because it might have fallen below the detection limit of the analytical techniques employed [5], in particular since Ti can form a broad range of hydride phases TiH_x with 0 < x < 2 [14] which makes it more difficult to detect experimentally. Gross *et al.* [3] showed that the kinetics can be enhanced either by doping NaAlH₄ with TiH₂ directly or through indirect doping by pre-reacting TiCl₂ with LiH. However, the improved reaction rates were only achieved after about 10 cycles. They suggested that this prolonged activation period allows for Ti diffusion and substitution into the NaAlH₄ lattice. The advantage of using TiH₂ as a dopant is not only to improve kinetics but it should also overcome the problem of hydrogen capacity loss associated with the use of Ti-halides [3].

Experiments have also shown that the milling conditions employed can play a crucial role in the formation of the catalytic species. Experiments on a (1:1) mixture of NaH with Al doped with Ti powder and milled under either an H₂ or an Ar atmosphere showed that the doped material prepared in the presence of hydrogen has significant improvements in hydrogenation rate and hydrogen capacity over the material prepared in the presence of argon. This gave an indication that the presence of

hydrogen affects the nature of the active Ti species [15]. Based on these [15] and other results [2, 3, 5, 6, 7, 9], it was suggested that the doped NaAlH₄ materials do not all contain the same active Ti species; rather, they may contain a variety of related active Ti species [15].

Using X-ray diffraction Wang *et al.* have identified (catalytically active) nano-crystalline Ti hydrides that were formed in situ by ball milling Ti powder with either a NaH/Al mixture or NaAlH₄ [16]. They also found that NaAlH₄ doped directly with commercial TiH₂ has quite similar catalytic activity as the material doped with metallic Ti, and a slight composition variation of the Ti hydrides was found by variation of the preparation conditions during the doping process [16]. They suggested that the formed Ti hydride phase(s) should be highly dispersed in the NaAlH₄ matrix. By using electron microscopy with energy dispersive X-ray analysis, the same group found that the TiH₂ particles obtained by milling NaH with Al and Ti-powder are randomly distributed in the as-prepared sample, while after cycling the TiH₂ particles stay near the centre of the segregated Al rich particles [17].

There are somewhat conflicting results in the literature with respect to the dehydrogenating kinetics of TiH₂ doped NaAlH₄ materials as compared to Ti(III) doped materials. Gross *et al.* [3] have shown that the desorption rates of TiH₂ doped samples are equivalent to those of doped materials with 1-2 mol.% of TiCl₃. Brinks *et al.* [18] have found that TiCl₃ and TiH₂ give comparable kinetics. Doping the alanate with Ti powder under a hydrogen atmosphere, resulting in TiH₂ formation, has shown slower dehydrogenation kinetics than those arising upon doping the alanate with TiF₃ [19]. The reason behind this variation in kinetics might be due to differences in composition of the Ti hydrides [16].

When ball-milling an Al₃Ti alloy in a hydrogen atmosphere, nano-sized TiH₂ inclusions were found [20]. Al₃Ti reacts with hydrogen and produces a TiH₂ phase distributed in the material [20]. After an intermetallic powder of Al₃Ti was milled under hydrogen and helium atmospheres, very small grains of an Al_{1.3}Ti_{0.7} phase were found [21]. Continuous heating of this material resulted in hydrogen desorption [21]. It was also found that a nano-crystalline Al₃Ti–TiH₂ composite forms during ball-milling of Al and Ti powders in a hydrogen atmosphere [22].

Theoretical studies employing density functional theory (DFT) and modeling Ti-doped NaAlH₄ using periodic boundary conditions have shown that Na-substitution is favored if the substituted metal (Na or Al) is not allowed to aggregate [23-25], i.e., if the substituted atom is located in the gas phase, while Al-substitution is favored if the substituted metal is allowed to aggregate [26-28]. Recently, Vegge performed DFT slab calculations to determine the deposition energy of Ti/TiH₂ and the substitutional energy for Ti@Al and Ti@Na-sites on the exposed surfaces [29]. TiH₂ adsorption was modelled by adding two hydrogen atoms to the titanium atom adsorbed on the surface to investigate the effect of changing the Ti-valence [29], since it was found to have a significant effect on hydrogen diffusion [23]. Vegge's results for the deposition energy of Ti and the substitutional energy for Ti@Al and Ti@Na-sites are consistent with the results of Løvvik *et al.* [26, 28]. Studying the interaction of Ti with (001) and (100) surfaces of NaAlH₄ Ti was found to be in the interstitial sites between three neighboring AlH₄ units. The resulting local structure around Ti atom is TiAlH₁₂ [30, 31].

Most of the theoretical work modeling Ti-doped NaAlH₄ has used periodic calculations. We use a different approach to study the Ti-doped NaAlH₄ system, employing a cluster model. One of the main reasons for choosing the cluster model is that this model might yield a more realistic description than a periodic model of NaAlH₄ particles of the size of 150-200 nm [10]. Another important reason for studying (small) cluster models can be found in the fact that particles much smaller than 100 nm can release some of the incorporated H₂ even *without* Ti at lower temperatures than in Ti-catalysed NaAlH₄ [32]. Also, a cluster model opens the possibility to model the complicated phase transitions taking place during (de-)hydrogenation.

In our previous work, we used a geometry optimized twenty three formula units NaAlH₄ (Z=23) cluster to introduce a new reference system: a Ti atom adsorbed on the surface of the cluster, assuming that some of the Ti can be present in mono-atomically dispersed form, which could constitute the active catalyst. By exchanging the Ti atom with Na or Al atoms or letting Ti occupy interstitial sites, we measured the stability relative to the newly chosen reference system. We found that the Ti atom preferably exchanges with a Na atom in the subsurface region or occupies an

interstitial site [33]. Then we looked for cooperative effects between two Ti atoms in the cluster. We found that the Ti dimer dissociates on the surface of the cluster and the resulting Ti atoms behave similarly to the mono-atomically dispersed case. After dissociation the two Ti atoms prefer to move to the subsurface region inside the cluster either to exchange with two Na atoms (preferred) or with neighbouring Na and Al atoms, such that the two Ti atoms end up close enough to each other to form a direct bond [34].

In the present work, we continue with our $Z=23$ model cluster to investigate the stability of TiH_2 and its interaction with NaAlH_4 . One of the important questions we address is whether TiH_2 prefers to exchange with Na or Al inside the NaAlH_4 cluster, and whether the exchange taking place involves a whole TiH_2 unit or only the Ti atom without the hydrogen atoms. We have determined the most stable adsorption and absorption geometries, focusing on the overall energetics. We have also looked into the local structure and bonding around the TiH_2 , and compared the results with the local structure around a single Ti atom determined in the previous work [33].

5.2 Method

Density functional theory (DFT) [35, 36] as implemented in the ADF code [37] has been used to calculate all the binding energies of the clusters. The bulk crystal structure of the 23 formula units ($Z=23$) cluster was used as initial geometry to perform a geometry optimization of the bare ($Z=23$) cluster (see also Ref. [33]), which then served as a starting point for geometry optimizations on the $\text{TiH}_2 + \text{NaAlH}_4$ system (see Section 5.3.1 below). The exchange-correlation energy is approximated at the generalized gradient approximation (GGA) level using the functional of Perdew *et al.* (PW91) [38]. A triple zeta plus one polarization function (TZP) type basis set is used with a frozen core of 1s on Al as well as Na and 1s2s2p for Ti. In our previous studies we found that it was important to consider both spin restricted and unrestricted calculations [33, 34]. All calculations in the present study have been done both at the spin restricted and unrestricted levels, and they confirm this conclusion. The spin unrestricted calculations were performed allowing one, two, three and four electrons to be unpaired. However, note that below only the values for the energetically most stable states are reported (together with the corresponding number of unpaired electrons). Other computational details can be found in Ref. [33].

The ADF code calculates the total binding energy relative to spin restricted spherically symmetric atoms. The only purpose of this reference state, is to provide a reference energy common to all calculated energies. When considering TiH₂ adsorbed/absorbed on/in the Z=23 model cluster our zero of energy has been set to that of the fully optimized bare Z=23 cluster plus TiH₂ in TiH₂ bulk. Note that we have defined the adsorption/absorption energies in such a way that a negative number means that it is stable with respect to TiH₂ in TiH₂ bulk. Our periodic bulk TiH₂ calculations have been performed using ADF-BAND [39] with the same basis and fit sets as used in the cluster calculations.

5.3 Results and Discussion

5.3.1 The adsorption of TiH₂ on the (001) surface of the cluster

The geometry optimized structure of the bare twenty three formula units (Z=23) NaAlH₄ cluster (see also Ref. [33]) was used as initial geometry to perform geometry optimizations for the TiH₂ + (NaAlH₄)₂₃ system. TiH₂ was adsorbed on the (001) surface of the optimized bare cluster (Fig. 5.1a) in different positions. The adsorption energies of TiH₂ on the relaxed clusters are listed in Table 5.1 and the surface geometries are displayed in Fig. 5.1. The TiH₂ was adsorbed between 4 AlH₄ units above the Na atom [TiH₂@top_4AlH₄], in the bridge site between 2 AlH₄ units [TiH₂@top_2AlH₄], and between 3 AlH₄ units [TiH₂@top_3AlH₄] as shown in Figs. 5.1b, 5.1c and 5.1d, respectively. We also tried to adsorb the TiH₂ above a single AlH₄ unit, but we could find no stable minimum for this geometry (the TiH₂ moved to the bridge site [TiH₂@top_2AlH₄]). Comparing the energy of the bare Z=23 cluster and TiH₂ in the gas phase [TiH₂+Z=23] with the adsorption energies for the three different adsorption sites described above (Table 5.1), TiH₂ is clearly found to be more stable on the surface of the cluster than in the gas phase. The adsorption energies for the three different sites on the surface show that the most stable adsorption site is TiH₂@top_4AlH₄. As seen from the side views of the TiH₂@top_4AlH₄ cluster in Fig. 5.1e and of the bare cluster in Fig. 5.1g, the surface Na atom is pushed down considerably when TiH₂ is adsorbed above it.

A similar displacement of the surface Na atom(s) to the subsurface region was also observed when one (two) Ti atom(s) was (were) adsorbed above the surface Na

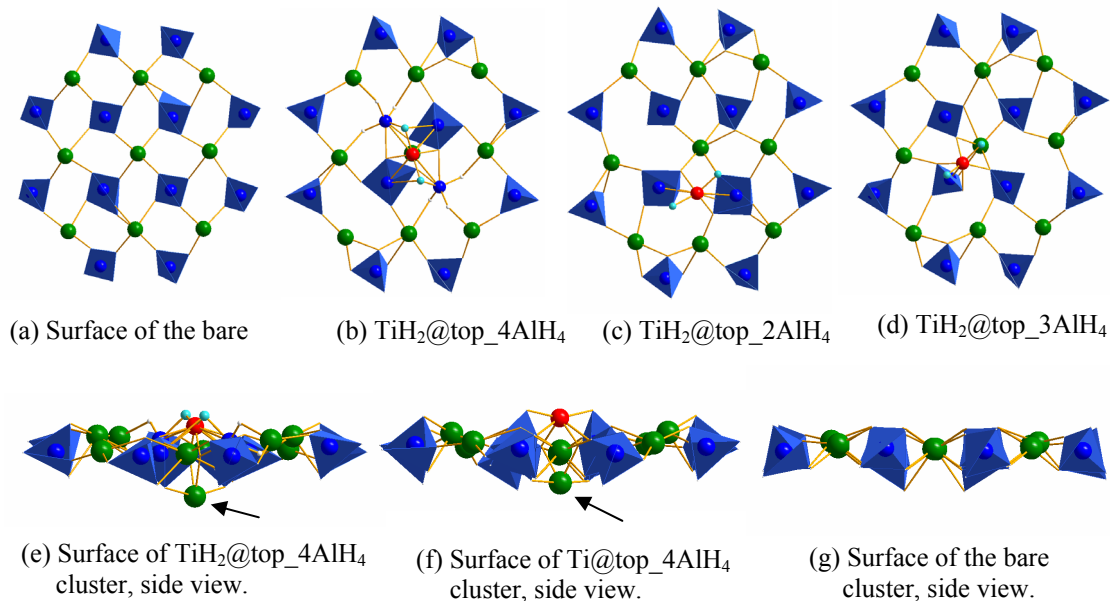


Fig. 5.1: The figure shows TiH_2 adsorbed in different positions on the (001) surface of the $Z=23$ model cluster viewed from above. The Na atoms are displayed as green balls, Ti as a red ball, the two hydrogen atoms of the TiH_2 as light blue balls, and Al as dark blue balls inside the tetrahedrons with the four hydrogen atoms at their corners. (a) The surface of the bare cluster. (b) A TiH_2 above Na atom between four AlH_4 units [$\text{TiH}_2@top_4\text{AlH}_4$]. (c) A TiH_2 between two AlH_4 units [$\text{TiH}_2@top_2\text{AlH}_4$]. (d) A TiH_2 between three AlH_4 units [$\text{TiH}_2@top_3\text{AlH}_4$]. (e) Side view of $\text{TiH}_2@top_4\text{AlH}_4$ cluster surface. (f) Side view of $\text{Ti}@top_4\text{AlH}_4$ cluster surface. (g) Side view of bare cluster surface. In the side views (e) and (f), the subsurface displaced Na atoms are indicated by arrows.

	E_a	$E_{\text{Rel.top}}$	n
$\text{TiH}_2@top_4\text{AlH}_4$	0.48	0.00	2
$\text{TiH}_2@top_3\text{AlH}_4$	2.40	1.92	2
$\text{TiH}_2@top_2\text{AlH}_4$	1.05	0.57	2
$\text{Ti}@NaH_2$	1.24	0.76	2
$\text{Ti}@AlH_2$	0.67	0.19	0
$\text{TiH}_2@Na$	-0.08	-0.56	0
$\text{TiH}_2@Al$	2.08	1.59	0
$\text{TiH}@NaH$	0.84	0.36	2
TiH_2+Z23	5.72	5.24	2

Table 5.1: The adsorption/absorption energies (E_a) are given for the TiH_2 system. The energy reference used is discussed in the method section. The notations used to refer to a given structure are defined in Figs. 5.1 and 5.2. All the energies are given in eV, and all results have been obtained from fully relaxed geometries. The number of unpaired electrons giving the lowest energy is denoted n .

atom(s) [33, 34]. The Na displacement resulting from a mono-dispersed Ti atom adsorbed on the surface, Ti@top_4AlH_4 [29] is compared to that of $\text{TiH}_2\text{@top_4AlH}_4$ in Figs. 5.1e and 5.1f, with the reference Na position in the bare cluster displayed in Fig. 5.1g. It is clear that in the case of $\text{TiH}_2\text{@top_4AlH}_4$ the Ti atom sits deeper into the surface and the Na atom is displaced even further into the subsurface region.

5.3.2 The stability of TiH_2 inside the cluster

We have also investigated the stability of the TiH_2 inside the cluster (a side view of the bare cluster is shown in Fig. 5.2a). The $\text{TiH}_2\text{@top_4AlH}_4$ cluster (Fig. 5.1b) was taken as a starting geometry for making TiH_2 exchanges with Na and Al. Two kinds of exchanges have been considered. First, the whole TiH_2 unit was exchanged with either a Na or Al atom [$\text{TiH}_2\text{@Na}$, $\text{TiH}_2\text{@Al}$], as shown in Figs. 5.2b and 5.2d, respectively. Next, only the Ti atom was exchanged with either a Na or an Al atom, leaving the two hydrogen atoms on the surface together with the exchanged Na or Al atom [Ti@NaH_2 , Ti@AlH_2], as shown in Figs. 5.2c and 5.2e, respectively. The reason for making the two different kinds of exchanges is, of course, to check whether the TiH_2 molecule prefers to move as a whole, or whether only its Ti atom is involved in the exchange. As may be seen in Table 5.1, the TiH_2 molecule prefers to exchange with the subsurface displaced Na atom [$\text{TiH}_2\text{@Na}$] (Fig. 5.2b). This exchange is found to be more stable than the adsorption of TiH_2 on the surface [$\text{TiH}_2\text{@top_4AlH}_4$] by 0.56 eV, indicating that TiH_2 prefers to move into the subsurface region of the cluster rather than to stay on the surface of NaAlH_4 . Note that the exchange takes place through moving the whole TiH_2 unit subsurface. Leaving the two hydrogen atoms with the exchanged Na atom on the surface to form a Ti@NaH_2 cluster is less stable by 1.32 eV compared to the $\text{TiH}_2\text{@Na}$ cluster, and also less stable than the starting geometry [$\text{TiH}_2\text{@top_4AlH}_4$] by 0.76 eV. Leaving one hydrogen atom with the exchanged Na atom on the surface and taking one H-atom with Ti to form a TiH@NaH cluster (Fig. 5.2f) is also unfavorable, being less stable by 0.92 eV compared to the $\text{TiH}_2\text{@Na}$ cluster. The exchanges with an Al atom are also unstable compared to $\text{TiH}_2\text{@Na}$: The Ti@AlH_2 and $\text{TiH}_2\text{@Al}$ exchanges are unstable by 0.75 and 2.15 eV, respectively, both also being unstable compared to the starting geometry. Note, however, that in the case of Ti exchange with an Al atom it is preferable to leave the two hydrogen atoms on the surface together with the exchanged Al atom.

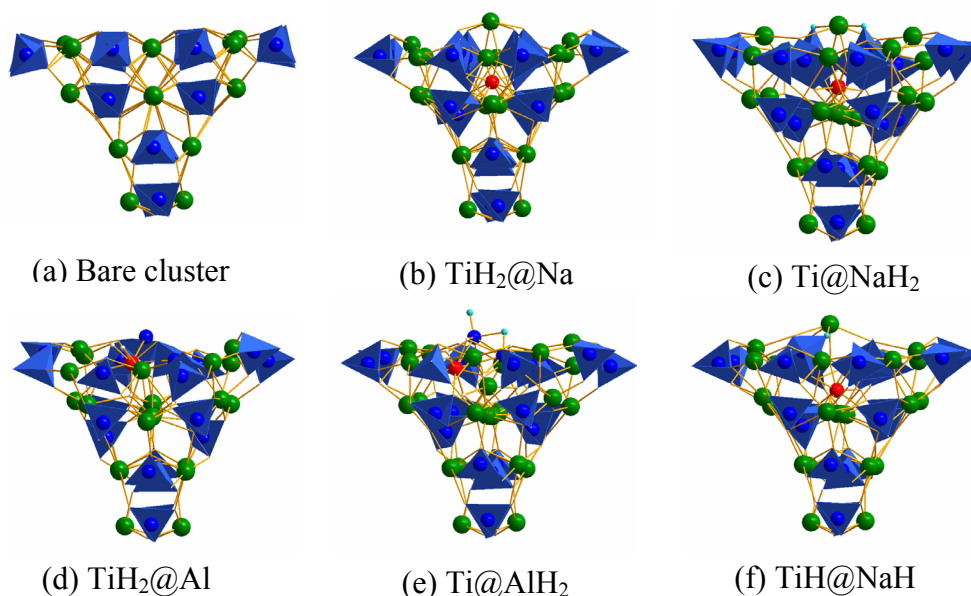


Fig. 5.2: TiH_2 absorbed in different positions in the $Z=23$ cluster. The atoms are displayed in the same way as in Fig. 5.1. (a) The bare cluster. (b) TiH_2 unit exchanged with a Na atom [$\text{TiH}_2@Na$]. (c) A Ti atom (of the TiH_2) exchanged with a Na atom while leaving the 2 H atoms on the Na atom [$\text{Ti}@NaH_2$]. (d) TiH_2 unit exchanged with an Al atom [$\text{TiH}_2@Al$]. (e) A Ti atom (of the TiH_2) exchanged with an Al atom while leaving the 2H atoms on the Al atom [$\text{Ti}@AlH_2$]. (f) TiH exchanged with a Na atom while leaving one H atom on the exchanged Na atom [$\text{TiH}@NaH$].

These results are very similar to what we have found when one or two Ti atoms were adsorbed on the surface of NaAlH_4 , or exchanged with Na or Al atoms [33, 34]: When restricting the possible outcomes to adsorption on the surface, the adsorbed species (Ti, 2Ti, or TiH_2) prefers to be on top of a Na atom between 4 AlH_4 units, and the surface Na atom is pushed subsurface as a result of the adsorption. However, the energetically most stable situation is in all cases found when the Ti-containing species is exchanged with the subsurface displaced Na atom.

5.3.3 The interaction of H_2 with a Ti, Na or Al atom on the surface of the cluster

By combining the present results with some of our previously published results [33] we have tried to address the question what would happen if a mono-dispersed atom (Ti, Na or Al) on the surface of the NaAlH_4 cluster interacts with H_2 . This is important for understanding the stability of the possible different structures formed during the de/hydrogenation processes. The relevant available data are presented in Fig. 5.3, showing an energy difference diagram for different structures.

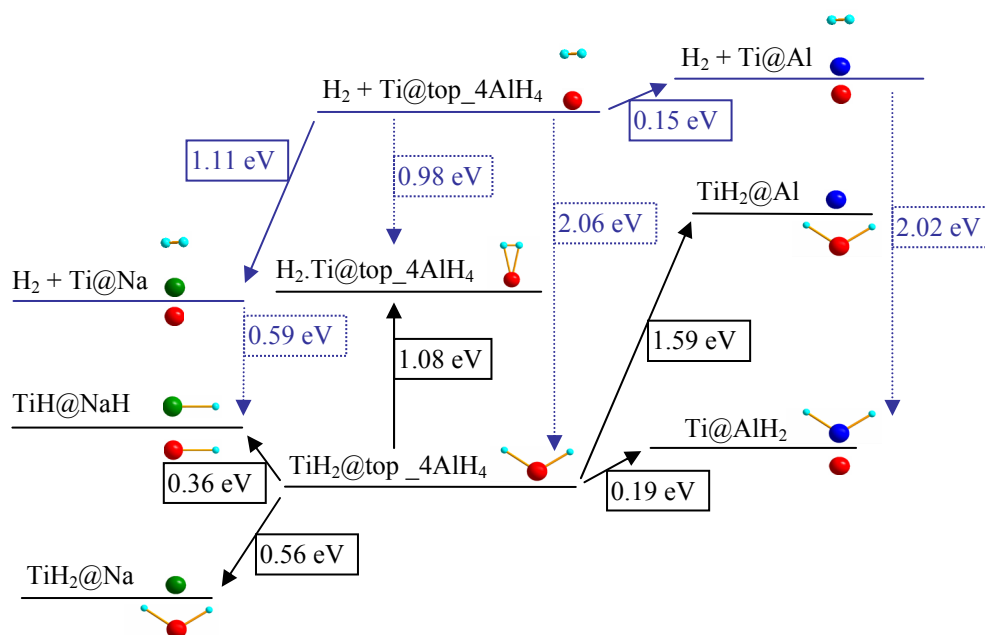


Fig. 5.3: Diagram showing the energy differences between a number of different structures. A simplified representation is shown for the $Z=23$ formula units NaAlH_4 cluster with a TiH_2 unit added: The horizontal lines in the figure (both blue and black) represent the surface of each cluster. The two hydrogen atoms are shown as two light blue balls, and the Ti, Na, and Al atoms as red, green, and dark blue balls, respectively. When the Ti atom is below a horizontal line it means that it has been exchanged with a Na or Al atom in the cluster, and the atom with which it has been exchanged is placed above the horizontal line. The arrows with their attached numbers indicate energy changes when moving between the different structures. All black lines and arrows represent results calculated in the present study. The full blue lines and arrows represent results presented in Ref. [33]. The dashed blue arrows represent results that have been obtained by combining the results from these two studies ([33] and the present work).

It is clear from the diagram that any excess of H_2 (e.g. stemming from the dehydrogenation of a nearby NaAlH_4 particle) would gain a significant amount of energy (in the order of 2 eV) if reacting with a NaAlH_4 surface containing Ti. Whether this will happen or not will probably depend on the state of the surface. If Ti has already changed place with Na, there is considerable energy (0.59 eV) to be gained by dissociating H_2 to form NaH on the surface and TiH subsurface, but there is probably a significant kinetic barrier for this process. If Ti is still at the surface, there is a large energy benefit for H_2 to react with Ti, and TiH_2 would probably be formed easily. Similarly, if H_2 is present at the time Ti is introduced to the surface, the

	Bare cluster	Ti@Na	TiH ₂ @Na
Al-H	1.62-1.65	1.69-1.86	1.65-1.84
Ti-Al		2.79-3.09	2.84-3.21
Ti-H		1.87-1.99	1.81-1.86

Table 5.2: A comparison between Al-H, Ti-Al and Ti-H bond lengths (in Å), in the bare cluster, the cluster with Ti exchanged with the subsurface displaced Na atom (Ti@Na) and the cluster with TiH₂ exchanged with the subsurface displaced Na atom (TiH₂@Na).

formation of TiH₂ seems to be highly beneficial: formation of TiH₂@top_4AlH₄ from H₂ + Ti@top_4AlH₄ is accompanied by a release of more than 2 eV of energy. Only some experimental studies have identified TiH₂, and the reason may be that H₂ was only present in a high enough concentration during the reaction of Ti with NaAlH₄ in some of the experiments.

5.3.4 The local structure around Ti

In our previous studies, we found that the situation in which Ti is exchanged with the subsurface displaced Na atoms is preferred energetically [33, 34]. This is also true for TiH₂. It is therefore interesting to compare the local bonding structures for these systems. On the one hand, as seen from the bond lengths in Table 5.2, the presence of a TiH₂ in TiH₂@Na leads to shorter Ti-H bonds and longer Ti-Al bonds than the presence of a Ti atom in Ti@Na. On the other hand, the presence of a Ti atom in Ti@Na leads to longer Al-H bonds than the presence of a TiH₂ in TiH₂@Na. Apparently, a Ti atom softens the Al-H bond more than a TiH₂ molecule, which might influence the dehydrogenation kinetics.

The Ti atom (TiH₂) in Ti(TiH₂)@top_4AlH₄ clusters is found to be surrounded by 4 close lying Al atoms, of which two are significantly closer, and may be said to be present in the first coordination sphere (CS), while 2 are in the second CS. The Ti-Al distances and coordination numbers for the adsorption states are close to those found in NaAlH₄+Ti after ball-milling (the material denoted SAH-start in Ref. [13] (see Table 5.3)). However, in the case of Ti(TiH₂)@Na, although the distances of Ti to the Al-atoms in the first three CSs are close to those found for the first two CSs of the NaAlH₄+Ti material after H₂ desorption, the total numbers of Al atoms in the first and second CS (6 vs 8.5) are not equal. This indicates that Ti(TiH₂)@Na can not be the

	Ti-Al [\AA] 1 st CS	n	Ti-Al [\AA] 2 nd CS	n	Ti-Al [\AA] 3 rd CS	n
TiH ₂ @top_4AlH ₄	2.83	2.0	2.94	2.0		
Ti@top_4AlH ₄	2.79	2.0	2.90	2.0		
TiH ₂ @Na	2.84	2.0	3.00	2.0	3.21	2.0
Ti@Na	2.79	2.0	2.92	2.0	3.09	2.0
SAH-start [13]	2.71	2.3	2.89	2.5		
SAH-125 [13]	2.76	3.9	2.92	4.6		

Table 5.3: A comparison of Ti-Al distances from our theoretical calculations and the experimentally measured values of Baldé *et al.* [13] in the first, second and third coordination sphere (CS). The number of Al atoms, n, at the indicated distance from Ti is also displayed.

major species in the material that results after heating to 125 C° (SAH-125 material in Ref. [13]).

5.3.5 Further support of the zipper model

Recently we introduced the so-called zipper model to explain how Ti could improve the kinetics in the NaAlH₄ system [34]. In this model, Ti works as a novel kind of catalyst by acting as a slider, eating itself into the nano-particle as it reacts away – effectively unzipping the structure (see Fig. 5.4). In this way, the fully hydrogenated alanate could be decomposed, and at the same time fresh surfaces could be exposed along the route of the zipper. Note that the most reactive of all structures is the one with Ti on the surface. The first reaction according to our zipper model is that Ti moves into the subsurface region of the structure replacing Na. In our model we assume that the Na atom left on the surface can easily react with other species present, because it is an exposed and under-coordinated atom.

In the present study evidence is found that it is rather likely that TiH₂ will be formed sometimes during this process, especially if H₂ is available in the gas phase when Ti is added to NaAlH₄. What would then happen? Are our present results in accordance with the proposed zipper model? Yes, they are. In the case that TiH₂ is formed, the TiH₂ will play the same role as Ti. The essence of the zipper model is that the exchange with a subsurface displaced atom is favored compared to other atomic rearrangements. In that sense the results for one Ti atom [33], two Ti atoms [34], and the present results for TiH₂ present the same, consistent picture: The energetically

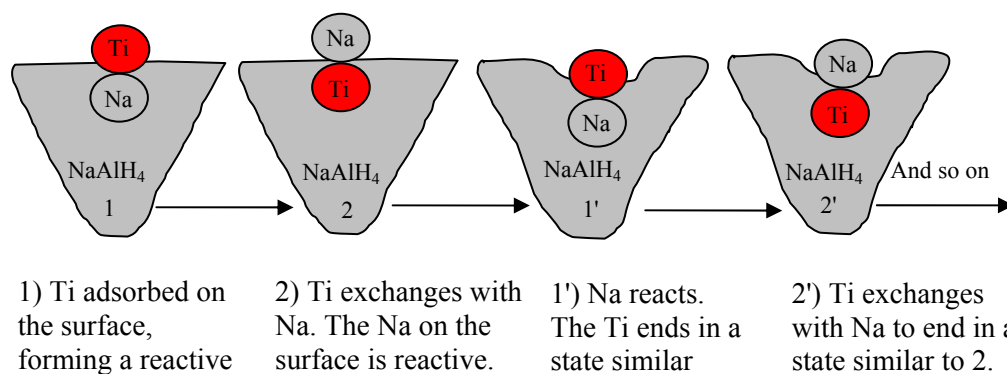


Fig. 5.4: A cartoon shows the zipper model. In Step 1, the $\text{Ti}(\text{H}_2)$ adsorbs on the surface of the cluster forming the most reactive surface. In step 2, the $\text{Ti}(\text{H}_2)$ exchanges with a Na atom in the subsurface region, ending with a reactive Na atom on the surface of the cluster. In step 3, the Na atom reacts with any species in the medium, resulting in 1'—a situation that is similar to 1. In step 4, the $\text{Ti}(\text{H}_2)$ again exchanges with a Na atom in the subsurface region, resulting in 2', a situation similar to 2. The process repeats itself until the whole NaAlH_4 species has reacted.

preferred situation is for Ti (TiH_2) to exchange with the subsurface displaced Na atom.

5.4 Conclusion

We have performed density functional theory calculations at the generalized gradient approximation (PW91) level for a NaAlH_4 cluster with TiH_2 adsorbed on (absorbed in) the (001) surface of the cluster. After studying the adsorption of the TiH_2 molecule on the surface, the TiH_2 molecule or its Ti atom was moved inside the cluster either by exchanging the whole TiH_2 molecule with Na or Al, or by exchanging only the Ti atom with Na or Al and leaving the two hydrogen atoms on the surface together with the exchanged atom. In the case that the possible outcomes were restricted to adsorption, we found that TiH_2 adsorbs on the surface above a Na atom, bonding with 4 AlH_4 units and pushing the surface Na atom into the subsurface region. However, it was energetically preferred to exchange the whole TiH_2 unit with the subsurface displaced Na atom. All other exchanges were unstable compared to the situation where TiH_2 was adsorbed on the surface. These results are consistent with our previous results for one and two Ti atoms interacting with the NaAlH_4 cluster. The results are also consistent with our recently proposed zipper model, in which the mechanism by

which the added TiH₂ promotes H₂ release is explained by the TiH₂ molecule working itself down into the alanate particle by replacing Na, effectively unzipping the structure.

5.5 References

- [1] L. Schlapbach, A. Züttel, *Nature*, 414, 353 (2001).
- [2] B. Bogdanovic, M. Schwickardi, *J. Alloys Compd.* 253, 1 (1997).
- [3] K. J. Gross, E. H. Majzoub, S. W. Spangler, *J. Alloys Compd.* 356–357, 423 (2003).
- [4] C. M. Jensen, R. Zidan, N. Mariels, A.; Hee, C. Hagen, *Int. J. Hydrogen Energy* 24, 461 (1999).
- [5] V. P. Balema, L. Balema, *Phys. Chem. Chem. Phys.* 7, 1310 (2005).
- [6] J. Graetz, J. J. Reilly, J. Johnson, A. Y. Ignatov, T. A. Tyson, *Appl. Phys. Lett.* 85, 500 (2004).
- [7] C. Weidenthaler, A. Pommerin, M. Felderhoff, B. Bogdanovic, F. Schüth, *Phys. Chem. Chem. Phys.* 5, 5149 (2003).
- [8] E. H. Majzoub, K. J. Gross, *J. Alloys Comp.* 356–357, 363 (2003).
- [9] H. W. Brinks, C. M. Jensen, S. S. Srinivasan, B. C. Hauback, D. Blanchard, K. Murphy, *J. Alloys Compd.* 376, 215 (2004).
- [10] H. W. Brinks, B. C. Hauback, S. S. Srinivasan, C. M. Jensen, *J. Phys. Chem. B* 109, 15780 (2005).
- [11] A. G. Haiduc, H. A. Stil, M. A. Schwarz, P. Paulus, J. J. C. Geerlings, *J. Alloys Compd.* 393, 252 (2005).
- [12] G. Streukens, B. Bogdanovic, M. Felderhoff, F. Schüth, *Phys. Chem. Chem. Phys.* 8, 2889 (2006).
- [13] C. P. Baldé, H. A. Stil, A. M. J. van der Eerden, K. P. de Jong, J. H. Bitter, *J. Phys. Chem. C* 111, 2797 (2007).
- [14] W. E. Wang, *J. Alloys Compd.* 238, 6 (1996).
- [15] P. Wang, C. M. Jensen, *J. Phys. Chem. B* 108, 15827 (2004).
- [16] P. Wang, X. D. Kang, H. M. Cheng, *J. Phys. Chem. B* 109, 20131 (2005).
- [17] X. D. Kang, P. Wang, H. M. Cheng, *J. Appl. Phys.* 100, 034914 (2006).
- [18] H. W. Brinks, M. Sulic, C. M. Jensen, B. C. Hauback, *J. Phys. Chem. B* 110, 2740 (2006).
- [19] P. Wang, C. M. Jensen, *J. Alloys Compd.* 379, 99 (2004).

- [20] K. Hashi, K. Ishikawa, K. Suzuki, K. Aoki, *Mater. Trans.* 43, 2734 (2002).
- [21] E. Illekova, P. Svec, D. Wexler, A. Calka, *Journal of Non-Crystalline Solids* 353, 1970 (2007).
- [22] K. I. Moon, K. Sub Lee, *J. Alloys Compd.* 264, 258 (1998).
- [23] J. Íñiguez, T. Yildirim, T. J. Udovic, M. Sulic, C. M. Jensen, *Phys. Rev. B* 70, 060101(R) (2004).
- [24] J. Íñiguez, T. Yildirim, *Appl. Phys. Lett.* 86, 103109 (2005).
- [25] C. M. Araújo, R. Ahuja, J. M. O. Guillén, P. Jena, *Appl. Phys. Lett.* 86, 251913 (2005).
- [26] O. M. Løvvik, S. M. Opalka, *Phys. Rev. B*, 71, 054103 (2005).
- [27] C. Y. W. Lee, J. K. Yoon, *J. Alloys Compd.* 416, 245 (2006).
- [28] O. M. Løvvik, S. M. Opalka, *Appl. Phys. Lett.* 88, 161917 (2006).
- [29] T. Vegge, *Phys. Chem. Chem. Phys.* 8, 4853 (2006).
- [30] J. Liu, Q. Ge, *J. Phys. Chem. B* 110, 25863 (2006).
- [31] J. Liu, Q. Ge, *Chem. Commun.* 1822 (2006).
- [32] C. P. Baldé, B. P. C. Hereijgers, J. H. Bitter, K. P. de Jong, *Angew. Chem. Int. Ed.* 45, 3501 (2006).
- [33] A. Marashdeh, R. A. Olsen, O. M. Løvvik, G. J. Kroes, *Chem. Phys. Lett.* 426, 180 (2006).
- [34] A. Marashdeh, R. A. Olsen, O. M. Løvvik, G. J. Kroes, *J. Phys. Chem. C* 111, 8206 (2007).
- [35] P. Hohenberg, W. Kohn, *Phys. Rev.* 136, B864 (1964).
- [36] W. Kohn, L. J. Sham, *Phys. Rev.* 140, A1133 (1965).
- [37] G. T. Velde, F. M. Bickelhaupt, E. J. Baerends, C. Fonseca Guerra, S. J. A. van Gisbergen, J. G. Snijders, T. Ziegler, *J. Comp. Chem.* 22, 931 (2001).
- [38] J. P. Perdew, J. A. Chevary, S. H. Vosko, K. A. Jackson, M. R. Pederson, D. J. Singh, C. Fiolhais, *Phys. Rev. B* 46, 6671 (1992).
- [39] G. T. Velde, E. J. Baerends, *Phys. Rev. B* 44, 7888 (1991).

Chapter 6

Why Some Transition Metals are Good Catalysts for Reversible Hydrogen Storage in Sodium Alanate, and Others are not: A Density Functional Theory Study

Sodium alanate (NaAlH_4) is a prototype system for storage of hydrogen in chemical form. However, a key experimental finding, that early transition metals (TMs) like Ti, Zr, and Sc are good catalysts for hydrogen release and re-uptake, while traditional hydrogenation catalysts like Pd and Pt are poor catalysts for NaAlH_4 , has so far gone unexplained. We have performed density functional theory calculations at the PW91 generalised gradient approximation level on Ti, Zr, Sc, Pd, and Pt interacting with the (001) surface of nanocrystalline NaAlH_4 , employing a cluster model of the complex metal hydride. A key difference between Ti, Zr, and Sc on the one hand, and Pd and Pt on the other hand is that exchange of the early TM atoms with a surface Na ion, whereby Na is pushed on to the surface, is energetically preferred over surface absorption in an interstitial site, as found for Pd and Pt. The theoretical findings are consistent with a crucial feature of the TM catalyst being that it can be transported with the reaction boundary as it moves into the bulk, enabling the starting material to react away while the catalyst eats its way into the bulk, and effecting a phase separation between a Na-rich and a Al-rich phase.

6.1. Introduction

The realisation of a hydrogen economy requires the development of an efficient system for on-board hydrogen storage [1]. At this stage, promising methods store hydrogen as a pressurised gas [2], a cryogenic liquid [3], an adsorbent to carbon nanotubes [4,5], to water in clathrate hydrates [6,7], and to metal organic frameworks (MOFs) [8,9], and in chemical form [10-12]. So far, all of these systems have their specific problems. Pressurising or liquefying hydrogen requires a significant fraction of the energy present in H_2 [1]. Carbon nanotubes seemed very promising at first [4], but their room temperature storage capacity would appear to be too low at close to 1 wt% [5]. At (close to) ambient conditions, the storage capacity presently achieved for

clathrates [7] and MOFs [8] is likewise too low. A recent overview of storage methods has been presented by Felderhoff *et al.* [13].

So far, the chemical storage system that comes closest to meeting practical requirements is the NaAlH₄ system [11]. Its theoretical reversible storage capacity is about 5.5 wt%. Hydrogen is released in two steps. According to thermodynamics, the first step, in which Na₃AlH₆, Al, and H₂ are produced, proceeds spontaneously at close to 30 °C. The second step, in which Na₃AlH₆ reacts to NaH, Al, and H₂ proceeds at close to 110 °C. A key point is that the release and re-uptake of H₂ can be made reversible by adding a catalyst like Ti, as demonstrated in 1997 by Bogdanovic and Schwickardi [10]. In much of the subsequent work aimed at improving the kinetics of the release and re-uptake of H₂, Ti was used (in the form of TiCl₃ [14] or of colloid nanoparticles [15,16]). However, other transition metals have also been tried. An intriguing observation is that traditional hydrogenation catalysts like Pd and Pt are poor catalysts for hydrogen release from NaAlH₄ [17], while early transition metals like Ti, Zr [17,18], and Sc [19], and actinides (Ce [19], Pr [19], and mischmetal (Mm, 42 at.%Ce, 31 at.% La, 18 at.% Nd, and 9 at.% Pr, [20]) are good catalysts (Sc, Ce, Pr [19] and Mm [20] all being even better than Ti). Another interesting observation is that adding different transition metals together may produce synergistic effects, as has been demonstrated for, for instance, Ti/Zr [18] and Ti/Fe [14].

Although much progress has been made at improving catalysed hydrogen release from and uptake in NaAlH₄, the kinetics of these processes is still too slow [11]. As a result, much recent work aimed at clarifying the role of the much used Ti catalyst has focussed on determining the form in which it is present. So far, Ti has been found to be present in at least three different forms. First, Ti has been observed to be present in Al as a Ti-Al alloy of varying compositions [21-27]. Second, Ti was observed to be present as TiH₂ upon doping a mixture of NaH and Al with pure Ti and ball milling [28,29], following a conjecture that TiH₂ [30] should be the active catalyst. Finally, there are experiments that suggest Ti to be present in NaAlH₄ itself [27,31,32].

Calculations employing periodic density functional theory (DFT) suggest substitution of Ti into the bulk lattice of NaAlH₄ to be energetically unfavourable if standard states of NaAlH₄, Na, Al, and Ti are used as reference states [33] or if reactant and

product states appropriate for describing doping reactions are used as reference states [34]. However, periodic DFT calculations also find substitution of Ti into the NaAlH₄ lattice to be more stable at the surface than in the bulk [34,35]. Calculations employing a cluster model of NaAlH₄ have shown that Ti atoms present on NaAlH₄(001) in monoatomically dispersed form prefer to exchange with a surface Na ion [36,37], and that the resulting situation (Ti in surface Na sites, the exchanged Na ion adsorbed on top of it) is energetically preferred over the case of two separate bulk phases of NaAlH₄ and Ti [37]. Furthermore, periodic DFT calculations likewise suggest that the initial reaction of TiCl₃ with NaAlH₄ can result in Ti substituting a Na surface ion [38]. Recent plane wave DFT calculations suggested that it is energetically even more favourable for Ti to occupy a surface interstitial site than to exchange with a surface Na ion, and give further support to the idea that Ti can be incorporated into the surface [39,40]. Recent experimental observations also give support to the idea that Ti can be present in the surface of NaAlH₄, immediately after doping with Ti [27].

The exact role of the much used Ti catalyst still remains elusive [11], although several ideas have been put forward. Isotope scrambling experiments provided evidence that exchange of gaseous D₂ with NaAlH₄ only occurred in the presence of Ti used as dopant [41]. This effect was attributed to the presence of a Ti-Al alloy [41], with support coming from DFT calculations that show that dissociation of H₂ on a surface of Al(001) with Ti alloyed into it can occur without barriers [42,43], whereas high barriers are encountered on low index surfaces of pure Al. However, the experimentalists pointed out that the hydrogen exchange observed to take place under steady state conditions occurs much faster than the full decomposition reaction, suggesting that the key role of Ti should be to enhance mass transfer of the solid as rate limiting step [41]. Experiments employing anelastic spectroscopy have suggested that Ti enhances bulk diffusion of H₂ through the alanate [44-46], but this point is controversial [47].

Addressing the role of Ti, calculations have shown that surface Ti facilitates defect formation in the surface of NaAlH₄, thanks to the ease with which Ti can change its oxidation state [48]. Another idea that has been suggested is that Ti enables the formation of mobile AlH₃ which would then enable the fast mass transfer required in

the solid state reactions releasing hydrogen [49,50], and volatile molecular aluminium hydride molecules have been identified during hydrogen release from Ti/Sn doped NaAlH₄ using inelastic neutron scattering spectroscopy [51]. Recent work has suggested that an additional role of Ti [52] or the associated anion [53,54] used in doping may be to improve the thermodynamics of the system. Perhaps most crucially, several experiments have shown that the release and uptake of H₂ are associated with massive mass transfer over long (micrometers) distances [14,23,55,56]. The idea that the crucial role of Ti is to enable mass transfer over large distances is further supported by experiments showing that partial decomposition of undoped NaAlH₄ particles is possible if they are very small (nano-sized), the decomposition starting at a temperature as low as 40 °C [57]. Also, recent isotope exchange experiments suggest that diffusion of a hydrogen containing species heavier than H (AlH₃, Al_xH_y, or NaH) constitutes the rate limiting step [58].

In Ref.[49], three basic mechanisms were proposed in which Ti could effect the long range mass transport of Al or Na required for de- and re-hydrogenation. In the first mechanism, long-range diffusion of metal species through the alanates to the catalyst would occur as a first step. Gross et al. [49] already proposed that this could involve the AlH₃ species. In the second mechanism, the driving force would be hydrogen desorption at the catalyst site, followed by long range transport of the metal species, the catalyst acting as a hydrogen dissociation and recombination site and possibly also as a nucleation site. In the third mechanism proposed, the catalyst itself would migrate through the bulk. In this mechanism, “the starting phase is consumed and product phases are formed at the catalyst while it ‘eats’ its way through the material” [49].

The goal of this Chapter is to determine the crucial aspect of the role good catalysts like Ti play in hydrogen release from NaAlH₄. The main idea underlying our work is that the explanation of the role of the catalyst should be based on a key experimental observation, that traditional hydrogenation catalysts like Pd and Pt [17] are poor catalysts for hydrogen release from NaAlH₄, while early transition metals like Ti [10,17], Zr [17], and Sc [19] are good catalysts for hydrogen release and re-uptake. Our starting point is a model in which the TM is adsorbed on the face of NaAlH₄ which has the lowest surface energy (the (001) face), the TM being present in monoatomically dispersed form. Such a situation can arise from ballmilling, a

technique that employs mechanical energy to achieve a fine dispersion of the catalyst, which has been in use in Ti-doping of NaAlH₄ since 1999 [18], or it can arise from the initial reaction of TiCl₃ with NaAlH₄ [38]. Our DFT calculations discussed below show that the bad catalysts, Pd and Pt, prefer to absorb interstitially in the surface of NaAlH₄, while the good catalysts, Ti, Zr, and Sc, all push Na ions out of the surface and thereby effect a separation between a Na-rich and an Al-rich phase, by exchanging with surface Na-ions. This result suggests that the crucial role of catalysts like Ti is indeed to promote long range mass transport of one of the metal ions, according to the third mechanism outlined above, in which the catalyst moves into the starting phase, eating its way through the material while moving Na ions outward.

The outline of this Chapter is as follows. Section 6.2 explains the DFT methodology we have used to study the interaction of isolated TM atoms with the (001) face of NaAlH₄. As explained there, we employ a cluster methodology, using a cluster with an exposed (001) face which is energetically, electronically, and structurally close to surface and bulk NaAlH₄, and which should form a good model system for nano-sized NaAlH₄ particles [36]. The DFT calculations are performed at the generalised gradient approximation (PW91) level [59]. In Section 6.3 we discuss the surface adsorption and absorption of the TM atoms on/in the (001) surface of NaAlH₄. This section is concluded with a discussion of the mechanism suggested by the DFT calculations. Our conclusions are summarised in Section 6.4.

6.2. Method

DFT calculations. The binding energies of all systems incorporating a NaAlH₄ cluster have been calculated using DFT [60,61] as implemented in the ADF code [62]. The exchange-correlation energy is approximated at the generalized gradient approximation (GGA) level, using the PW91 functional [59]. The basis set used is of a triple zeta plus one polarization function (TZP) type. A frozen core was chosen of 1s on Al as well as Na, and of 1s2s2p on Ti as well as Sc. On Pd and Zr, the frozen core was 1s2s2p3s3p3d, and 1s2s2p3s3p3d4s4p4d on Pt. The general accuracy parameter of ADF [62] was set to 4.0 based on a series of convergence tests. In many of the calculations we applied a non-zero electronic temperature to overcome problems with the SCF convergence. However, we ensured that we eventually ended up in the electronic ground state by gradually cooling the electrons. The standard ADF fit sets

(for the TZP basis sets) used to represent the deformation density were replaced by the fit sets corresponding to the quadruple zeta plus four polarization functions type basis sets to achieve results of high enough accuracy.

In our previous studies we found that it was important to consider both spin restricted and spin unrestricted calculations [36,37]. All calculations in the present study have therefore been done at both the spin restricted and the spin unrestricted level. The spin unrestricted calculations were performed allowing one, two, three and four electrons to be unpaired. Below, only the value for the energetically most stable state is reported in the tables. The calculations involving Zr, Pd, and Pt incorporated scalar relativistic corrections, employing the ZORA method [63]. Other computational details of the cluster calculations can be found in Chapters 2–4.

The bulk crystal structure of a semi-spherical NaAlH₄ cluster containing 23 formula units ($Z=23$) was used as the initial geometry to perform a geometry optimisation of a bare cluster, with a large exposed (001) surface (Chapter 3). The (001) face was selected because it has been shown to be the most stable crystal face of NaAlH₄ [64]. The geometry optimised $Z=23$ cluster is energetically, electronically, and structurally close to surface and bulk NaAlH₄, and should form a good model system for nano-sized NaAlH₄ particles (Chapter 3). In all geometry optimisations of both the bare cluster and the cluster interacting with a TM atom, I use the standard ADF convergence criteria concerning the force, step length and the energy to locate the minimum.

The optimized bare $Z=23$ cluster formed the starting point of geometry optimisations of the TM + NaAlH₄ system, where TM is Sc, Ti, Zr, Pd, or Pt. Specifically, the TM atom was put at various sites on the (001) surface (adsorption), and in various interstitial sites in the subsurface region (absorption). We also tried exchanging the TM atom with either a surface Na atom or a surface Al atom, placing the exchanged Na or Al atom at various sites on the surface of the substituted cluster to find the lowest energy TM + ($Z=23$) cluster with Na or Al exchanged with a surface adsorbed TM atom. The three initial adsorption geometries, the four initial absorption geometries used in exploring exchanges with Na and Al, and the four initial interstitial absorption geometries are all shown in Fig. 6.1. Note that in this Chapter, we explored a larger variety of geometries for Ti than in Chapter 3.

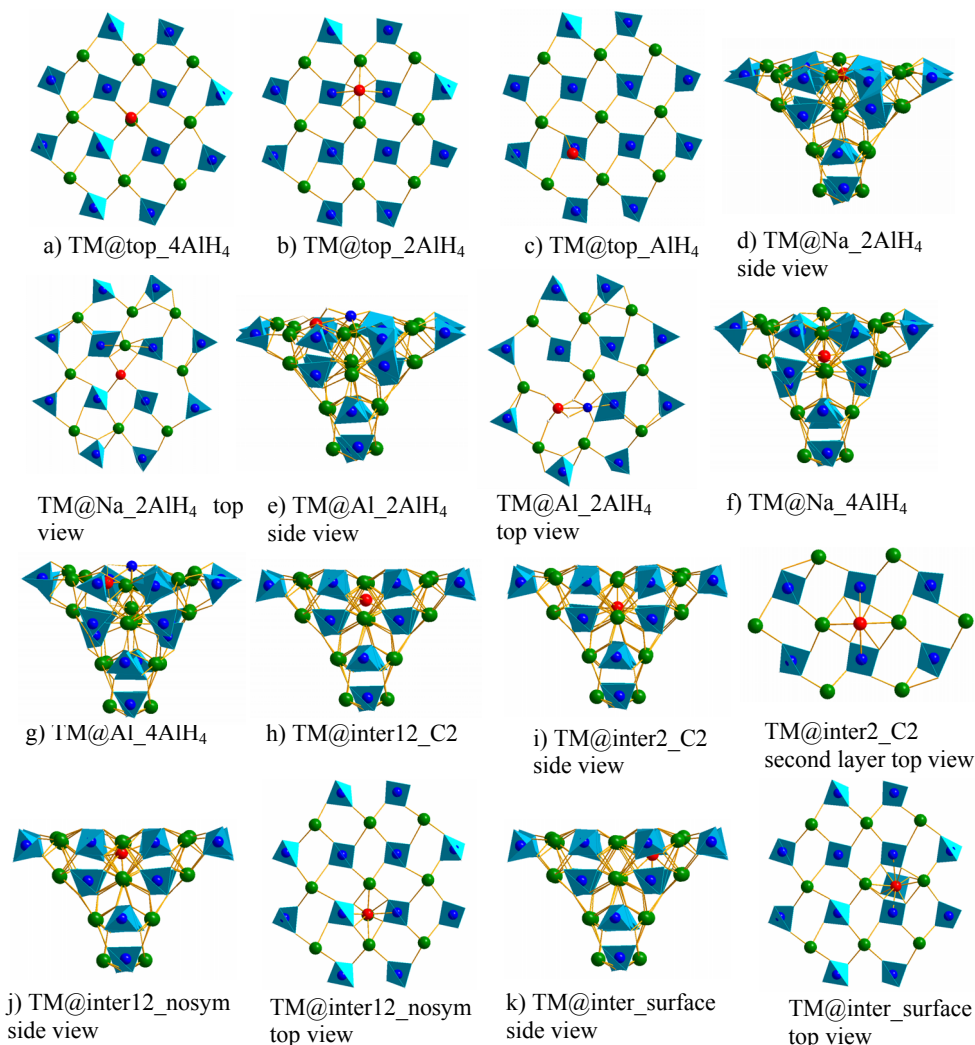


Fig. 6.1: Starting geometries are shown for all geometry optimisations of the TM atom interacting with the (001) surface of the Z=23 NaAlH₄ cluster: (a) The TM atom adsorbed above a first layer Na atom between four AlH_4^- units [TM@top_4AlH₄], (b) between two AlH_4^- units [TM@top_2AlH₄], and (c) above one AlH_4^- unit [TM@top_AlH₄]. Absorption geometries, where (d) the TM atom replaces Na in the surface layer and the exchanged Na atom adsorbs between two AlH_4^- units [TM@Na_2AlH₄], (e) the TM atom replaces Al in the surface layer and the exchanged Al atom adsorbs between two AlH_4^- units [TM@Al_2AlH₄], (f) the TM atom replaces Na in the surface layer and the exchanged Na atom adsorbs between four AlH_4^- units [TM@Na_4AlH₄], (g) the TM atom replaces Al in the surface layer and the exchanged Al atom adsorbs between four AlH_4^- units [TM@Al_4AlH₄]. Absorption geometries, where (h) the TM atom is in an interstitial site between the first and second layer, on the C₂ axis [TM@inter12_C2], (i) in an interstitial site in the second layer on the C₂ axis [TM@inter2_C2], (j) in an interstitial site in between the first two layers, but not on the C₂ axis [TM@inter12_nosym], and (k) in an interstitial site in the surface layer (TM@inter_surface).

The ADF code calculates the total binding energy relative to spin restricted spherically symmetric atoms. This is an unphysical reference state, but *all* our calculations have been done relative to this same state of reference. However, since we have some freedom in how to define our energy reference, we have chosen reference systems with a definite physical meaning. When considering one TM atom adsorbed/absorbed on/in the ($Z=23$) cluster our zero of energy has been set to that of the fully optimized bare $Z=23$ cluster plus one TM atom in TM bulk. In this way the energy reported for a specific TM + NaAlH₄ system represents the energy gained by taking one TM atom out of TM bulk and putting it on/in the $Z=23$ cluster. Our adsorption/absorption energies are defined in such a way that a negative number means that it is stable with respect to the bare ($Z=23$) cluster + one TM atom in TM bulk. The energies of the bulk TM systems have been computed using the periodic ADF-BAND code [65] using the same basis and fit sets as employed in the cluster calculations.

6.3. Results and Discussion

6.3.1 Adsorption of TM atoms on NaAlH₄(001)

The TM atoms (Sc, Ti, Zr, Pd, Pt) were adsorbed on the (001) surface of the geometry optimized ($Z=23$) NaAlH₄ cluster in different positions, after which a geometry optimisation of the whole system was performed. Three different starting geometries were attempted. In one geometry, the TM atom sits above a surface Na atom in between 4 AlH_4^- units (a structure denoted TM@top_4AlH₄, Fig. 6.1a). In the second geometry, the TM atom sits in between two AlH_4^- units (denoted TM@top_2AlH₄, Fig. 6.1b). In the third adsorption geometry, the TM atom sits on top of a surface AlH_4^- unit (TM@top_AlH₄, Fig. 6.1c). In almost all cases, the TM atom remained in more or less the same position in the relaxed structures. The adsorption energies of the relaxed clusters are listed in Table 6.1. The final optimised geometry is shown in Figs. 6.2a-6.6a for the most favourable adsorption geometry for each TM atom.

As can be seen from Table 6.1, when restricted to surface adsorption the Sc, Ti, and Zr atoms all prefer to be above the surface Na atom, with co-ordination to hydrogen atoms from four surrounding AlH_4^- units (Figs. 6.2a-6.4a). Of these three atoms, Sc perturbs the arrangement of the surface atoms of the NaAlH₄ cluster most. Also,

TM	Pt	Pd	Sc	Ti	Zr
Relative Energies	E_{rel}	E_{rel}	E_{rel}	E_{rel}	E_{rel}
$E_{Z23} + \text{TM@bulk}$	0.00	0.00	0.00	0.00	0.00
TM@top_4AlH ₄	-1.16	-0.84	-0.44	0.61	0.86
TM@top_2AlH ₄	-1.59	-1.47	0.76	1.55	1.59
TM@top_AlH ₄	-1.44	-0.01	0.45	1.77	2.13
TM@Na_2AlH ₄	-1.67	-2.04	-1.97	-2.15	-2.94
TM@Al_2AlH ₄	-1.13	-1.43	0.09	1.03	0.47
TM@Na_4AlH ₄	-1.01	-1.58	-1.51	-0.50	-1.35
TM@Al_4AlH ₄	-0.57	-0.13	-1.33	0.76	-0.08
TM@inter12_C2	-1.38	-1.82	0.43	-0.07	0.60
TM@inter2_C2	-1.79	-1.59	0.12	-0.18	0.95
TM@inter_nosym	-2.14	-2.19	-0.61	1.31	-0.97
TM@inter_surface	-2.16	-1.94	-1.03	-0.25	0.03

Table 6.1. The interaction energies (in eV) resulting from geometry optimisations of the transition metal atoms Pt, Pd, Sc, Ti, and Zr adsorbing on or absorbing in the (001) face of NaAlH₄ are given for each system. Both absolute and relative values are presented, where the relative values are relative to the bare cluster and the TM atom in TM bulk. The notations used in the first column are explained in Fig. 6.1.

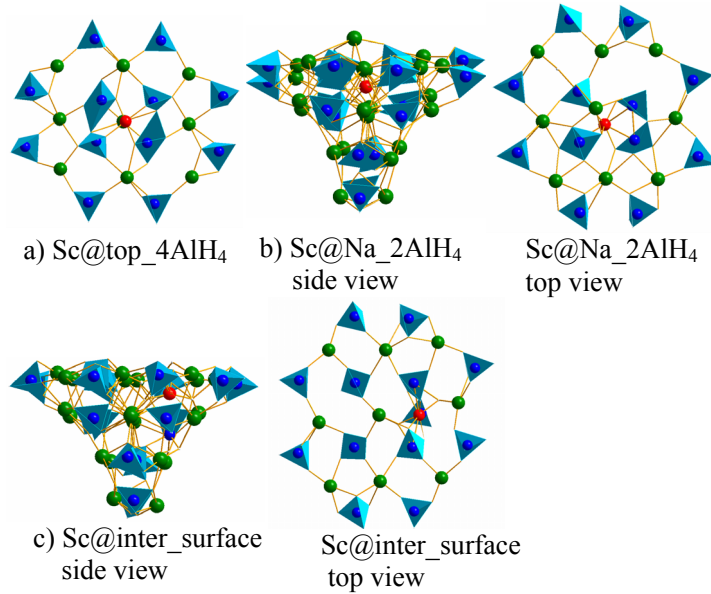


Fig. 6.2: Final optimised geometry for the Sc atom adsorbed on /absorbed in different positions relative to the (001) surface of the ($Z=23$) NaAlH₄ cluster, for the most favourable cases concerning adsorption, absorption with exchange, and absorption in an interstitial site: (a) the Sc atom adsorbed above a first layer Na atom between four AlH_4^- units [Sc@top_4AlH₄]; (b) the Sc atom replaces Na in the surface layer and the exchanged Na atom adsorbs between two AlH_4^- units [Sc@Na_2AlH₄]; (c) the Sc atom absorbs in an interstitial site in the surface layer (Sc@inter_surface).

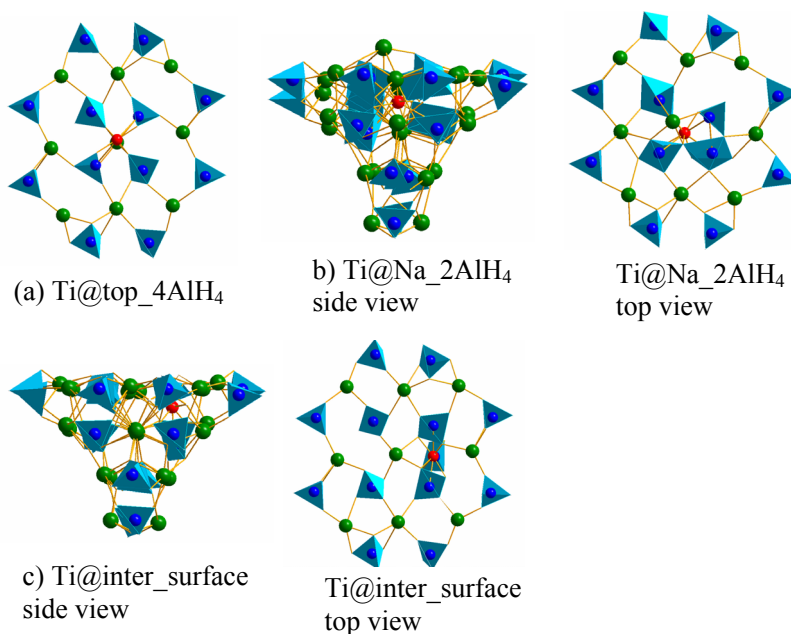


Fig. 6.3: Final optimised geometry for the Ti atom adsorbed on /absorbed in different positions relative to the (001) surface of the ($Z=23$) NaAlH₄ cluster, for the most favourable cases concerning adsorption, absorption with exchange, and absorption in an interstitial site: (a) the Ti atom adsorbed above a first layer Na atom between four AlH_4^- units [Ti@top_4AlH₄]; (b) the Ti atom replaces Na in the surface layer and the exchanged Na atom adsorbs between two AlH_4^- units [Ti@Na_2AlH₄]; (c) the Ti atom adsorbs in an interstitial site in the surface layer (Ti@inter_surface).

adsorption of monodispersed Sc to the NaAlH₄(001) face is energetically preferred above the situation where the NaAlH₄ and Sc are separate and the Sc atom is in atom bulk. In contrast, for the other two atoms, the energetically preferred situation is for the TM atom to be in TM bulk and separate from NaAlH₄.

The energy difference between NaAlH₄ and TM bulk and the TM atom surface adsorbed to the NaAlH₄(001) face is smaller for Ti than for Zr. Interestingly, the stability of the TM atom adsorbed to the NaAlH₄(001) face correlates well with the quality of the catalyst for dehydrogenation, Sc being the best catalyst [19], followed by Ti and then by Zr [17].

The TM atoms Pt and Pd preferentially adsorb at a different site when compared to Sc, Ti, and Zr: the Pt and Pd atoms prefer to adsorb on a “bridge site” between 2 AlH₄

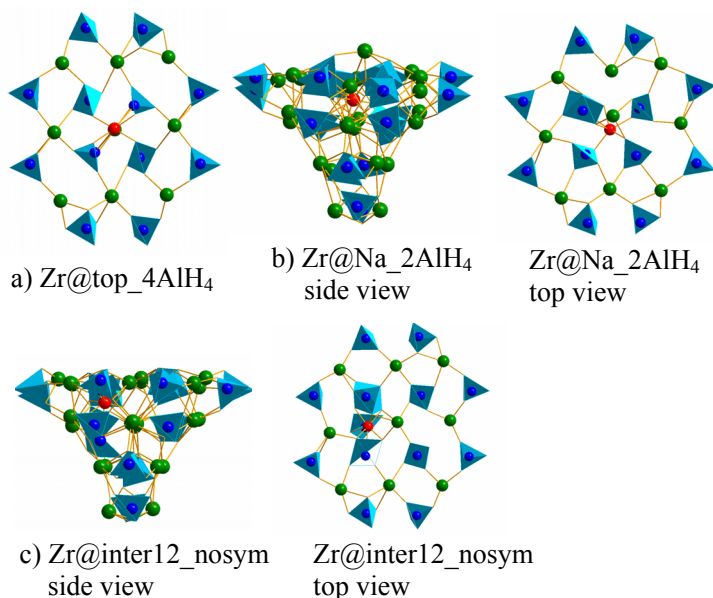


Fig. 6.4: Final optimised geometry for the Zr atom adsorbed on /absorbed in different positions relative to the (001) surface of the (Z=23) NaAlH₄ cluster, for the most favourable cases concerning adsorption, absorption with exchange, and absorption in an interstitial site: (a) the Zr atom adsorbed above a first layer Na atom between four AlH₄⁻ units [Zr@top_4AlH₄]; (b) the Zr atom replaces Na in the surface layer and the exchanged Na atom adsorbs between two AlH₄⁻ units [Zr@Na_2AlH₄]; (c) the Zr atom adsorbs in an interstitial site in between the first two layers, but not on the C2 axis [Zr@inter12_nosym].

units (Figs. 6.5a and 6.6a and Table 6.1). Just like Sc, Pt and Pd atoms prefer being adsorbed to the NaAlH₄(001) face over being in their bulk phases. However, in this case this property does not correlate to the quality of the catalyst for dehydrogenation of NaAlH₄, Sc being a very good catalyst, but Pt and Pd being very poor catalysts [17].

6.3.2 Absorption of TM atoms in the surface of NaAlH₄(001)

Next, we tried to absorb the TM atoms in the surface of NaAlH₄(001), either by exchanging the TM atom with a surface Na or Al atom, or by putting the TM atom in an interstitial position (see Table 6.1 for the energy of the relaxed TM + (Z=23) cluster systems, and Figs. 6.2b-6.6b and 6.2c-6.6c). When making an exchange, the exchanged atom (Na or Al) was either put on a bridge site between two AlH₄⁻ units (TM@Na_2AlH₄ or TM@Al_2AlH₄ Figs. 6.1d and 6.1e), or put in a site between four AlH₄⁻ units (TM@Na_4AlH₄ and TM@Al_4AlH₄, Figs. 6.1f and 6.1g). In

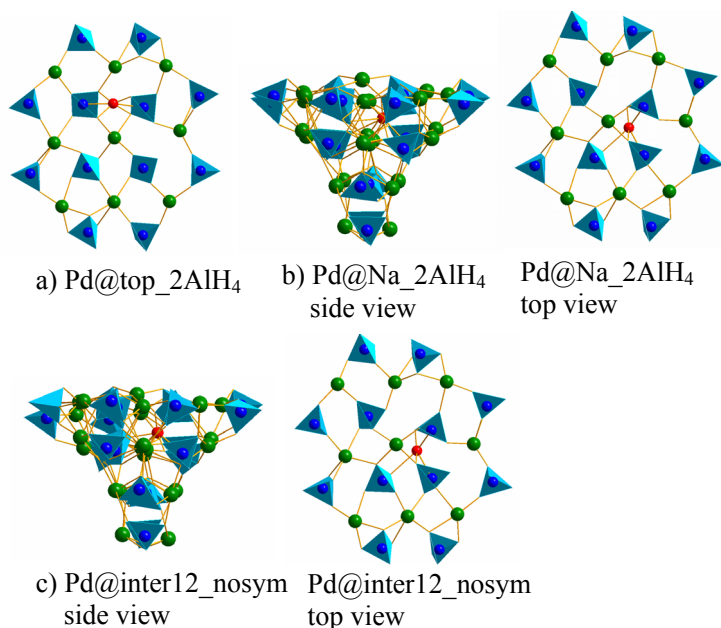


Fig. 6.5: Final optimised geometry for the Pd atom adsorbed on /absorbed in different positions relative to the (001) surface of the ($Z=23$) NaAlH_4 cluster, for the most favourable cases concerning adsorption, absorption with exchange, and absorption in an interstitial site: (a) the Pd atom adsorbed above a first layer Na atom between two AlH_4^- units [Pd@top_2AlH₄]; (b) the Pd atom replaces Na in the surface layer and the exchanged Na atom adsorbs between two AlH_4^- units [Pd@Na_2AlH₄]; (c) the Pd atom adsorbs in an interstitial site in between the first two layers, but not on the C_2 axis [Pd@inter12_nosym].

putting the TM atom in an interstitial site, four different possibilities were tried. In the first case, the TM atom was placed initially in between the first 2 layers on the C_2 -axis (TM@inter12_ C_2) (Fig. 6.1h). In the second case, the TM atom was placed within the second layer, again on the C_2 -axis (TM@inter2_ C_2) (Fig. 6.1i).

In the third case the TM atom was placed initially in between the first 2 layers, but not on the C_2 -axis (TM@inter12_nosym), in a position above a Na ion (Fig. 6.1j). Finally, in the fourth case the atom was placed initially in a surface interstitial site above an AlH_4^- unit, as investigated previously by Liu and Ge [(39,40), Fig. 6.1k).

Again, we find a difference between Sc, Ti, and Zr on the one hand, and Pt and Pd on the other hand (see Table 6.1). The Sc, Ti, and Zr atoms all prefer to exchange with a surface Na atom, leaving the Na atom on the surface on a site where it is in between 2 AlH_4^- units (TM@Na_2AlH₄, Figs. 6.2b-6.4b), and high above the surface. In all

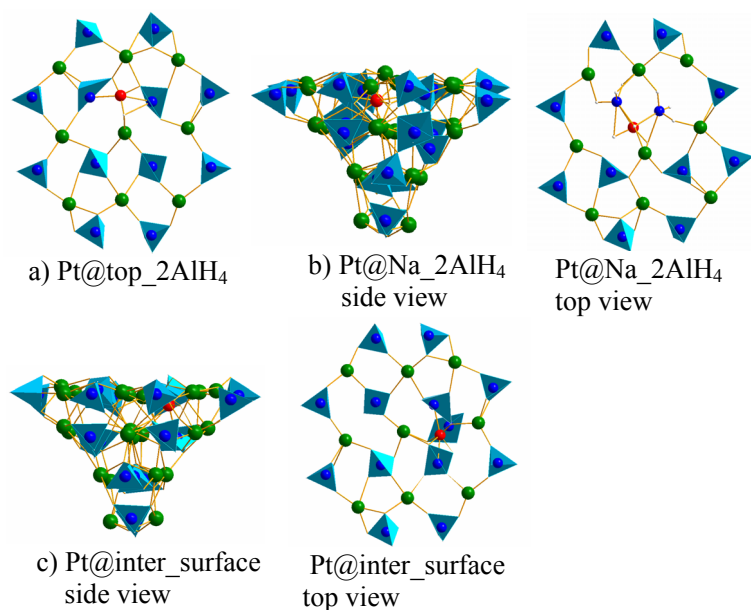


Fig. 6.6: Final optimised geometry for the Pt atom adsorbed on /absorbed in different positions relative to the (001) surface of the ($Z=23$) NaAlH_4 cluster, for the most favourable cases concerning adsorption, absorption with exchange, and absorption in an interstitial site: (a) the Pt atom adsorbed above a first layer Na atom between two AlH_4^- units [Pt@top_2AlH₄]; (b) the Pt atom replaces Na in the surface layer and the exchanged Na atom adsorbs between two AlH_4^- units [Pt@Na_2AlH₄]; (c) the Pt atom adsorbs in an interstitial site in the surface layer (Pt@inter_surface).

three cases, the TM@Na_2AlH₄ absorbed case is also preferred over the energetically most favourable adsorption case, TM@top_4AlH₄.

Furthermore, in all cases the TM@Na_2AlH₄ absorbed case is also preferred over the case where the TM atom is in its bulk phase but separate from NaAlH_4 . On the other hand, the Pt and Pd atoms prefer to be in an interstitial position, in either the TM@inter_nosym site (Pd, Fig. 6.5c) or the TM@inter_surface site (Pt, Fig. 6.6c), and in this case no Na ion is pushed out of the surface. Considering only the exchanges, for Pd and Pt the TM@Na_2AlH₄ geometry is preferred over the other two exchange geometries, as was the case for Sc, Ti and Zr, but in the TM@Na_2AlH₄ geometries the exchanged Na ion is hardly pushed out of the surface for Pd and Pt (Figs. 6.5a and 6.6a), in contrast to what is found for Sc, Ti, and Zr

(Figs. 6.2a, 6.3a, and 6.4a). The difference between the preferred absorption sites correlates well with catalyst activity: Sc, Ti, and Zr, which exchange with Na and push Na on to the surface, are good catalysts [17,19], while Pt and Pd, which prefer to go interstitial and leave surface Na ions in their place, are bad catalysts [17].

A few extra comments are in order. The first is that, in our previous work on a single Ti-atom adsorbed to the (001) face of NaAlH₄ (Chapter 3), we did not yet consider the exchange where the exchanged atom (Na or Al) was put on a bridge site, in between 2 AlH₄⁻ units (for instance, the most favourable TM@Na_2AlH4 structure of Fig. 6.1d). Instead, in the previous work only the exchanges with the Na atom in between 4 AlH₄⁻ units were considered (for instance, TM@Na_4AlH4). For the latter geometry, in our calculations the exchange with Na is also favoured over the absorption in the surface interstitial site for Ti, in contrast with the results of plane wave periodic DFT calculations by Liu and Ge [39,40]. However, the energy difference between the Ti@Na_4AlH4 and the Ti@inter_surface geometries is rather small in our cluster calculations (0.25 eV), the difference apparently being small enough to make the preference concerning these two sites become dependent on the model (cluster vs. plane wave in Refs. [39,40]). The energy difference between the Ti@Na_2AlH4 and the Ti@inter_surface geometries is much larger in our calculations (1.9 eV), and we would expect the Ti@Na_2AlH4 geometry to also be the preferred one in plane wave DFT calculations. The idea to explore the TM@Na_2AlH4 geometry arose when we were doing calculations on Pd and Pt adsorbing on the (001) face of NaAlH₄, and discovered that these atoms preferred to adsorb between 2 rather than between 4 AlH₄⁻ units, giving rise to the question of whether the same might be true for Na adsorbing to a substituted surface.

A second comment to be made is that for Pd and Pt the favoured exchange geometry is likewise TM@Na_2AlH4 (Figs. 6.5b and 6.6b) rather than TM@Na_4AlH4 (see

also Table 6.1). The final point to be made is that for Sc and Ti the most favourable interstitial site is TM@inter_surface, while for Zr it is the TM@inter_nosym site.

6.3.3 Interpretation with a zipper model for mass transport

The results are best explained if one assumes that the most important function of the catalyst is to arrange for mass transport to enable a phase separation between a Na rich phase and an Al rich phase. The “zipper mechanism” outlined below is essentially a specific example of the third mechanism for mass transport discussed by Gross *et al.* [49], in which the catalyst moves into the starting phase and “eats” its way into the material, moving one of the two metal atoms (in our case Na) out of it. A difference in mass transport is exactly what distinguishes the absorption behaviour of the good catalysts (Sc, Ti, and Zr) from the absorption behaviour of the bad catalysts (Pt and Pd): the good catalysts prefer to push a Na atom on to the surface by exchanging with it, penetrating the surface and bringing about a mass separation between a Na rich and a Na poor phase. In contrast, the bad catalysts (Pt and Pd) are able to penetrate the surface, but they do not actively enforce mass separation by exchanging with either Na or Al and transporting the exchanged atom away to sit above the surface. Instead, they simply absorb in an interstitial site.

We have previously invoked a “zipper model” [37] to explain the effect one of the good catalysts, Ti, may have, and the same model can be applied to Sc and Zr. In this model, the catalytically active TM-atom acts as a slider, eating itself into a NaAlH₄ nanoparticle as it reacts away, effectively unzipping the structure. The Na ion transported away to sit on the surface should form the nucleus of a Na rich phase (Na₃AlH₆ or NaH), while the TM atom moving into the NaAlH₄, being surrounded, could act as a nucleus for an Al rich phase (Al with the TM atom alloyed into it). The precise ordering of the catalytic activity of Sc, Ti, and Zr can be explained assuming that two things are needed for the catalyst to be good: (1) it should prefer to exchange with a surface atom, which would lead to the desired mass transport, (2) it should be possible to initially have the catalyst present on the surface in mono-atomically

dispersed form. Assumption 2 would explain why Sc is the best catalyst (it actually prefers being present on the surface in mono-atomically dispersed form over being separate from NaAlH₄ in its bulk phase, and why Ti is a better catalyst than Zr (less energy is needed to keep Ti separate from its bulk phase and present in monoatomic form on the surface than for Zr). In the latter two cases, the energy required to have the TM be present in monoatomic form on the surface could, for instance, be provided in mechanical form, through ballmilling.

6.4. Conclusions.

We have performed DFT calculations on the interaction of a single TM atom (Sc, Ti, Zr, Pd, and Pt) with the (001) face of NaAlH₄, using a nano-sized cluster model. In the DFT calculations, the PW91 GGA was used, and both spin restricted and spin unrestricted calculations were performed. The calculations involving Zr, Pd, and Pt incorporated scalar relativistic corrections, employing the ZORA method. The calculations were performed in an attempt to explain a key experimental finding, that Sc, Ti, and Zr are good catalysts for hydrogen uptake and release, while the traditional hydrogenation catalysts Pt and Pd are poor catalysts for hydrogen storage in NaAlH₄. The key difference found between the good catalysts (Sc, Ti, and Zr) and the bad catalysts (Pt and Pd) is that the good catalysts prefer to exchange with a surface Na atom, while the bad catalysts prefer to absorb in an interstitial site. Thus, the good catalysts are seen to initiate mass transport of the heavy metal atoms, and to bring about an initial separation between a Na-rich and a Al-rich phase. The calculations therefore suggest the catalyst to effect mass transport according to one of three mechanisms postulated earlier by Gross *et al.* [49], in which the catalyst moves into the starting phase and “eats” its way into the material, moving one of the two metal atoms (in this case Na) out of it.

A difference found among the good catalysts that correlates with their activity is that, for the best of the three good catalysts (Sc), atomic adsorption of the catalyst on the

(001) face of NaAlH₄ is energetically preferred over the case where the TM atom is in the bulk TM phase, whereas atomic adsorption is not favoured for the Ti and Zr catalyst, and is most unfavourable for the worst of the three catalysts (Zr). This suggests that the ability to disperse the catalyst in atomic form over the surface of NaAlH₄ may also be important to the functioning of the catalyst, and that this ability may be used to distinguish the “best catalysts” from the class of “good catalysts”. I believe that our calculations have revealed some key points about what are good catalysts for effecting hydrogen release from and uptake in NaAlH₄, and I hope that experiments can be done to confirm the interpretations given above of what are features of good catalysts.

6.5. References

- [1] L. Schlapbach, A. Züttel, *Nature* 414, 353 (2001).
- [2] R. S. Irani, *MRS Bull.* 27, 680 (2002).
- [3] J. Wolf, *MRS Bull.* 27, 684 (2002).
- [4] A. C. Dillon, K. M. Jones, T. A. Bekkedahl, C. H. Kiang, D. S. Bethune, M. J. Heben, *Nature* 386, 377 (1997).
- [5] A. Züttel, S. Orimo, *MRS Bull.* 27, 705 (2002).
- [6] W. L. Mao, H-k Mao, A. F. Goncharov, V. V. Struzhin, Q. Guo, J. Hu, J. Shu, R. J. Hemley, M. Somayazulu, Y. Zhao, *Science* 297, 2247 (2002).
- [7] L. J. Florusse, C. J. Peters, J. Schoonman, K. C. Hester, C. A. Koh, S. F. Dec, K. N. Marsh, E. D. Sloan, *Science* 306, 469 (2004).
- [8] N. L. Rosi, J. Eckert, M. Eddaoudi, D. T. Vodak, J. Kim, M. O’Keeffe, O. M. Yaghi, *Science* 300, 1127 (2003).
- [9] Z. Zhao, B. Xiao, A. J. Fletcher, K. M. Thomas, D. Bradshaw, M. J. Rosseinsky, *Science* 306, 1012 (2004).
- [10] B. Bogdanovic, M. Schwickardi, *J. Alloys Comp.* 253-254, 1 (1997).
- [11] F. Schüth, B. Bogdanovic, M. Felderhoff, *Chem.Comm.* 2249-58 (2004).
- [12] W. Grochala, P. P. Edwards, *Chem.Rev.* 104, 1283 (2004).
- [13] M. Felderhoff, C. Weidenthaler, U. von Helmolt, U. Eberle, *Phys. Chem. Chem. Phys.* 9, 2643 (2006).

- [14] B. Bogdanovic, R. A. Brand, A. Marjanovic, M. Schwickardi, J. Tölle, J. Alloys Comp. 302, 36 (2000).
- [15] B. Bogdanovic, M. Felderhoff, S. Kaskel, A. Pommerin, K. Schlichte, F. Schüth, Adv.Mater. 15, 1012 (2003).
- [16] M. Fichtner, O. Fuhr, O. Kircher, J. Rothe, Nanotechnology 14, 778 (2003).
- [17] D. L. Anton, J. Alloys Comp. 356-357, 400 (2003).
- [18] R. A. Zidan, S. Takara, A. G. Hee, C. M. Jensen, J. Alloys Comp. 285, 119 (1999).
- [19] B. Bogdanovic, M. Felderhoff, A. Pommerin, F. Schüth, N. Spielkamp, Adv. Mater. 18, 1198 (2006).
- [20] D. Pukazhselvan, M. S. L. Hudson, B. K. Gupta, M. A. Shaz, O. N. Srivastava, J. Alloys Comp. 439, 243 (2007).
- [21] E. H. Majzoub, K. J. Gross, J. Alloys Comp. 356-357, 363 (2003).
- [22] C. Weidenthaler, A. Pommerin, M. Felderhoff, B. Bogdanovic, F. Schüth, Phys. Chem. Chem. Phys. 5, 5149 (2003).
- [23] M. Felderhoff, K. Klementiev, W. Grunert, B. Spliethoff, B. Tesche, J. M. Bellosta von Colbe, B. Bogdanovic, M. Hartel, A. Pommerin, F. Schuth, C. Weidenthaler, Phys. Chem. Chem. Phys. 6, 4369 (2004).
- [24] J. Graetz, J. J. Reilly, J. Johnson, A. Yu, T. A. Tyson, Appl. Phys. Lett. 85, 500 (2004).
- [25] A. G. Haiduc, H. A. Stil, M. A. Schwarz, P. Paulus, J. J. C. Geerlings, J. Alloys Comp. 393, 252 (2005).
- [26] A. Léon, O. Kircher, M. Fichtner, J. Rothe, D. Schild, J. Phys. Chem.B 110, 1192 (2006).
- [27] C. P. Baldé, H. A. Stil, A. M. J. van der Eerden, K. P. de Jong, J. H. Bitter, J. Phys. Chem.C 111, 2797 (2007).
- [28] X. D. Kang, P. Wang, H. M. Cheng, J. Appl. Phys. 100, 034914 (2006).
- [29] H. W. Brinks, M. Sullic, C. M. Jensen, B. C. Hauback, J. Phys.Chem.B 110, 2740 (2006).
- [30] V. P. Balema, L. Balema, Phys. Chem. Chem. Phys. 7, 1310 (2005).
- [31] D. Sun, T. Kiyobayashi, H. T. Takeshita, N. Kuriyama, C. M. Jensen, J. Alloys Comp. 337, L8 (2002).
- [32] A. Léon, O. Kircher, H. Rösner, B. Décamps, E. Leroy, M. Fichtner, A. Percheron-Guégan, J. Alloys Compd. 414, 190 (2006).

- [33] O. M. Løvvik, S. M. Opalka, *Phys. Rev. B* 71, 054103 (2005).
- [34] O. M. Løvvik, S. M. Opalka, *Appl. Phys. Lett.* 88, 161917 (2006).
- [35] J. Íñiguez, T. Yildirim, *Appl. Phys. Lett.* 86, 103109 (2005).
- [36] A. Marashdeh, R. A. Olsen, O. M. Løvvik, G. J. Kroes, *Chem. Phys. Lett.* 426, 180 (2006).
- [37] A. Marashdeh, R. A. Olsen, O. M. Løvvik, G. J. Kroes, *J. Phys. Chem. C* 111, 8206 (2007).
- [38] T. Vegge, *Phys. Chem. Chem. Phys.* 8, 4853 (2006).
- [39] J. Liu, Q. Ge, *Chem. Commun.* 1822-24 (2006).
- [40] J. Liu, Q. Ge, *J. Phys. Chem. B* 110, 25863-68 (2006).
- [41] J. M. Bellosta von Colbe, W. Schmidt, M. Felderhoff, B. Bogdanovic, F. Schüth, *Angew. Chem. Int. Ed.* 45, 3663 (2006).
- [42] S. Chaudhuri, J. T. Muckerman, *J. Phys. Chem. B* 109, 6952 (2005).
- [43] S. Chaudhuri, J. Graetz, A. Ignatov, J. J. Reilly, J. T. Muckerman, *J. Am. Chem. Soc.* 128 11404 (2006).
- [44] O. Palumbo, R. Cantelli, A. Paolone, C. M. Jensen, S. S. Shrinivan, *J. Phys. Chem. B* 109, 168 (2005).
- [45] O. Palumbo, A. Paolone, R. Cantelli, C. M. Jensen, S. S. Shrinivan, *J. Phys. Chem. B* 110, 9105 (2006).
- [46] O. Palumbo, A. Paolone, R. Cantelli, C. M. Jensen, R. Ayabe, *Mater. Sci. Eng. A* 442, 75 (2006).
- [47] J. Voss, Q. Shi, H. S. Jacobsen, M. Zamponi, K. Lefman, T. Vegge, *J. Phys. Chem. B* 111, 3886 (2007).
- [48] J. Íñiguez, T. Yildirim, *J. Phys. Condens. Matter* 19, 176007 (2007).
- [49] K. J. Gross, S. Guthrie, S. Takara, G. Thomas, *J. Alloys Comp.* 297, 270 (2000).
- [50] R. T. Walters, J. H. Scogin, *J. Alloys Comp.* 379, 135 (2004).
- [51] Q. J. Fu, A. J. Ramirez-Cuesta, S. C. Tsang, *J. Phys. Chem. B* 110, 711 (2006).
- [52] G. Streukens, B. Bogdanovic, M. Felderhoff, F. Schüth, *Phys. Chem. Chem. Phys.* 8, 2889 (2006).
- [53] P. Wang, X. D. Kan, H. M. Cheng, *Chem. Phys. Chem.* 6, 2488-91 (2005).
- [54] L. C. Yin, P. Wang, X. D. Kang, C. H. Sun, H. M. Cheng, *Phys. Chem. Chem. Phys.* 9, 1499 (2007).
- [55] B. Bogdanovic, M. Felderhoff, M. Germann, M. Härtel, A. Pommerin, F. Schüth, C. Weidenthaler, B. Zibrowius, *J. Alloys Comp.* 350, 246 (2003).

- [56] G. J. Thomas, K. J. Gross, N. Y. C. Yang, C. Jensen, *J. Alloys Comp.* 330-332, 702 (2002).
- [57] C. P. Baldé, B. P. C. Hereijgers, J. H. Bitter, K. P. de Jong, *Angew. Chem. Int. Ed.* 45, 3501 (2006).
- [58] W. Lohstro, M. Fichtner, *Phys. Rev. B* 75, 184106 (2007).
- [59] J. P. Perdew, J. A. Chevary, S. H. Vosko, K. A. Jackson, M. R. Pederson, D. J. Singh, C. Fiolhais, *Phys. Rev. B* 46, 6671 (1992).
- [60] P. Hohenberg, W. Kohn, *Phys. Rev.* 136, B864 (1964).
- [61] W. Kohn, L. J. Sham, *Phys. Rev.* 140, A1133 (1965).
- [62] G. te Velde, F. M. Bickelhaupt, E. J. Baerends, S.v. Gisbergen, J. G. Snijders, T. Ziegler, *J. Comput. Phys.* 22, 931 (2001).
- [63] E. van Lenthe, E. J. Baerends, J. G. Snijders, *J. Chem. Phys.* 101, 9783 (1994).
- [64] T. J. Frankcombe, O. M. Løvvik, *J. Phys. Chem. B* 110, 622 (2006).
- [65] G. te Velde, E. J. Baerends, *Phys. Rev. B* 44, 7888 (1991).

Chapter 7

Zero point energy corrected dehydrogenation enthalpies of $\text{Ca}(\text{AlH}_4)_2$, CaAlH_5 and $\text{CaH}_2+6\text{LiBH}_4$

The dehydrogenation enthalpies of $\text{Ca}(\text{AlH}_4)_2$, CaAlH_5 and $\text{CaH}_2+6\text{LiBH}_4$ have been calculated using density functional theory calculations at the generalized gradient approximation level, including harmonic phonon zero point energy correction. The dehydrogenation of $\text{Ca}(\text{AlH}_4)_2$ is exothermic, indicating a metastable hydride. Calculations for CaAlH_5 including ZPE effects indicate that it is not stable enough for a hydrogen storage system operating near ambient conditions. The destabilized combination of LiBH_4 with CaH_2 is a promising system after ZPE-corrected enthalpy calculations. The calculations show that including ZPE effects in the harmonic approximation for the dehydrogenation of $\text{Ca}(\text{AlH}_4)_2$, CaAlH_5 and $\text{CaH}_2+6\text{LiBH}_4$ has a significant effect on the calculated reaction enthalpy.

7.1 Introduction

Hydrogen is widely regarded as an attractive alternative to fossil fuels for transport and other mobile applications, being lightweight, nontoxic and producing only water at the point of end use. The lack of suitable high density storage remains one of the main problems holding back practical implementations [1]. Though many storage systems have been proposed, no currently known system meets desired targets of storage density, hydrogen availability and energy efficiency, let alone cost. Chemical hydrides show much promise, but the (de)hydrogenation kinetics for these systems needs to be improved.

A decade ago Bogdanovic and Schwickardi found that the hydrogenation and dehydrogenation kinetics and storage reversibility of NaAlH_4 are significantly improved by adding small amounts of Ti [2]. In light of this discovery, light element complex metal hydrides (especially the alanates) are promising materials for practical hydrogen storage. In general light element complex metal hydrides have high volumetric and gravimetric hydrogen densities, essential properties for mobile applications.

$\text{Ca}(\text{AlH}_4)_2$ is one such high hydrogen density alanate of great interest, exhibiting 7.9 wt. % hydrogen content in total. It decomposes to CaH_2 , Al and H_2 in a two-step process with the formation of a CaAlH_5 intermediate in the first step, as indicated in Eqs. (7.1) and (7.2) [3–5]. Overall the decomposition can be described as the reaction in Eq. (7.3). Many researchers have neglected the CaAlH_5 intermediate, considering only Eq. (7.3).



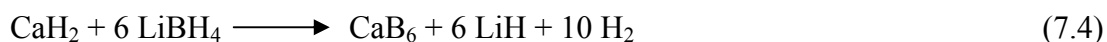
The ground state $\text{Ca}(\text{AlH}_4)_2$ crystal structure of space group $Pbca$ has been determined by theoretical prediction from density functional theory (DFT) band-structure calculations [6], with the simulated X-ray diffraction pattern agreeing well with the powder pattern subsequently measured [7]. The crystal structure of the CaAlH_5 has also been predicted using DFT calculations, revealing a $P2_1/n$ space group and facilitating refinement of the structure from measured X-ray diffraction patterns [7]. The intermediate CaAlH_5 is the first penta-hydride known in the family of complex metal hydrides, in which tetra- and hexa-hydrides abound.

The energy changes for the reactions in Eqs. (7.1)–(7.3) have previously been calculated without including the zero point energy (ZPE) [7]. These calculations indicate that the first step, Eq. (7.1), is exothermic, and thus irreversible. The second step, Eq. (7.2), is promising since 4.2 wt. % of H_2 can be released. The dehydrogenation energy for the second step is calculated to be 39.9 kJ/mole H_2 without the ZPE correction. This value lies within the target range for hydrogen storage materials [1].

It is now well known that including ZPE effects (in the harmonic approximation) for the dehydrogenation of complex metal hydrides has a significant effect on the calculated reaction enthalpy [9–13]. Including ZPE corrections typically reduces the calculated energy change by 10–20 kJ/mol H_2 [9].

Alapati *et al.* have calculated the dehydration enthalpies for many destabilized hydride systems [8] without including ZPE in their study. One of the reactions studied

with an enthalpy change that appears to be favourable for hydrogen storage applications is a mixture of CaH₂ with LiBH₄ (reaction 7.4). The energy change for this reaction is found to be 62.7 kJ/mol H₂ [8].



In a subsequent paper, Alapati *et al.* extended their reaction set to over 340 possible combinations of materials [14]. Vibrational effects were included for a number of promising destabilized hydride systems, including the reaction shown in Eq. (7.4) above. For this reaction, including ZPE reduces the dehydrogenation enthalpy by 20.3 kJ/mol H₂ to 42.4 kJ/mol H₂.

In the present work we have calculated ZPE corrections for reactions 7.1 and 7.2, and thus for the more often considered reaction 7.3. We have also repeated the calculations performed by Alapati *et al.* [14] on reaction 7.4 as a representative sample of their ZPE corrections for mixed hydride systems.

7.2 Method

Plane wave density functional theory [15] was used to calculate potential energies using the program VASP [16]. The PW91 generalized gradient approximation exchange-correlation functional [17] was used with the projector augmented wave (PAW) method [18, 19]. Γ -centred k -space grids and plane wave basis set cutoff energies were selected to converge the total energy of each system to better than 1 meV per conventional crystallographic unit cell. Initial crystal structures were taken from Weidenthaler *et al.* [7] for Ca(AlH₄)₂ and CaAlH₅, from Wyckoff [20] for CaH₂ and from Schmitt *et al.* [21] for CaB₆.

Harmonic phonon densities of states were calculated by the direct method [22] as implemented in PHONON [23]. In this implementation the second derivatives required to construct the dynamical matrices used in the direct method are determined by finite differencing from force calculations. Two-sided differences were used in the calculations described here. Typical atomic displacements used were in the range 0.05–0.10 Å. Conventional unit cells were used in the phonon calculations for Ca(AlH₄)₂ and CaAlH₅. 2×2×2 supercells were used for CaH₂ and CaB₆.

From the frequency-dependent harmonic phonon density of states $g(\omega)$ thus obtained the vibrational ZPE can be calculated, per unit cell, as

$$E_{ZPE} = \frac{\hbar r}{2} \int_0^{\infty} \omega g(\omega) d\omega \quad (7.5)$$

where \hbar is Planck's constant divided by 2π and r is the number of degrees of freedom in the unit cell. Similar integrals over $g(\omega)$ can be used to evaluate the vibrational free energy and the entropy [24]. In this work the ZPE was evaluated at the lattice parameters that minimised the potential energy. No attempt was made to include the effect of vibrations on the equilibrium geometry (for example by applying the quasiharmonic approximation), since this has been shown to have a negligible effect on the dehydrogenation enthalpy for a closely related system [10].

7.3 Results and Discussion

In previous work the crystal structure of CaAlH_5 has been given in the non-standard space group $P2_1/n$ [7]. This crystal structure was transformed into the standard space group $P2_1/c$ using standard methods [25]. The resulting $P2_1/c$ representation of the CaAlH_5 structure was reoptimized. The resulting crystallographic data for CaAlH_5 in the $P2_1/c$ space group is given in Table 7.1 and the crystal structure is shown in Figs. 7.1a and 7.1b. The crystal structures of $\text{Ca}(\text{AlH}_4)_2$ is shown in Fig. 7.1c.

The optimized CaB_6 structure was similar to the experimentally determined $Pm\bar{3}m$ structure, with $a=4.1469 \text{ \AA}$ and the boron atoms in 6f positions with $x=0.2017$. All other structures used in this work have been published previously [7, 10].

Fig. 7.2 shows the calculated phonon density of states for $\text{Ca}(\text{AlH}_4)_2$, CaAlH_5 , CaB_6 and CaH_2 . The phonon density of states of $\text{Ca}(\text{AlH}_4)_2$ exhibits similar features to densities of states calculated for other similar complex metal hydrides [9, 11, 26], with contributions from Al–H stretching modes, AlH_4 bending modes and modes involving relative motion of the ions clearly separated into high, medium and low frequency groups. On the other hand, in the CaAlH_5 structure (Fig. 7.1a) the aluminium and hydrogen do not exist in distinct molecular ions, forming instead chains of corner-sharing AlH_6 octahedra (Fig. 7.1b). This is reflected in the phonon

Atom	site	Atomic coordinates
Ca	4e	(0.7737, 0.7703, 0.0419)
Ca	4e	(0.3313, 0.7293, 0.1451)
Al	4e	(0.8015, 0.6946, 0.3105)
Al	4e	(0.2097, 0.7840, 0.3400)
H	4e	(0.9487, 0.8096, 0.2757)
H	4e	(0.6063, 0.7150, 0.1393)
H	4e	(0.1051, 0.6493, 0.1948)
H	4e	(0.2652, 0.6014, 0.4511)
H	4e	(0.4350, 0.7866, 0.3665)
H	4e	(0.0088, 0.3072, 0.5176)
H	4e	(0.6970, 0.8891, 0.3402)
H	4e	(0.2637, 0.9452, 0.4615)
H	4e	(0.1189, 0.9758, 0.2143)
H	4e	(0.3544, 0.4351, 0.6642)

Table 7.1: Relative internal coordinates of atoms of the standard crystallographic space group $P2_1/c$ of CaAlH_5 . The lattice parameters are $a=8.3247 \text{ \AA}$, $b=6.9665 \text{ \AA}$, $c= 12.3668 \text{ \AA}$ and $\beta=127.938^\circ$.

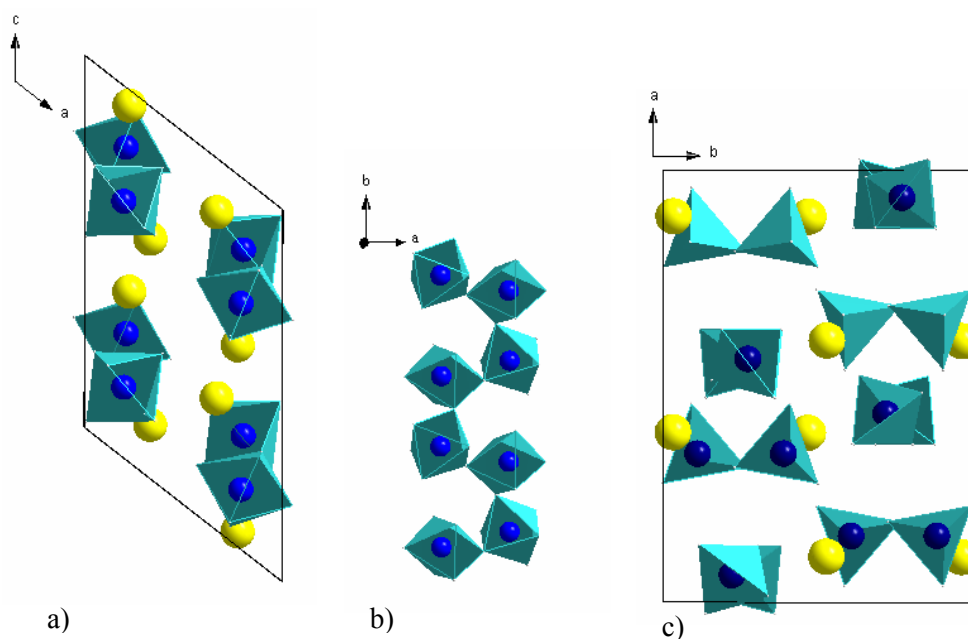


Fig. 7.1: (a) The crystal structure of CaAlH_5 viewed down the b axis. (b) The helical arrangement of corner sharing $[\text{AlH}_6]$ octahedra in CaAlH_5 . (c) The crystal structure of $\text{Ca}(\text{AlH}_4)_2$.

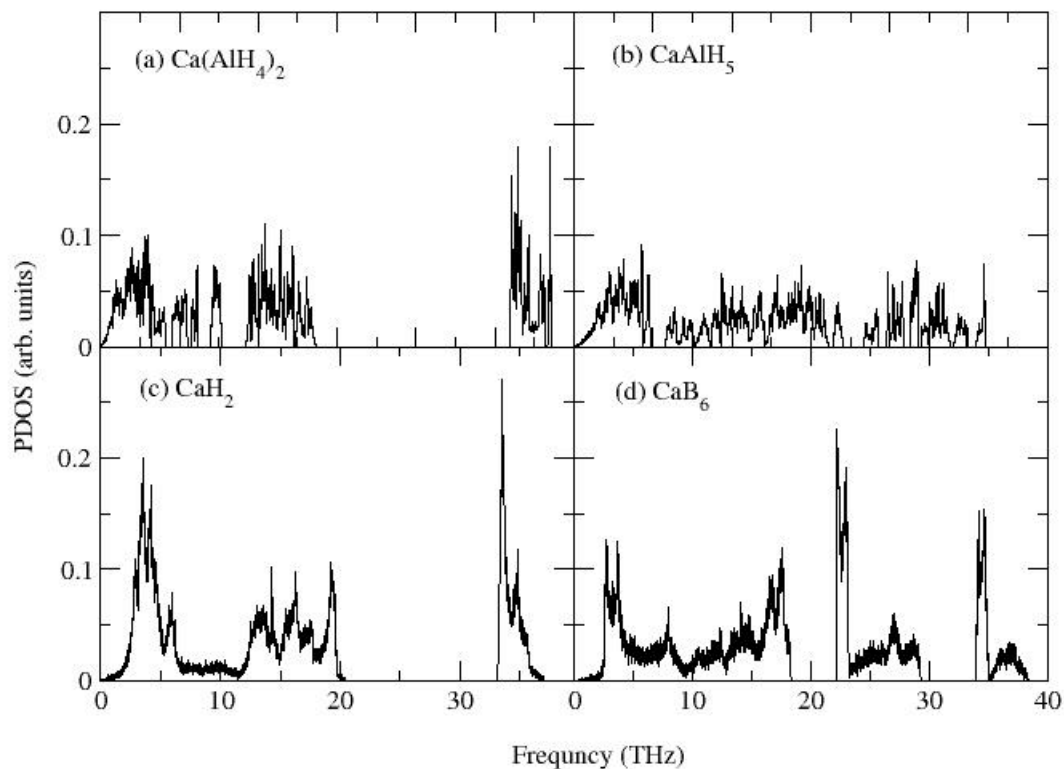


Fig. 7.2: Phonon density of states for (a) $\text{Ca}(\text{AlH}_4)_2$, (b) CaAlH_5 , (c) CaH_2 and (d) CaB_6 .

	Potential energy	ZPE
$\text{Ca}(\text{AlH}_4)_2$	-38.6758	1.5776
CaAlH_5	-24.8555	1.0231
CaH_2	-10.3251	0.2919
CaB_6	-45.0062	0.7863

Table 7.2: Calculated potential energy (as calculated by VASP, relative to spherically symmetric, isolated reference atoms) and ZPE for calcium-containing phases calculated in this work (eV/formula unit).

density of states, with the (now coupled) Al–H bending and stretching modes spread over a much greater frequency range than for $\text{Ca}(\text{AlH}_4)_2$. Indeed, the phonons in the three groups of modes are sufficiently coupled that the frequency ranges at which they occur almost overlap.

From the calculated phonon density of states, the ZPE per unit cell was calculated via Eq. (7.5) for all the calcium-containing phases in reactions 7.1–7.4 [$\text{Ca}(\text{AlH}_4)_2$, CaAlH_5 , CaH_2 and CaB_6]. These are shown in Table 7.2. The ZPEs for LiBH_4 and

Reaction	ΔH Without ZPE	ΔH With ZPE	$-\Delta(\Delta H)$
$\text{Ca}(\text{AlH}_4)_2 \longrightarrow \text{CaAlH}_5 + \text{Al} + 3/2\text{H}_2$	-5.3	-12.3	7.0
$\text{CaAlH}_5 \longrightarrow \text{CaH}_2 + \text{Al} + 3/2\text{H}_2$	40.3	22.0	18.4
$\text{Ca}(\text{AlH}_4)_2 \longrightarrow \text{CaH}_2 + 2\text{Al} + 3\text{H}_2$	17.5	4.8	12.7
$\text{CaH}_2 + 6\text{LiBH}_4 \longrightarrow \text{CaB}_6 + 6\text{LiH} + 10\text{H}_2$	60.2	40.7	19.5

Table 7.3: Low temperature and pressure enthalpy changes for dehydrogenation reactions (kJ/mol H₂).

Al have been published previously [10, 27]. For H₂ the ZPE was calculated in the harmonic approximation with vibrational frequency 4401 cm⁻¹.

Table 7.3 shows the calculated enthalpy changes for the dehydrogenation reactions shown in Eqs. (7.1)–(7.4). In all cases the inclusion of ZPE reduced the enthalpy change on dehydrogenation appreciably. For the “elementary” steps (that is, excluding the overall reaction 7.3), the magnitudes of the reductions were of the order that has come to be expected [9].

Without ZPE, our calculated enthalpy changes are in accord with those published by Alapati *et al.* [14] for reactions 7.3 and 7.4. The small discrepancies are easily accounted for as differences in details such as energy and geometry optimization convergence thresholds. Alapati *et al.* also published a ZPE-corrected enthalpy change for reaction 7.4, which likewise agrees with our calculated value. The change in the calculated enthalpy upon inclusion of ZPE, the focus of the calculations performed in this work, agrees even more closely, differing by less than 1 kJ/mol H₂. The calculated dehydrogenation enthalpy, including ZPE effects, lies within the target range for hydrogen storage systems. Clearly, this is not a novel result, being previously reported. However, this represents an important independent validation of a representative example of the extensive calculations reported by Alapati *et al.*

It has been shown [3, 5] that the dehydrogenation represented in reaction 7.3 is the sum of two steps, reactions 7.1 and 7.2. With or without ZPE contributions, the first step of the decomposition of calcium alanate was calculated to be significantly exothermic, and thus uninteresting from the point of view of hydrogen storage. The second step, itself accounting for a storage capacity of 4.2 wt. %, has a potential

energy change on dehydrogenation that does lie within the desired enthalpy change range for a hydrogen storage material [7]. However, adding contributions from ZPE reduces this calculated enthalpy change to significantly below the 30 kJ/mol H₂ lower limit [1] of the target enthalpy change range. These results are in accord with those of Wolverton and Ozoliņš [28].

In their screening of destabilized hydride storage systems, Alapati *et al.* [14] considered separately systems that involved combining Ca(AlH₄)₂ with another complex metal hydride, on the basis that the decomposition of Ca(AlH₄)₂, with its low reaction enthalpy, was likely to compete with the destabilized path. The enthalpy change calculated for the dehydrogenation of Ca(AlH₄)₂ to CaH₂, reaction 7.3, is lowered by the first step being exothermic. The dehydrogenation enthalpy for CaAlH₅ is also below the lower limit for hydrogen storage systems and is thus in principle subject to the same considerations as Ca(AlH₄)₂ from the point of view of “short-circuiting” destabilization schemes. Hence while potential attractive destabilization schemes involving CaAlH₅ are likely to be at best metastable, experimental tests of such destabilization schemes should be designed with the CaAlH₅ intermediate in mind, rather than the more traditional alanate Ca(AlH₄)₂. In particular, rehydrogenation of a calcium- and aluminium-containing system would be expected to stop at CaAlH₅ rather than continuing to Ca(AlH₄)₂.

7.4 Conclusions

We have performed density functional theory calculations at the generalized gradient approximation level for the dehydrogenation reactions of Ca(AlH₄)₂, CaAlH₅ and CaH₂+6LiBH₄. Harmonic ZPE effects were included. Ca(AlH₄)₂ was confirmed to be a metastable hydride, and thus unsuitable as a medium for a cyclable hydrogen storage system. CaAlH₅ is stable, but calculations including ZPE effects indicate that it is not stable enough for a hydrogen storage system operating near ambient conditions. ZPE-corrected enthalpy calculations confirm that the destabilized combination of LiBH₄ with CaH₂ is a promising system, as previously reported.

7.5 References

- [1] L. Schlapbach, A. Züttel, *Nature* 414, 353 (2001).
- [2] B. Bogdanovic, M. Schwickardi, *J. Alloys Compd.* 253, 1 (1997).

- [3] M. Mamatha, B. Bogdanovic, M. Felderhoff, A. Pommerin, W. Schmidt, F. Schuth, C. Weidenthaler, *J. Alloys Compd.* 407, 78 (2006).
- [4] N. N. Mal'tseva, A. I. Golovanova, T. N. Dymova, Aleksandrov, D. P. Russ, *J. Inorg. Chem.* 46, 1793 (2001).
- [5] M. Mamatha, C. Weidenthaler, A. Pommerin, M. Felderhoff, F. Schuth, *J. Alloys Compd.* 416, 303 (2006).
- [6] O. M. Løvvik, *Phys. Rev. B* 71, 144111 (2005).
- [7] C. Weidenthaler, T. J. Frankcombe, M. Felderhoff, *Inorg. Chem.* 45, 3849 (2006).
- [8] S. V. Alapati, J. K. Johnson, D. S. Sholl, *J. Phys. Chem. B* 110, 8769 (2006).
- [9] T. J. Frankcombe, *J. Alloys Compd.* 446–447, 455 (2007).
- [10] T. J. Frankcombe, G. J. Kroes, *Phys. Rev. B* 73, 174302 (2006).
- [11] K. Miwa, N. Ohba, S. Towata, Y. Nakamori, S. Orimo, *Phys. Rev. B* 69, 245120 (2004).
- [12] X. Ke, I. Tanaka, *Phys. Rev. B* 71, 024117 (2005).
- [13] J. F. Herbst, L. G. Hector, Jr., *Phys. Rev. B* 72, 125120 (2005).
- [14] S. V. Alapati, J. K. Johnson, D. S. Sholl, *Phys. Chem. Chem. Phys.* 9, 1438 (2007).
- [15] R. G. Parr, W. Yang, *Density-Functional Theory of Atoms and Molecules*, Oxford University Press, New York 1989.
- [16] G. Kresse, J. Furthmüller, *Phys. Rev. B* 1996, 54, 11169.
- [17] J. P. Perdew, J. A. Chevary, S. H. Vosko, K. A. Jackson, M. R. Pederson, D. J. Singh, C. Fiolhais, *Phys. Rev. B* 46, 6671 (1992).
- [18] G. Kresse, D. Joubert, *Phys. Rev. B* 59, 1758 (1999).
- [19] P. E. Blöchl, C. J. Först, J. Schimpl, *Bull. Mat. Sci.* 26, 33 (2003).
- [20] R. W. G Wyckoff, *Crystal Structures*, 2nd edition, John Wiley and Sons, New York, 1963.
- [21] K. Schmitt, C. Stückl, H. Ripplinger, B. Albert, *Solid State Sci.* 3, 321 (2001).
- [22] K. Parlinski, Z. Q. Li, Y. Kawazoe, *Phys. Rev. Lett.* 78, 4063 (1997).
- [23] K. Parlinski, *Software PHONON*, Institute of Nuclear Physics, Crakow 2005.
- [24] A. A. Maradudin, E. W. Montroll, G. H. Weiss, I. P. Ipatova, *Theory of lattice dynamics in the harmonic approximation*, *Solid State Physics Supplement* vol. 3, Academic Press, New York 1971.
- [25] H. Suh, I. K. Oh, Y. K. Yoon, M. J. Kim, *Journal of the Korean Physical Society* 19, 280 (1986).

- [26] A. Peles, M. Y. Chou, Phys. Rev. B 73, 184302 (2006).
- [27] T. J. Frankcombe, G. J. Kroes, Chem. Phys. Lett. 423, 102 (2006).
- [28] C. Wolverton, V. Ozoliņš, Phys. Rev. B 75, 064101 (2007).

Summary

In the hydrogen economy, hydrogen is used as a clean energy carrier in the transport sector. Extracting energy from hydrogen using a fuel cell or an internal combustion engine avoids the emission of the harmful greenhouse gas CO₂, provided that the hydrogen was made in a “clean way”, for instance, using solar or wind energy to electrolyze water, or using steam reforming with CO₂ sequestration. However, to bring about the hydrogen economy a number of challenges have to be met. Scientific and technological advances are needed to (i) produce fuel cells at acceptable costs, (ii) to produce “clean” (CO₂ free) hydrogen at acceptable costs, and (iii) to store hydrogen in cars in tanks of not too high weight and volume, again at acceptable costs. This thesis focuses on the third challenge, hydrogen storage.

Sodium alanate (NaAlH₄) contains 5.5 weight percent hydrogen which, in principle, can be released from the storage material and put back into it at close to ambient pressures and temperatures. For about ten years now, it is known that adding transition metal atoms in some form (for example, Ti, in TiCl₃) makes the hydrogen release from and uptake in the material reversible, and improves the kinetics of these processes enormously, although the kinetics of hydrogen uptake is still too slow. Unfortunately, it is still not clear what the role of the transition metal catalyst is. If this would be understood, it might be possible to suggest better catalysts or combinations of catalysts. The main goal of this thesis has therefore been to determine, by computation, how the catalyst acts. In addition, calculations were performed on the decomposition of two calcium alanates, to determine zero-point energy corrected enthalpies of dehydrogenation for these compounds, and to determine whether destabilization of LiBH₄ by CaH₂ might improve the performance of this material.

In order to determine the role of transition metal catalysts like Ti, calculations were performed using density functional theory (DFT) employing the PW91 generalized gradient approximation (GGA). The adsorption of transition metal atoms on and their absorption in the energetically most stable (001) surface of NaAlH₄ was studied employing a cluster model of NaAlH₄ with an exposed (001) face. Geometry optimizations were performed to arrive at a good model for the bare NaAlH₄ cluster,

which contained 23 formula units and was of semi-spherical shape. To model the interaction with one or two transition metal atoms, these atoms were put on various places on or in the surface of the NaAlH₄ cluster, also considering initial geometries in which the transition metal atom replaces a surface Na or Al atom, which is then put on the surface of the cluster. Geometry optimizations were then performed on the transition metal atom(s) interacting with the NaAlH₄ cluster using both spin-restricted and unrestricted DFT calculations, to determine the position of the transition metal atom(s) relative to the cluster atoms, and thereby make inferences about the possible role of the transition metal catalyst. In the modeling of heavier transition metal catalysts, such as Zr, Pd, and Pt, relativistic corrections were incorporated using the ZORA method. All electronic structure calculations involving NaAlH₄ were performed using the Amsterdam Density Functional (ADF) code. Because experiments showed that hydrogenated Ti (TiH₂) is also a good catalyst for hydrogen release, calculations on a TiH₂ “molecule” interacting with the NaAlH₄ cluster were also performed.

In **chapter 3**, a “good” NaAlH₄ model cluster was determined that could be used to study the interaction of transition metal atoms with the (001) face of NaAlH₄. It was found that large geometry optimized clusters (tetragonal clusters of 20 and 42 NaAlH₄ formula units, and semispherical clusters of 23 and 45 NaAlH₄ formula units) are energetically, electronically and structurally close to surface and bulk NaAlH₄, and therefore form good model systems for nano-sized NaAlH₄ particles. A semispherical cluster of 23 NaAlH₄ formula units was chosen as an appropriate model system, and then doped with a Ti atom. Using this mono-atomically dispersed Ti adsorbed on the surface of NaAlH₄ as a reference system, Ti was found to preferably substitute a lattice Na atom at the surface. It was found that it is important to allow for spin polarisation when performing calculations on Ti interacting with the NaAlH₄ cluster.

In **chapter 4**, the interaction of a NaAlH₄ cluster with two Ti atoms, either as a dimer or two separated Ti atoms, and adsorbed on the (001) surface of the cluster, was studied. The calculations on surface adsorption were supplemented with a large number of calculations where one or two Ti atoms had been either inserted into interstitial sites or exchanged with a surface Na or Al atom. The calculations showed that: (i) Beginning with the case that a Ti dimer is adsorbed on the surface, it is

energetically preferred for the Ti dimer to dissociate on the surface of the cluster. The most stable adsorption position results when the resulting separate Ti atoms are both above first layer Na surface atoms. These surface Na atoms are found to be displaced into the subsurface region of the cluster, allowing each Ti atom to interact with 4 AlH₄ units. (ii) After dissociation the two Ti atoms prefer to move inside the cluster to the subsurface region, as was also found in **chapter 3** for a single Ti atom interacting with the (001) surface. If the two Ti atoms move inside the cluster, exchange with two subsurface displaced Na atoms is preferred, and overall this represents the energetically most favorable case. Absorbing two Ti atoms in interstitial sites close to each other (5.8 – 7.4 Å) is clearly unfavorable; instead, the thermodynamically most stable situation is for Ti atoms to move into Na positions far away from each other. A zipper model was proposed, in which the mechanism by which the added Ti promotes H₂ release is explained by the Ti atom working itself down into the alanate particle, effectively unzipping the structure.

In **chapter 5**, the interaction of TiH₂ with the (001) face of NaAlH₄ was studied, again using the cluster model. The adsorption of the TiH₂ molecule on the surface was investigated. Also, the TiH₂ molecule or its Ti atom was moved inside the cluster either by exchanging the whole TiH₂ molecule with Na or Al, or by exchanging only the Ti atom with Na or Al and leaving the two hydrogen atoms on the surface together with the exchanged atom. Restricting the possible outcomes to adsorption, TiH₂ was found to adsorb on the surface above a Na atom, bonding with 4 AlH₄ units and pushing the surface Na atom into the subsurface region, as was found before for a single Ti atom in **chapter 3**. However, it was energetically preferred to exchange the whole TiH₂ unit with the subsurface displaced Na atom, as also found for one Ti atom in **chapter 3**. All other exchanges were unstable compared to the situation where TiH₂ was adsorbed on the surface. These results are also consistent with our results for two Ti atoms interacting with the NaAlH₄ cluster, as presented in **chapter 4**. The results are also consistent with the zipper model presented in **chapter 4**. In this model, the mechanism by which the added TiH₂ promotes H₂ release involves the TiH₂ molecule working its way into the alanate particle by replacing Na and pushing the Na atom on the surface, effectively unzipping the NaAlH₄ structure.

In **chapter 6**, the role of transition metal catalysts in promoting de- or rehydrogenation was investigated coming from another angle. Rather than only addressing the popular Ti catalyst, the following question was asked: why are Sc, Ti, and Zr good catalysts for promoting hydrogen release from and uptake in NaAlH_4 , while traditional hydrogenation catalysts, like Pd and Pt, are poor for NaAlH_4 ?

The key difference found between the good catalysts (Sc, Ti, and Zr) and the bad catalysts (Pt and Pd) was that the good catalysts prefer to exchange with a surface Na atom and push the Na atom on to the surface, while the bad catalysts prefer to absorb in an interstitial site. Thus, the good catalysts initiate mass transport of the heavy metal atoms, and bring about an initial separation between a Na-rich and an Al-rich phase. The calculations therefore suggest the catalyst to effect mass transport according to one of three mechanisms postulated earlier by Gross *et al.* In this mechanism, the catalyst moves into the starting phase and “eats” its way into the material, moving one of the two metal atoms (in this case Na) out of it.

A difference found among the good catalysts, which correlates with their activity, is that, for the best of the three good catalysts (Sc), atomic adsorption of the catalyst on the (001) face of NaAlH_4 is energetically preferred over the case where the transition metal (TM) atom is in the bulk TM phase. Instead, atomic adsorption is not favored for the Ti and Zr catalyst, and it is most unfavorable for the worst of the three catalysts (Zr). This suggests that the ability to disperse the catalyst in atomic form over the surface of NaAlH_4 should be important to the functioning of the catalyst, and that this ability can be used to separate the “best catalysts” from the class of “good catalysts”. It is my belief that the calculations have revealed some key points about what are good catalysts for effecting hydrogen release from and uptake in NaAlH_4 , and I hope that experiments can be done to confirm the interpretations given above of what are features of good catalysts.

In **chapter 7**, DFT calculations were performed on the dehydrogenation reactions of $\text{Ca}(\text{AlH}_4)_2$, CaAlH_5 and $\text{CaH}_2+6\text{LiBH}_4$. The DFT model used was somewhat different from that employed in the calculations on NaAlH_4 . A periodic model was used of the hydrogen storage materials, using the plane wave DFT code VASP, with the PW91 GGA. Harmonic phonon densities of states (DOSs) were calculated by the direct

method using the PHONON code. From these DOSs, zero-point energy (ZPE) corrections to the dehydrogenation enthalpies were computed. $\text{Ca}(\text{AlH}_4)_2$ was confirmed to be a meta-stable hydride, and thus unsuitable as a medium for a cyclable hydrogen storage system. CaAlH_5 was confirmed to be stable, but calculations including ZPE effects indicate that it is not stable enough for a hydrogen storage system operating near ambient conditions. ZPE-corrected enthalpy calculations confirm that the destabilized combination of LiBH_4 with CaH_2 is a promising system, as previously reported. The computed ZPE corrected dehydrogenation enthalpies were in good agreement with recent DFT results of other research groups. The computed phonon DOS of CaAlH_5 differs qualitatively from that found for other alanates, because in CaAlH_5 the aluminium and hydrogen atoms do not exist in distinct molecular ions.

Samenvatting.

Een cluster dichtheidsfunctionaaltheorie studie aan de interactie van het waterstofopslagsysteem NaAlH_4 met overgangsmetaal- katalysatoren.

In de waterstofeconomie wordt waterstof gebruikt als een schone energiedrager in de transportsector. Energie onttrekken uit waterstof met gebruik van een brandstofcel of een interne verbrandingsmotor vermijdt de emissie van het schadelijke broeikasgas CO_2 , mits het waterstof wordt gemaakt op een schone manier, bijvoorbeeld, met gebruik van zonne- of windenergie om water te electrolyseren, of via “steam reforming” met CO_2 sequestratie. Echter, om de waterstofeconomie te realiseren moeten een aantal uitdagingen overwonnen worden. Wetenschappelijke en technologische doorbraken zijn nodig op de gebieden van: (i) de productie van brandstofcellen tegen acceptabele kosten, (ii) de productie van “schoon” (CO_2 vrij) waterstof tegen acceptabele kosten, en (iii) de opslag van waterstof in auto's, in tanks met een niet te hoog gewicht en volume, opnieuw tegen acceptabele kosten. Dit proefschrift richt zich op de derde uitdaging, waterstofopslag.

Natriumalanaat (NaAlH_4) bevat 5.5 gewichtsprocent waterstof dat, in principe, afgegeven kan worden uit het opslagmateriaal en er weer in opgenomen kan worden bij omstandigheden die niet ver af liggen van heersende drukken en temperaturen. Voor ongeveer 10 jaar is nu bekend dat toevoegen van overgangsmetaal-atomen in een bepaalde vorm (bijvoorbeeld, Ti, in TiCl_3) de waterstofopslag in het materiaal reversibel maakt, en dat het de kinetiek van de afgifte en opname van waterstof enorm verbetert, hoewel de kinetiek van de opname nog steeds te langzaam is. Helaas is nog steeds niet duidelijk wat de rol van de overgangsmetaalkatalysator is. Als dit begrepen zou zijn, zou het mogelijk moeten zijn betere katalysatoren of combinaties van katalysatoren te suggereren. Het belangrijkste doel van dit proefschrift is daarom geweest om te bepalen hoe de katalysator zijn werk doet, met gebruik van computerberekeningen. Eveneens worden berekeningen gepresenteerd aan de decompositie van twee calciumalenen, om de nulpunsvibratie-energiegecorrigeerde enthalpieën van dehydrogenering van deze verbindingen te bepalen, en te bepalen of destabilisatie van LiBH_4 door CaH_2 de werking van dit materiaal zou kunnen verbeteren.

Om de rol van overgangsmetaalkatalysatoren zoals Ti te bepalen zijn berekeningen gedaan met dichtheidsfunctionaaltheorie (DFT), met gebruik van de PW91 functionaal. De adsorptie van overgangsmetaal-atomen op en de absorptie van die atomen in het energetisch meest stabiele (001) oppervlak van NaAlH_4 is bestudeerd met gebruik van een clustermodel van NaAlH_4 met een (001) oppervlak. Geometrie-optimalisaties zijn gedaan om te komen tot een goed model van het vrije NaAlH_4 cluster, dat 23 formule-eenheden bevat en de vorm heeft van een halve bol. Om de interactie te kunnen modelleren met een of twee overgangsmetaal-atomen, zijn deze atomen geplaatst op verschillende plekken op of in het oppervlak van het NaAlH_4 cluster. Hierbij zijn eveneens initiële geometrieën beschouwd waarin het overgangsmetaal-atoom een oppervlakte Na of Al atoom vervangt, dat dan op het oppervlak van het cluster werd geplaatst. Vervolgens zijn geometrie-optimalisaties gedaan aan het (de) overgangsmetaal-atoom (-atomen) in interactie met het NaAlH_4 cluster, met gebruik van zowel “spin-restricted” als “spin-unrestricted” DFT berekeningen, om de positie van het (de) overgangsmetaal-atoom (-atomen) t.o.v. de clusteratomen te bepalen, om op die manier te komen tot een interpretatie van de mogelijke rol van de overgangsmetaalkatalysator. In het modelleren van zwaardere overgangsmetaalkatalysatoren, zoals Zr, Pd, en Pt, zijn relativistische correcties toegepast met gebruik van de zogenaamde ZORA methode. Alle elektronenstructuur-berekeningen aan systemen met daarin NaAlH_4 zijn gedaan met gebruik van het Amsterdam Density Functional (ADF) computerprogramma. Omdat experimenten hebben laten zien dat gehydrogeneerd Ti (TiH_2) ook een goede katalysator is voor waterstofafgifte, zijn eveneens berekeningen gedaan aan een TiH_2 “molecuul” in interactie met een NaAlH_4 cluster.

In **hoofdstuk 3** is een “goed” NaAlH_4 clustermodel bepaald dat gebruikt kan worden om de interactie van overgangsmetaal-atomen met het (001) oppervlak van NaAlH_4 te bestuderen. Er is gevonden dat grote geometriegeoptimaliseerde clusters (tetragonale clusters met daarin 20 of 42 NaAlH_4 formule-eenheden, en halfronde clusters van 23 en 45 NaAlH_4 formule-eenheden) energetisch, elektronisch, en in structureel opzicht sterk lijken op oppervlakte- en bulk- NaAlH_4 , en dat die clusters daarom goede modelsystemen vormen voor NaAlH_4 deeltjes met nanogrootte. Een halfronde cluster van 23 NaAlH_4 formule-eenheden is gekozen als een geëigend model systeem, en vervolgens gedoteerd met een Ti atoom. Met gebruik van dit mono-atomair

gedispergeerde Ti geadsorbeerd op het oppervlak van NaAlH_4 als referentie systeem, werd gevonden dat Ti bij voorkeur een oppervlakte N atoom vervangt. Eveneens werd gevonden dat het belangrijk is om spinpolarisatie toe te staan in het doen van berekeningen aan een Ti-atoom in interactie met een NaAlH_4 cluster.

In **hoofdstuk 4** wordt de interactie van een NaAlH_4 cluster met twee Ti atomen bestudeerd, met het Ti beschouwd zowel als dimeer als als gescheiden Ti atomen, in beide gevallen geadsorbeerd op het (001) oppervlak van het cluster. De berekeningen aan oppervlakte-adsorptie zijn gecomplementeerd met berekeningen waarin één of twee Ti atomen ofwel werden opgenomen in interstitiële sites, dan wel uitgewisseld werden met een oppervlakte Na of Al atoom. De berekeningen lieten zien dat: (i) Beginnend met het geval dat een Ti dimeer geadsorbeerd is op een oppervlak, het energetisch gezien voordelig is voor het Ti dimeer om te dissociëren op het oppervlak van het cluster. De meest stabiele adsorptiepositie ontstaat als de resulterende, gescheiden Ti atomen zich beiden bevinden boven Na oppervlakte atomen. In de gevonden geometrie zijn de oppervlakte Na atomen ietwat verplaatst naar de regio van het cluster beneden het oppervlak, zodat elk Ti atoom interactie kan hebben met 4 AlH_4 eenheden. (ii) Na dissociatie is het energetisch gezien voordelig voor de Ti atomen om zich in het oppervlak van het cluster te begeven, zoals ook was gevonden in **hoofdstuk 3** voor een enkel Ti atoom in interactie met het (001) oppervlak. In dit proces is de uitwisseling met twee oppervlakte Na atomen energetisch gezien het meest voordelig. Adsorptie van twee Ti atomen in interstitiële sites die zich dicht bij elkaar bevinden ($5.8 - 7.4 \text{ \AA}$) is zeer ongunstig; de thermodynamisch meest stabiele situatie ontstaat wanneer de Ti atomen oppervlakte Na atomen vervangen met grote afstand van elkaar. Een “ritsmodel” is voorgesteld, waarin het mechanisme waardoor het toegevoegde Ti waterstofafgifte bevordert wordt verklaard door het idee dat het Ti atoom zich een weg baant naar het binnenste van het alenaatdeeltje, en op die manier het deeltje als het ware openritst.

In **hoofdstuk 5** werd de interactie van TiH_2 met het (001) oppervlak van NaAlH_4 bestudeerd, opnieuw met gebruik van het clustermodel. De adsorptie van het TiH_2 molecuul op het oppervlak is onderzocht. Ook zijn situaties onderzocht waarin het TiH_2 molecuul of daarvan het Ti atoom in het cluster werd gebracht, of door uitwisseling van het gehele TiH_2 molecuul met Na of Al, of door uitwisseling van het

Ti atoom met Na of Al, met achterlating van de waterstofatomen op het oppervlak tezamen met het uitgewisselde atoom (Na of Al). Als de mogelijke uitkomsten worden beperkt tot adsorptie wordt gevonden dat TiH_2 adsorbeert aan het oppervlak boven een Na atoom, met binding aan 4 AlH_4 eenheden en onder wegduwen van het Na atoom in de richting van de bulk, zoals gevonden is voor één Ti atoom in **hoofdstuk 3**. Echter, energetisch gezien is het voordelig om de gehele TiH_2 eenheid te verwisselen met een oppervlakte Na atoom, zoals ook is gevonden voor één Ti atoom in **hoofdstuk 3**. Alle andere uitwisselingen waren onstabiel vergeleken met de situatie waarin TiH_2 was geadsorbeerd op het oppervlak. Deze resultaten zijn eveneens consistent met onze resultaten voor twee Ti atomen in interactie met het NaAlH_4 cluster, zoals gepresenteerd in **hoofdstuk 4**. De resultaten zijn ook consistent met het “ritsmodel” dat is gepresenteerd in **hoofdstuk 4**. In dit model geldt dat, in het mechanisme waardoor het toegevoegde TiH_2 waterstofafgifte bevordert, het TiH_2 molecuul zich een weg baant naar het binnenste van het alenaatdeeltje door Na te vervangen en het Na atoom uit het deeltje weg te duwen naar het oppervlak ervan, op die manier de NaAlH_4 structuur als het ware openritsend.

In **hoofdstuk 6** is de rol van overgangsmetaalkatalysatoren ten aanzien van het bevorderen van de de- of re-hydrogenering onderzocht vanuit een ander gezichtspunt. In plaats van alleen naar de populaire Ti-katalysator te kijken is de volgende vraag gesteld: waarom zijn Sc, Ti, en Zr goede katalysatoren voor waterstofafgifte uit en waterstofopname in NaAlH_4 , hoewel traditionele hydrogeneringskatalysatoren, zoals Pd en Pt, slecht zijn voor NaAlH_4 ?

Het belangrijkste verschil dat is gevonden tussen de goede katalysatoren (Sc, Ti, en Zr) en de slechte katalysatoren (Pt en Pd) was dat de goede katalysatoren er de voorkeur aan geven te verwisselen met een oppervlakte Na atoom en het Na atoom naar buiten duwen, het oppervlak op, waar de slechte katalysatoren er de voorkeur aan geven te absorberen in een interstitiële site. Dit betekent dat de goede katalysatoren massatransport initiëren van de relatief zware metaal atomen, en een initiële scheiding bewerkstelligen tussen een Na-rijke en een Al-rijke fase. De berekeningen suggereren dat de katalysator massatransport bewerkstelligt volgens één van de drie eerder gepostuleerde mechanismen door Gross *et al.* In dit mechanisme begeeft de

katalysator zich in de beginfase en “eet” zich vervolgens het materiaal in, terwijl het één van de twee metaalatomen (in dit geval Na) naar buiten werkt.

Een verschil dat is gevonden tussen de goede katalysatoren, dat correleert met hun activiteit, is dat, voor de beste van de drie goede katalysatoren (Sc), atomaire adsorptie van de katalysator op het (001) oppervlak van NaAlH₄ energetisch geprefereerd is over het geval waarin het overgangsmetaal (TM) atoom zich in de bulk TM fase bevindt. In tegenstelling hiermee geldt dat atomaire adsorptie niet gunstig is voor de Ti en Zr katalysatoren, en het meest ongunstig is voor de slechtste van de drie katalysatoren (Zr). Dit suggereert dat het vermogen om de katalysator in atomaire vorm over het oppervlak van NaAlH₄ te dispergeren belangrijk is voor het functioneren van de katalysator, en dat dit vermogen gebruikt kan worden om de “beste katalysatoren” te onderscheiden van de klasse van “goede katalysatoren”. Ik durf dan ook te stellen dat de berekeningen op belangrijke punten hebben laten zien wat goede katalysatoren voor waterstof-afgifte uit en -opname in NaAlH₄ onderscheidt van slechte katalysatoren, en ik hoop dat experimenten gedaan kunnen worden om de interpretaties die hier boven gegeven zijn ten aanzien van wat kenmerken zijn van goede katalysatoren te bevestigen.

In **hoofdstuk 7** zijn DFT-berekeningen gedaan aan de dehydrogeneringsreacties van Ca(AlH₄)₂, CaAlH₅ en CaH₂+6LiBH₄. Het DFT-model dat is gebruikt verschilt van het model dat is gebruikt in de berekeningen aan NaAlH₄. Een periodiek model is gebruikt voor de waterstofopslagmaterialen, met gebruik van het vlakke-golf DFT programma VASP, en de PW91-functionaal. Harmonische fonon toestandsdichtheden (DOSs) zijn berekend met de “directe methode” met gebruik van de PHONON code. Uit deze toestandsdichtheden zijn nulpuntsvibratieënergie (ZPE) correcties berekend op de dehydrogeneringsenthalpieën. Ca(AlH₄)₂ werd bevestigd een meta-stabiele hydride te zijn, en daarmee ongeschikt te zijn als een medium voor een reversibel waterstofopslag systeem. Voor CaAlH₅ werd bevestigd dat dit een stabiele hydride is, maar berekeningen die ZPE effecten meenemen laten zien dat dit materiaal niet stabiel genoeg is voor een waterstofopslagsysteem dat bij heersende omstandigheden kan functioneren. ZPE-gecorrigeerde enthalpieberekeningen bevestigen dat de gedestabiliseerde combinatie van LiBH₄ met CaH₂ een veelbelovend systeem is, zoals eerder gerapporteerd. De berekende ZPE-gecorrigeerde dehydrogeneringsenthalpieën

waren in goede overeenstemming met recente DFT resultaten van andere onderzoeksgroepen. De berekende fonon-DOS van CaAlH_5 verschilt kwalitatief van die gevonden voor andere alenaten, omdat in CaAlH_5 de aluminium- en waterstofatomen niet bestaan in afzonderlijke moleculaire ionen.

Curriculum Vitae

Ali Awad Marashdeh

I was born on 1 March 1973 in Ramtha, Jordan. I passed the general secondary education examination (Tawjihi) in 1991. In 1991, I started my undergraduate study at Yarmouk University in the faculty of science to study chemistry. I obtained my B.Sc. degree in chemistry in 1995. After that I worked in different fields for two years. In September 1997, I started my master study in Mu'tah University in the chemistry department. I finished the master courses in 1999. I worked my master project under the supervision of Professor Salim Khalil in theoretical chemistry. My research involved a theoretical study of Keto-Enol tautomerism of substituted acyclic and cyclic propanones (XCH_2COCH_3 and XCH_2COCH_2) and the influence of different substitutes ($X = H, F, OH, CN, NH_2, NO_2, CH_3, CF_3, OCH_3$) on the stability of either the keto or enol form. All substituents were found to decrease the stability of the keto form, particularly in the case of electron withdrawing capacity (e. g. NO_2 and CF_3).

On 1 February 2004, I moved to the theoretical chemistry group at the Leiden Institute of Chemistry (LIC), Leiden University, to work as a PhD student under the direct supervision of Dr. R. A. Olsen and Prof. dr. G. J. Kroes, where I am till now. My research focuses on the theoretical modeling of the storage of hydrogen in $NaAlH_4$. The aim is to determine the role played by catalysts like Ti, Zr, Sc, Pd and Pt.

During my PhD research, I have attended several conferences and workshops at which I presented my work. I have attended the winter school "Theoretische Chemie en Spectroscopie" which was held in Belgium twice, in 2004 and 2005. I have attended the winter school MSSC2004, Ab Initio Modeling in Solid State Chemistry" at Imperial Collage in London in 2004. I have attended a Gordon conference (Hydrogen-Metal Systems, in 2005) and "MH2006", the International Symposium on Metal-Hydrogen Systems which was held in Hawaii in 2006. I attended the International Workshop on Functional Materials for Mobile Hydrogen Storage which was held in Hamburg in 2006. Here in the Netherlands I attended the 1st EU Network

Hydrogen2 Meeting SRTCA which was held at Shell in 2007. I have been to the ACTS meetings five times and to the “Spectroscopie en Theorie” national conference in Lunteren four times. I have also attended three “HRSMC” symposiums. In December 2006, I visited both the Centre for Materials Science and Nanotechnology at University of Oslo and the Institute for Energy Technology at Kjeller, where I gave talks about my work.

Publication list

- A Theoretical Study of Substituted Stepwise Fluorinated Cyclopropanone Keto-Enol System. El-Alali, A.; Marashdeh, A. A.; Khalil S. M. *Z. Naturforsch* **2003**, *58a*, 749–755.
- A density functional theory study of Ti-doped NaAlH₄ clusters. Marashdeh, A.; Olsen, R. A.; Løvvik, O. M.; Kroes, G.-J. *Chem. Phys. Lett.* **2006**, *426*, 180–186.
- NaAlH₄ Clusters with Two Titanium Atoms Added. Marashdeh, A.; Olsen, R. A.; Løvvik, O. M.; Kroes, G.-J. *J. Phys. Chem. C* **2007**, *111*, 8206–8213.
- A density functional theory study of the TiH₂ interaction with a NaAlH₄ cluster. Marashdeh, A.; Olsen, R. A.; Løvvik, O. M.; Kroes, G.-J., submitted.
- Zero point energy corrected dehydrogenation enthalpies of Ca(AlH₄)₂, CaAlH₅ and CaH₂+6LiBH₄, Marashdeh, A.; Frankcombe, T. J., submitted.
- Why Some Transition Metals are Good Catalysts for Reversible Hydrogen Storage as Sodium Alanate, and Others do not: A Density Functional Theory Study. Marashdeh, A.; Versluis, J. W.; Olsen, R. A.; Løvvik, O. M.; Kroes, G.-J., in preparation.

Acknowledgment

All praise is due to Allah SWT with his compassion and mercifulness to give me health, patience, hearing, sight, heart, mind and knowledge. By which I manage to understand the beauty of sciences as I learned in this thesis.

This dissertation would not be finished without the support, encouragement and help of many people who I appreciate.

My mother (Fatima), she was with me in every single step of my life. Her courage and invocations were the energy suppliers to me in all my life until the last minutes in her life. My father, he gave me the courage and support. Until now, I have gotten all the support, kindness and patience from my lovely wife. My daughter is the source of happiness in my life. I want to thank also my brothers, sisters and all my family members.

The collaboration with Ole Martin Løvvik at the University of Oslo and fruitful scientific discussions with him have influenced significantly my thesis. Terry Frankcombe has helped me to work with the VASP and PHONON codes to make the periodic calculations. I thank my colleagues in the theoretical chemistry group for the scientific discussions that taught me many things that helped me during my research.